Doctorial Dissertation (Censored)

博 士 論 文 (要約)

Enzymatic Synthesis of Cu^{II}-responsive Deoxyribozymes through Incorporation of Artificial Ligand-type Nucleotides

（金属配位子型人工ヌクレオチドを導入した
Cu^{II}応答性デオキシリボザイムの酵素合成）

A Dissertation Submitted for the Degree of Doctor of Philosophy
December 2019
令和元年１２月博士（理学）申請

Department of Chemistry, Graduate School of Science,
The University of Tokyo
東京大学大学院理学系研究科
化学専攻

Takahiro Nakama
中 間 貴 寛

Abstract

1. Introduction

Metal-mediated base pairs, which consist of ligand-bearing nucleotides and a bridging metal ion, have gained much attention as functional units of DNA-based supramolecules and nanoarchitectures[1]. For example, hydroxypyridone (**H**) nucleotides form a 2:1 complex with a Cu^{II} ion (**H**–Cu^{II}–**H**) in a DNA duplex[2] and **H**–Cu^{II}–**H** base pairing was utilized for the DNA-templated Cu^{II} assembly[3] and the control of DNA conductivity[4]. In spite of the great potential for metal-dependent regulation of DNA functions, metal-mediated unnatural base pairs have scarcely been applied to metal-responsive DNA materials. This is mainly because chemical synthesis of artificial ligand-bearing oligonucleotides is often cumbersome and time-consuming.

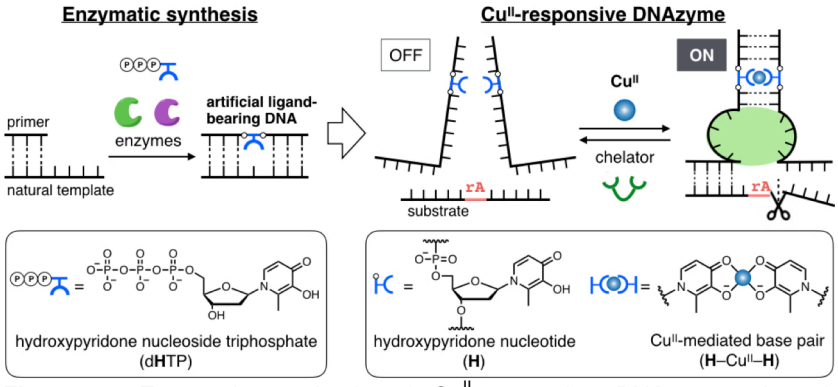

Figure 1. Enzymatic synthesis of Cu^{II}-responsive DNAzymes through incorporation of hydroxypyridone (**H**) nucleotides. rA: adenosine ribonucleotide.

Herein, I report efficient enzymatic methods to synthesize artificial DNA strands containing **H** nucleotides (Figure 1). Enzymatic reactions were expected to incorporate hydroxypyridone nucleoside triphosphate (d**H**TP) under mild conditions without any protecting group of the ligand moiety. I subsequently applied the enzymatic synthesis to develop Cu^{II}-responsive deoxyribozymes (DNAzymes). **H** nucleotides were incorporated into reported DNAzymes so that the formation of one **H**–Cu^{II}–**H** base pair can regulate their catalytic activities.

2. Enzymatic synthesis of artificial ligand-bearing DNA strands

Polymerase incorporation of d**H**TP was first investigated using a natural DNA template. I expected that unnatural **H** nucleotides can be introduced into the opposite site of natural nucleobases through misincorporation by a DNA polymerase. An exonuclease-deficient Klenow fragment (KF exo–) was found to incorporate one d**H**TP in a quantitative manner when the opposite base (X) was A or T.

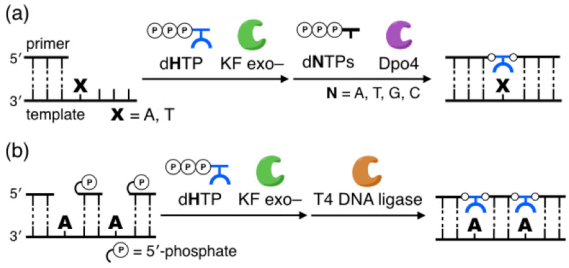

Figure 2. Enzymatic synthesis of artificial DNA strands bearing **H** nucleotides utilizing a natural DNA template. (a) Two-step primer extension using two DNA polymerases. (b) Incorporation of multiple **H** nucleotides using a polymerase and a ligase.

Next, the subsequent primer extension with natural nucleoside triphosphates (dNTPs) was examined to obtain a fully-elongated strand (Figure 2a). However, KF exo– hardly incorporated any dNTPs presumably due to the inhibition of primer elongation by the **H**–X mismatch. In contrast, a lesion bypass DNA polymerase, Dpo4 incorporated dNTPs after the **H** to afford a full-length product in over 90% yield. The product was characterized by MALDI-TOF mass spectrometry and an exonuclease-digestion experiment. This two-step primer extension allowed for the incorporation of a single **H** nucleotide into any sequences to afford **H**-containing DNA strands.

The incorporation of multiple **H** nucleotides was also accomplished using a polymerase and a ligase (Figure

2b). **H** nucleotides were appended to the 3′-ends of DNA strands by KF exo– and the **H**-bearing strands were subsequently connected through ligation by T4 DNA ligase.

In addition, I investigated the enzymatic synthesis of DNA strands containing consecutive **H** nucleotides. Dpo4 polymerase was found to incorporate three consecutive **H** nucleotides with the aid of Mn^{II} ions as a cofactor. **H**-oligomers (e.g. 5′-G**HHH**C-3′) were also enzymatically incorporated into a DNA strand by T4 DNA ligase.

These enzymatic methods enabled the incorporation of **H** nucleotides at prearranged internal positions without any protecting groups by using commercially available enzymes.

3. Development of Cu^{II}-responsive split DNAzymes

DNAzymes are catalytically active DNA molecules and applied to biosensors, logic gates, and molecular machines. Thus, regulation of DNAzyme activities by external stimuli is highly demanded for developing more sophisticated DNA-based systems.

The first Cu^{II}-responsive DNAzyme was developed based on a split design. A known RNA-cleaving DNAzyme (E5 DNAzyme[5], Figure 3a) was divided into two strands, and **H** nucleotides were incorporated into its stem site. The split DNAzyme was expected to restore its catalytic activity upon addition of Cu^{II} ions through the formation of a **H**–Cu^{II}–**H** base pair (Figure 3b). I prepared 11 **H**-bearing DNA stands by the two-step primer extension (Figure 2a) to investigate the optimal position of the **H**–**H** pair. The Cu^{II}-dependent catalytic activity of each DNAzyme was evaluated with an equimolar substrate in the absence and in the presence of one equivalent of Cu^{II} ions. As a result, the highest on/off ratio (~5) was observed with a DNAzyme containing a **H**–**H** at the third position, which is referred to as "split **H**-DNAzyme".

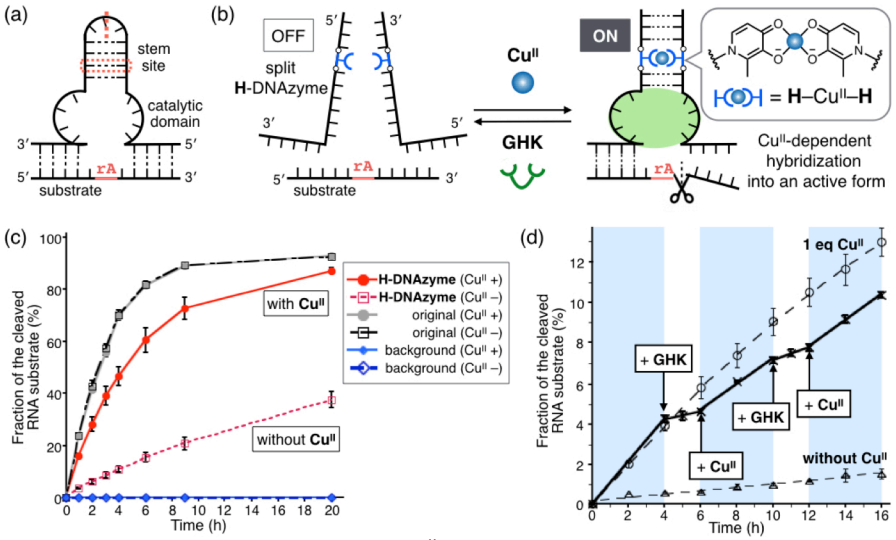

Figure 3. Development of a split Cu^{II}-responsive DNAzyme (**H**-DNAzyme). (a) Original E5 RNA-cleaving DNAzyme. (b) Reversible Cu^{II}-dependent regulation of the DNAzyme activity by the formation of a **H**–Cu^{II}–**H** base pair. (c) RNA-cleaving activity of the split **H**-DNAzyme and the original E5 DNAzyme in the absence and in the presence of one equivalent of Cu^{II} ions. (d) Iterative switching of the activity of the **H**-DNAzyme by the alternate addition of one equivalent of Cu^{II} ions and a Cu^{II}-binding peptide (GHK). [DNAzyme] = 1.0 μM, [substrate] = 10 μM, [$CuSO_4$] = 1.0 μM in 10 mM HEPES (pH 7.0), 1 M NaCl, 10 mM $MgCl_2$, 25 °C. *N* = 3. Error bars indicate standard errors.

The RNA-cleaving activity of the split **H**-DNAzyme was examined with 10 equivalents of the substrate (Figure 3c). The time-course analysis clarified that the split **H**-DNAzyme catalytically cleaved the substrate in the presence of Cu^{II} ions at the 5.5-times higher initial rate than that under the Cu^{II}-free condition. No substrate cleavage was observed with Cu^{II} ions but without any DNAzymes, which evidenced that the DNAzyme activity itself was enhanced by Cu^{II}.

The metal specificity of the split **H**-DNAzyme was examined with 11 kinds of transition metal ions. Among them, only Cu^{II} ions enhanced the activity while the other ions had no effect on the RNA-cleaving reaction.

The reversible regulation of the DNAzyme activity was demonstrated by the addition and removal of Cu^{II} ions. The addition Cu^{II} ions in the course of the reaction immediately increased the RNA-cleaving activity. When a

Cu^{II}-binding peptide (GHK) was added as a chelator, the activity was immediately diminished to almost the same level as that in the absence of Cu^{II} ions. Moreover, the two-cycle switching of the DNAzyme activity was demonstrated by the alternate addition of Cu^{II} ions and the Cu^{II}-binding peptide (Figure 3d).

4. Development of Cu^{II}-responsive single-stranded DNAzymes

第 4 章
本章については、５年以内に論文誌で刊行予定のため、非公開。

5. Multimetal-dependent regulation of DNAzyme activities

Based on its high metal specificity, the split **H**-DNAzyme was applied to metal-dependent orthogonal regulation of DNAzyme activities using well-known Hg^{II}-mediated thymine base pairs (T–Hg^{II}–T) as well as **H**–Cu^{II}–**H** (Figure 5a). A novel Hg^{II}-responsive DNAzyme (T-DNAzyme) was developed by introducing four T–T mismatches into E5 DNAzyme. The metal-dependent activation of **H**-DNAzyme and T-DNAzyme was examined with a mixture of both DNAzymes and their substrates. When one equivalent of Cu^{II} ions was added, the activity of **H**-DNAzyme was enhanced eight-fold while T-DNAzyme showed the same activity (Fig. 5b). On the other hand, the addition of Hg^{II} ions selectively increased the activity of T-DNAzyme. In the presence of both Cu^{II} and Hg^{II} ions, both DNAzymes were activated by two- to three-fold. Furthermore, the selective deactivation of the DNAzymes was also demonstrated by the removal of Cu^{II} or Hg^{II} ions using corresponding chelating agents. In

this way, the orthogonal regulation of the DNAzymes was achieved through the metal-specific formation of **H**–Cu^{II}–**H** and T–Hg^{II}–T base pairs.

A DNAzyme that responds to two metal ions was also developed through the incorporation **H** nucleotides into a reported Ag^{I}-dependent RNA-cleaving DNAzyme[7]. In the absence of Ag^{I} ions, no substrate cleavage was observed. The addition of only Ag^{I} ions but without Cu^{II} ions yielded little cleaved substrate. The activity of the modified DNAzyme was restored only when both Cu^{II} and Ag^{I} ions were added. Therefore, it displayed an AND-gate behavior using the two metal ions as inputs, which is applicable to DNA-based logic gates, multiplexer, and computing circuits.

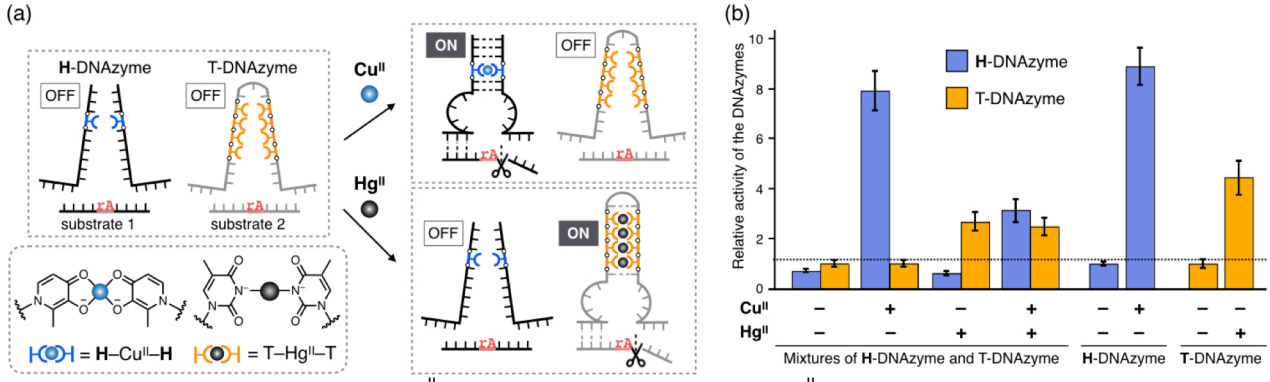

Figure 5. Orthogonal activation of a Cu^{II}-responsive **H**-DNAzyme and a Hg^{II}-responsive T-DNAzyme. (a) Design of the orthogonal activation. (b) Metal-dependent activation of **H**-DNAzyme and T-DNAzyme. Cu^{II} and/or Hg^{II} ions were added to a mixture of **H**-DNAzyme and T-DNAzyme. [**H**-DNAzyme] = [T-DNAzyme] = 1.0 μM, [substrate 1] = [substrate 2] = 2.0 μM, [$CuSO_4$] = 0 or 1.0 μM (1 equiv for **H**–**H**), [$Hg(ClO_4)_2$] = 0 or 4.0 μM (1 equiv for T–T) in 10 mM HEPES (pH 7.0), 1 M $NaNO_3$, 10 mM $Mg(NO_3)_2$, 25 °C, 3 h. *N* ≥ 3. Error bars indicate standard errors. The activities of the individual DNAzymes under the same condition are also shown.

6. Conclusion

In my doctorial study, I have established the enzymatic synthesis of artificial ligand-bearing DNA strands and developed Cu^{II}-responsive DNAzymes. Compared to the conventional chemical synthesis, the enzymatic methods allowed for the protection-free incorporation of hydroxypyridone (**H**) nucleotides without any specialized equipment. Cu^{II}-responsive DNAzymes were synthesized by the enzymatic incorporation of **H** nucleotides. Because Cu^{II} ions rarely interfere with natural nucleotides and selectively bind to **H** nucleotides, the rational designs of metal-responsive DNAzymes were accomplished. The RNA-cleaving activities of both split and single-stranded DNAzymes were reversibly regulated by the formation of one **H**–Cu^{II}–**H** base pair. Moreover, multimetal-dependent regulation of DNAzyme activities was also demonstrated. The Cu^{II}-responsive DNAzymes developed here will be utilized for the metal-triggered control of DNA-based molecular machines and logic gates.

These facile enzymatic methods and design concepts would be applicable to other artificial ligand-bearing nucleotides. Accordingly, this study would provide a powerful tool to develop DNA materials that respond to diverse metal ions.

References

[1] Y. Takezawa *et al.*, *Chem. Lett.* **2017**, *46*, 622–633. [2] K. Tanaka *et al.*, *J. Am. Chem. Soc.* **2002**, *124*, 12494–12498. [3] K. Tanaka *et al.*, *Science* **2003**, *299*, 1212–1213. [4] S. Liu *et al.*, *Angew. Chem. Int. Ed.* **2011**, *50*, 8886–8890. [5] R. R. Breaker *et al.*, *Chem. Biol.* **1995**, *2*, 655–660. [6] D. A. Berry *et al.*, *Tetrahedron Lett.* **2004**, *45*, 2457–2461. [7] J. Liu *et al.*, *Anal. Chem.* **2016**, *88*, 4014–4020.

Abbreviations

A	absorbance
A	adenine
Ac	acetyl
AcOH	acetic acid
AMP	adenosine monophosphate
AP site	apurinic/apyrimidinic site
Asc	ascorbate
ATP	adenosine triphosphate
a.u.	arbitrary unit
BER	base excision repair
bp	base pair
BSA	bovine serum albumin
C	cytosine
ca.	circa
calcd.	calculated
dATP	deoxyadenosine triphosphate
dCTP	deoxycytidine triphosphate
dGTP	deoxyguanosine triphosphate
d**H**TP	hydroxypyridone nucleoside triphosphate
DNA	deoxyribonucleic acid
dNTP	natural deoxynucleoside triphosphates
Dpo4	*Sulfolobus solfataricus* DNA Polymerase IV
DTT	dithiothreitol
dTTP	deoxythymidine triphosphate
ε	molar extinction coefficient
EDTA	ethylenediaminetetraacetic acid
EPR	electron paramagnetic resonance
ESI-TOF	electron spray ionization
FAM	6-carboxyfluorescein
FRET	fluorescence resonance energy transfer
G	guanine
GHK	glycine-histidine-lysine

H	hydroxypyridone
HEPES	4-(2-hydroxyethyl)-1-piperazineethanesufonic acid
HPA	hydroxypicolinic acid
HPLC	high performance liquid chromatography
HSAB	hard-soft acid-base
KF exo–	Klenow fragment of DNA polymerase I (3′→5′ exo–)
M	molar
MALDI	matrix assisted laser desorption ionization
MeCN	acetonitrile
MS	mass spectrometry
m/*z*	mass-to-charge ratio
obs.	observed
PAGE	polyacrylamide gel electrophoresis
PC	pyrrolocytosine
PCR	polymerase chain reaction
PEG	polyethylene glycol
Phos	5′-phosphate
PNK	polynucleotide kinase
rA	adenosine ribonucleotide
RNA	ribonucleic acid
T	thymine
TdT	terminal deoxynucleotidyl transferase
TEAA	triethylammonium acetate
T_m	melting temperature
TOF	time-of-flight
tpy	terpyridine
Tris	tris(hydroxymethyl)aminomethane
U	uracil
UV	ultraviolet
Vis	visible
XNA	xeno nucleic acid

Contents

Chapter 1.

General Introduction

1-1. DNA supramolecular chemistry

DNA (Deoxyribonucleic acid) is generally perceived as a carrier of genetic information. DNA is a polymer of deoxyribonuleotides which consist of a deoxyribose, a phosphate group, and a nucleobase (Figure 1-1a). Four natural nucleobases, adenine (A), cytosine (C), guanine (G), and thymine (T) selectively form two types of Watson–Crick base pairs through hydrogen bonding, A–T and G–C (Figure 1-1b). The complementary base pairing leads to the formation of the DNA double-helical structure based on its sequence information (Figure 1-1c). This elgant suparamolecular structure relies not only on the hydrogen bonding between the base pairs, but also on stacking of nucleobases, eletrostatic interactions, and hydrophobic effects in water.[1] Mismatch pairs other than A–T and G–C significantly decrease the thermal stability of a DNA duplex, resulting in the selectivle hybridization to a complementry DNA strand. This sequence-spefiic assembly allows for the construction of well-organized supramolecular structures. Therefore, DNA has attracted much attention in the fields of supramolecular chemistry and nanotechnology.

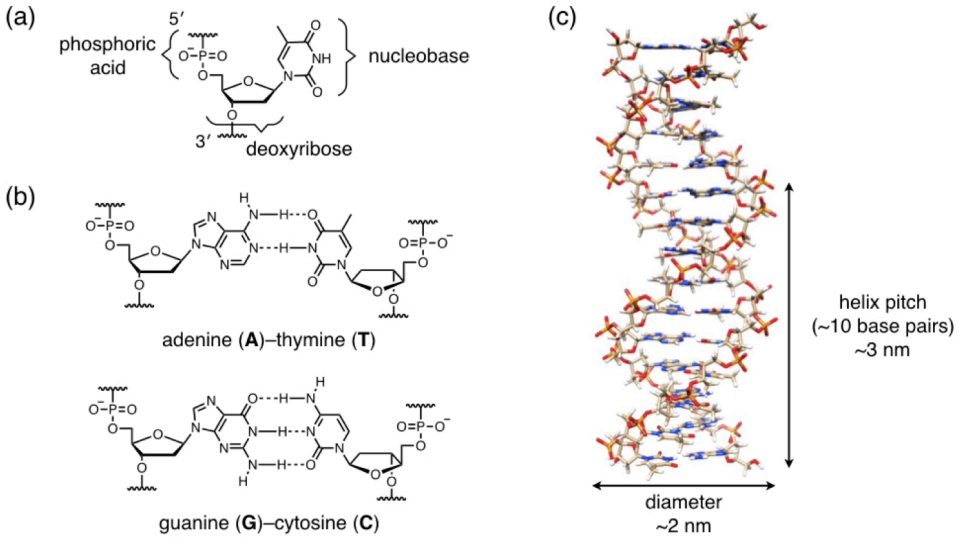

Figure 1-1. Structures of a nucleotide (a), Watson–Crick base pairs (b), and a DNA duplex (c).

Since Seeman proposed a concept of "DNA nanotechnology,"[2] a variety of sophisticated DNA structures have been fabricated.[3] Seeman et al. constructed a DNA cubic structure by designing sequences of DNA juncitons (Figure 1-2a).[4] Rosemund established a method to fabricate 2D nanostructures called DNA origami (Figure 1-2b).[5] New strategies have been extensively explored

for the construction of larger structuers, including 3D nanostructures, with atomic-scale control.[6] The highly ordered structures have provided many novel applications in nanotechnology. For example, Dietz et al. contorlled the distance between two molecules with ångström precision by adjusting the angle of a DNA hinge structure (Figure 1-2c).[7] Dietz, Simmel et al. constructed a DNA membrane channel, which was further applied to single-molecule analysis (Figure 1-2d).[8]

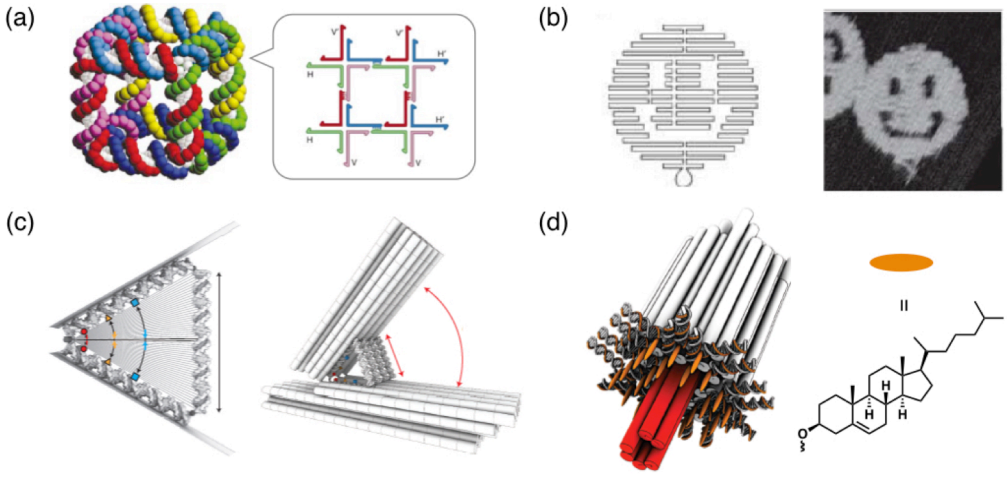

Figure 1-2. DNA nanoarchitectures and their applications. (a) A DNA cubic nanostructure. Reproduced from ref. [4]. Copyright 1991 Nature Publishing Group. (b) A DNA origami nanostructure. Reprinted from ref. [5]. Copyright 2006 Nature Publishing Group. (c) A DNA device that places molecules with ångström precision. Reprinted from ref. [7]. Copyright 2016 Nature Publishing Group. (d) A DNA membrane channel. The end of architecture was modified with cholesterol to insert lipid bilayer. Reproduced from ref. [8]. Copyright 2012 American Association for the Advancement of Science.

DNA also allows for the development of supramolecular assemblies, in which each component is precisely arranged based on DNA sequneces and structures.[9] Sleiman et al. fabricated DNA polygons and placed different gold nanoparticles in precise location through DNA hybridizaiton to the construct (Figure 1-3a).[10,11] Mirkin et al. constructed assemlies of nanoparticles in different lattice strucutres with a careful design of linker DNA strands (Figure 1-3b).[12,13] Accordingly, sequence-specfic assembly of DNA strands enbles the construction of supramolecular structures composed of well-organized molecules and nanomaterials.

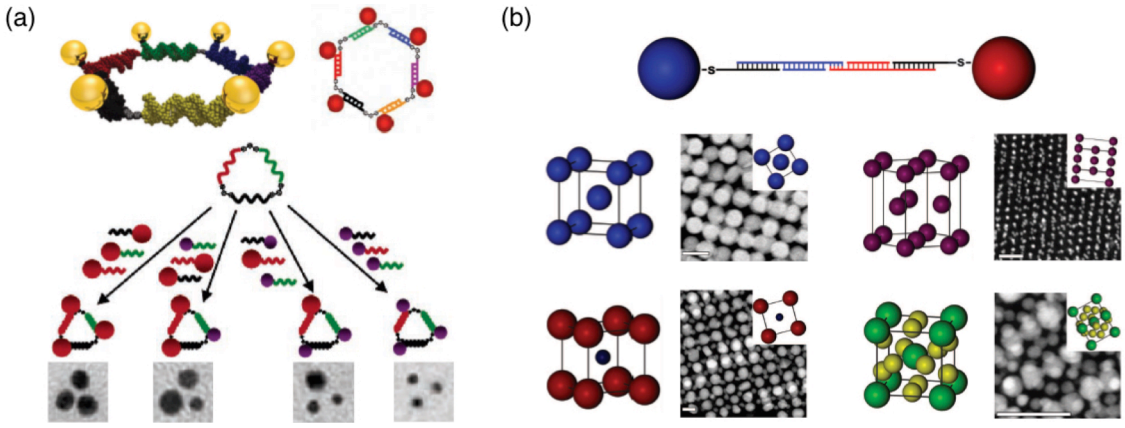

Figure 1-3. DNA-guided assembly of nanoparticles. (a) Assembly of gold nanoparticles on DNA polygons. Reproduced from [10] and [11]. Copyright 2006 Wiley-VCH and 2007 American Chemical Society. (b) DNA-mediated assembly of nanoparticles in different lattice patterns. Reprinted from ref. [13]. Copyright 2011 American Association for the Advancement of Science.

For the functionalization of these DNA-based supramolecular structures and assemblies, the dynamic control by external stimuli is of great importance. The strand displacement reaction, which triggers strand exchange through toehold-mediated hybridization, can afford dynamic functions using DNA strands as inputs (Figure 1-4a).[14,15] By exploiting this reaction, a variety of DNA-based nanoswitches, nanodevices, and molecular machines have been constructed. Turberfield et al. developed a DNA nanoswitch, which opened and closed repetitively through the DNA strand displacement reactons (Figure 1-4b).[16] Gothelf, Kjems et al. applied the strand displacement to open a lid of a DNA nanobox by adding oligonucleotides as extenal stimuli (Figure 1-4c).[17] Pierce et al. developed a molecular machine called a DNA walker, which moves unidirectonally on a DNA track driven by the strand displacement reactions (Figure 1-4d).[18] In a similar manner, many DNA-based molecular machines have been fabricated by employing the strand displacement reaction.[19]

The strand displacement reaction can be also applied to molecular computing circuits.[14,15,20,21] For instance, an AND logic gate can be constructed by designing the successive strand displaement reactions that proceed only when two input DNA strands are added (Figure 1-5a).[14] Winfree et al. develoeped logic circuits consisting of more than 100 DNA strands.[20] The complex system allowed for the dynamic circuits that yielded oscillatory signlas (Figure 1-5c).[21]

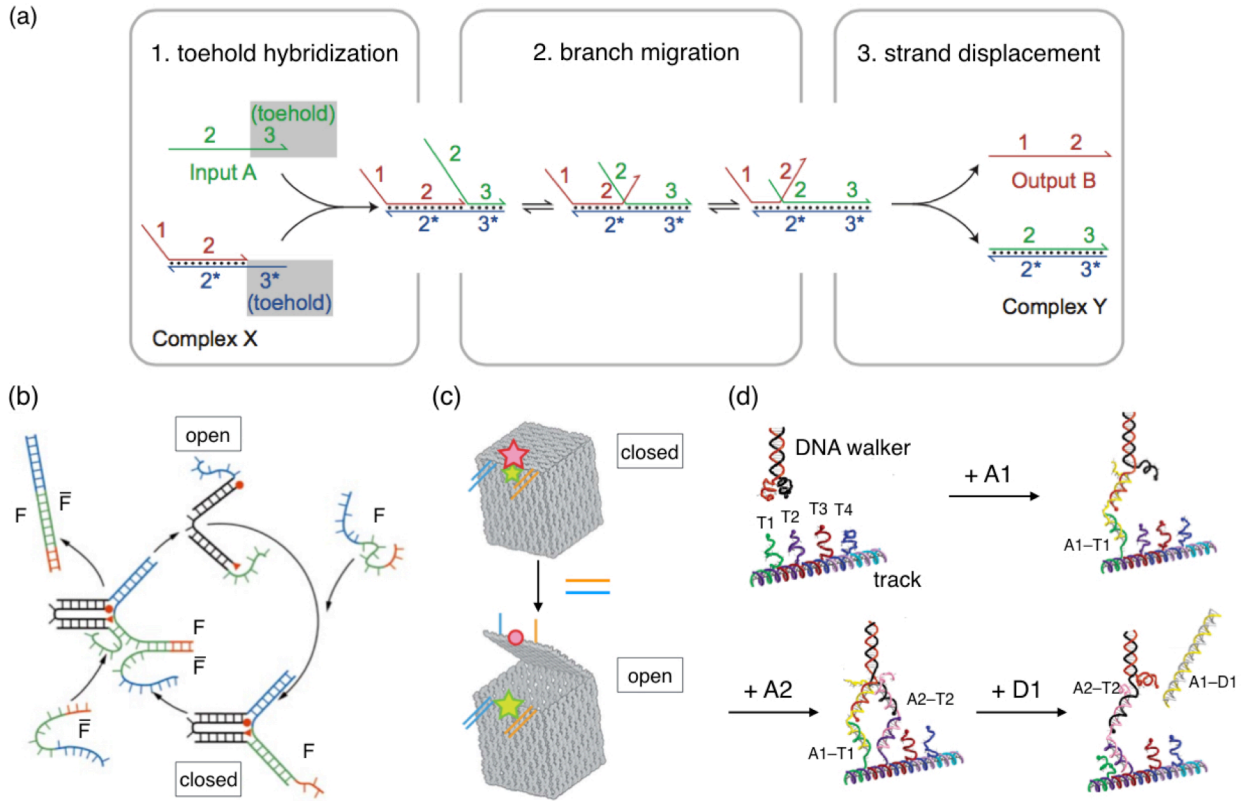

Figure 1-4. Strand displacement reaction and its applications. (a) Schematic representation of processes in the strand displacement reaction. Reprinted from ref. [14]. Copyright 2011 Nature Publishing Group. (b) DNA tweezers that change their structure by the strand displacement reaction. Reproduced from ref. [16]. Copyright 2000 Nature Publishing Group. (c) A DNA nanobox that opens through the strand displacement. Reproduced from ref. [17]. Copyright 2009 Nature Publishing Group. (d) A DNA walker that unidirectionally moves driven by the strand displacement reactions. Reproduced from ref. [18]. Copyright 2004 American Chemical Society.

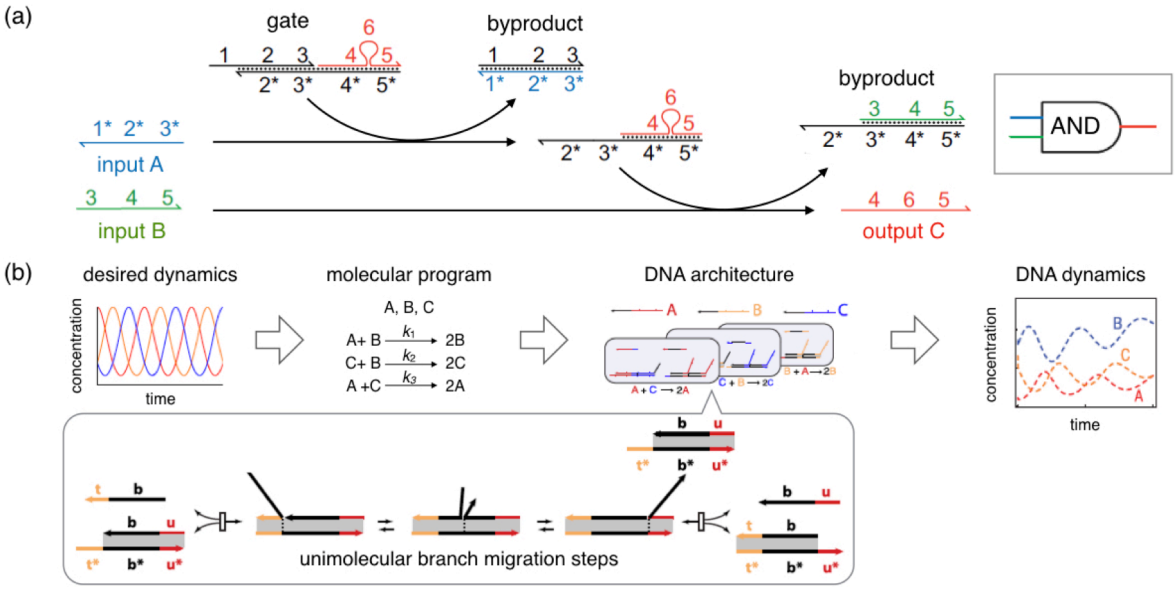

Figure 1-5. DNA logic gates and computing circuits based on the strand displacement reactions. (a) Schematic representation of a DNA-based AND logic gate utilizing the strand displacement. Reproduced from ref. [14]. Copyright 2011 Nature Publishing Group. (b) A DNA dynamic circuit that exhibits oscillatory signals. Reproduced from ref. [21]. Copyright 2017 American Association for the Advancement of Science.

Accordingly, DNA provides a robust platform for the developement of supramolecules and nanoarchitechtures based on its sequence-specific assembly. To fabricate more functionalized materials, new methods to dynamically control DNA supramolecules by external stimuli are highly demanded, not limited to the strand displacement reaction. Such stimulus-rsponsive DNA supramolecules can be developed through the incorporation of DNAzymes, the functionalization by chemical modifications, and the use of metal-mediared artificial base pairing, which will be discussed later.

1-2. Deoxyribozymes (DNAzymes)

DNA molecules can act not only as frameworks of supramolecules and nanoarchitectures but also as their functional cores. Some DNA strands with a given sequence are known to possess a unique function such as binding ability to a target molecule (i.e. DNA aptamer).[22,23] Among them, deoxyribozymes or DNAzymes, which can catalyze a chemical reaction, have attracted much attention.[24] After Breaker and Joyce found the first DNAzyme that cleaves RNA strands,[25] many DNAzymes have been discovered by means of in vitro selection.[26]

An overview of the in vitro selection method is depicted in Figure 1-6. A pool of oligonucleotides with a randomized sequence is subjected to a selection process in the presence of a cofactor to find out sequences that can catalyze a target reaction. After treating the pool under a specific reaction condition, only catalytically active species are released from the solid support, thus separated from inactive DNA strands. The recovered active DNA strands are amplified by PCR and then used for the next cycle of screening. As the number of the cycles increases, more active DNA molecules predominantly remain. DNAzymes with different catalytic activities can be obtained by changing the selection conditions.

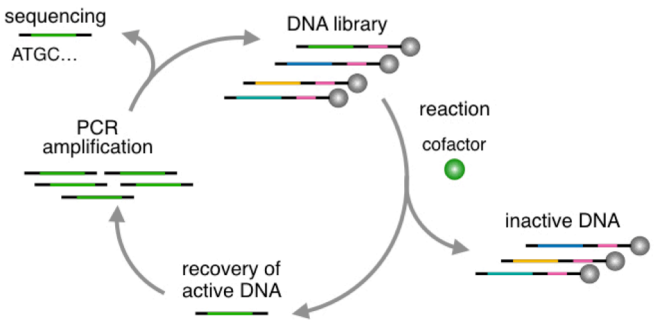

Figure 1-6. Overview of the in vitro selection method to discover DNAzymes.

The selection method has afforded numerous DNAzymes that catalyze various kinds of chemical reactions (Figure 1-7). As well as the first report,[25] many groups discovered RNA-cleaving DNAzymes, which can cleave a phosphodiester bond of an RNA substrate at a specific position (Figure 1-7a).[27] The DNAzymes induce the intramolecular nucleophilic attack of 2′-oxygen on the adjacent phosphate group with the aid of a cofactor (Figure 1-7b).[28] Some

DNAzyme can also promote DNA cleavage via an oxidative and hydrolysis mechanism.[29,30] Szostak et al. found E47 DNAzyme that ligates DNA strands by jointing 5′-hydroxy and 3′-phosphorimidazolide groups (Figure 1-7c).[31] Particular G-quadruplex DNA sequences can bind to hemin and the resulting complexes show a peroxidase-like activity to oxidize small-molecules (Figure 1-7d).[32] This DNAzyme reaction has been often utilized for colorimetric assays using chromogenic substrates such as ABTS (2,2'-azino-bis(3-ethylbenzothiazoline-6-sulfonic acid).[33] DNAzymes can also catalyze other chemical reactions including phosphorylation,[34] hydrolysis of ester bonds,[35] and Diels–Alder reaction.[36]

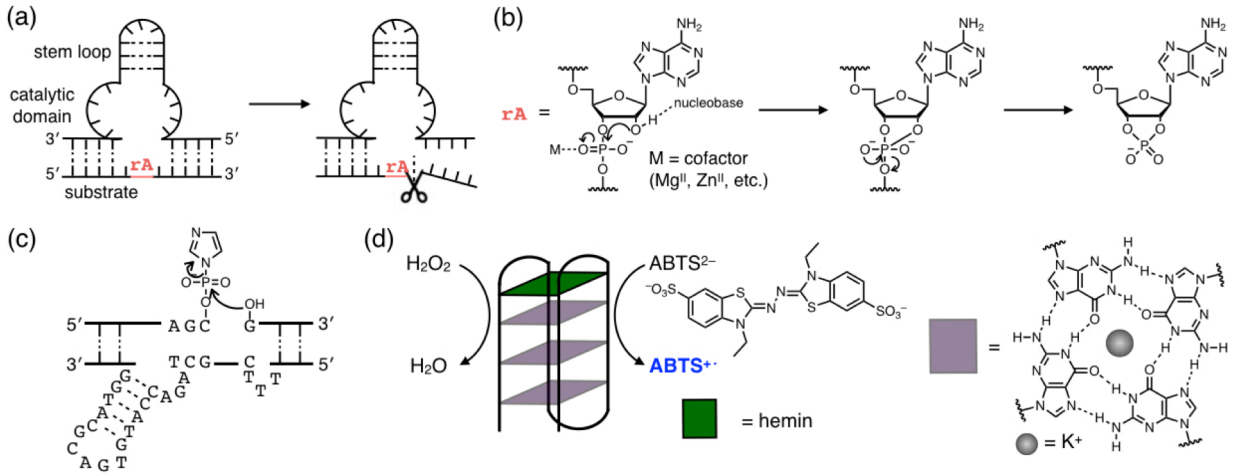

Figure 1-7. Examples of DNAzymes. (a) RNA-cleaving DNAzyme. (b) Proposed mechanism of the RNA-cleaving reaction by DNAzymes. (c) DNAzyme with a DNA ligase activity. (d) Peroxidase-mimicking G-quadruplex DNAzyme.

Although the mechanisms of most DNAzyme reactions have been poorly understood, two crystal structures of DNAzymes have been recently reported.[37,38] The structure of 8–17 RNA-cleaving DNAzyme (Figure 1-8) validates that folding of the DNAzyme and the resulting intrinsic tertiary interactions are essential for the RNA hydrolysis.[38]

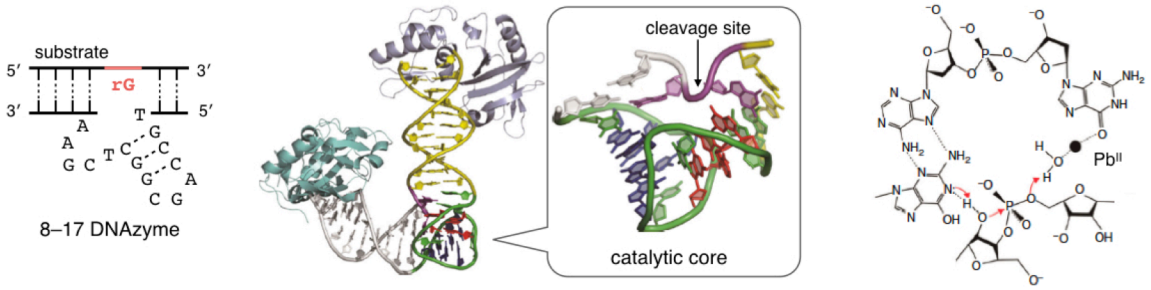

Figure 1-8. Crystal structure of 8–17 RNA-cleaving DNAzyme. Proposed mechanism based on the crystal structure is also shown. Reproduced from ref. [38]. Copyright 2017 Nature Publishing Group.

DNAzymes have been widely utilized as functional units in the fields of DNA supramolecular chemistry and nanotechnology. They have been applied to biosensors,[23,39] therapeutic agents,[40] and tools for oligonucleotide synthesis.[41] One of the most promising applications is a functional element in DNA computing circuits.[42] Chemical reactions catalyzed by DNAzymes can often generate output signals detectable by spectroscopic methods. When the output is an oligonucleotide, the output signal can be transferred to the following DNA-based systems as an input, thus resulting in cascade reactions for computing circuits. Up to now a great number of logic gates, multiplexers, and computing circuits have been constructed using DNAzymes as key components. For instance, Stojanovic et al. developed logic gates by introducing DNA-binding sites into an RNA-cleaving DNAzyme (Figure 1-2-4a).[43,44] Only when correct input oligonucleotides were added, the DNAzyme cleaved a fluorophore-labeled substrate, thus yielding a FRET signal as an output. Willner et al. demonstrated cascade gate systems with the use of several DNAzymes in the same

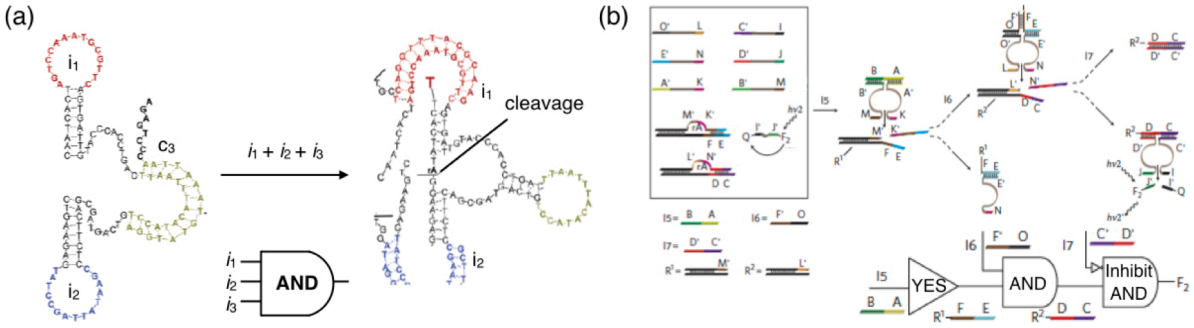

Figure 1-9. DNAzyme-based logic gates and computing circuits. (a) An AND-gate DNAzyme that responds to three input oligonucleotides. Reproduced from ref. [44]. Copyright 2006 American Chemical Society. (b) A logic gate cascade composed of three RNA-cleaving DNAzymes. Reproduced from ref. [45]. Copyright 2010 Nature Publishing Group.

solution (Figure 1-9b).[42,45,46] After the cleavage of the substrates by the DNAzymes, the released strands transferred the output signal to the following logic gates, which enabled the complex computing circuits.

Chemical reactions by DNAzymes can be also utilized as a power source of DNA-based molecular machines. Mao et al. developed a DNA motor[47] (Figure 1-10a) and a DNA walker[48] (Figure 1-10b) by exploiting RNA-cleaving DNAzymes. These DNA machines autonomously moved by consuming RNA substrates. Yan et al. demonstrated that DNA walkers can unidirectionally move along the defined pathway on DNA origami architectures.[49] Liu et al. applied DNA walkers to multistep chemical synthesis (Figure 1-10c).[50] Different substrates were attached on a DNA track, and the amino group on a DNA walker sequentially reacted with the substrates while the walker moved in a unidirectional way.

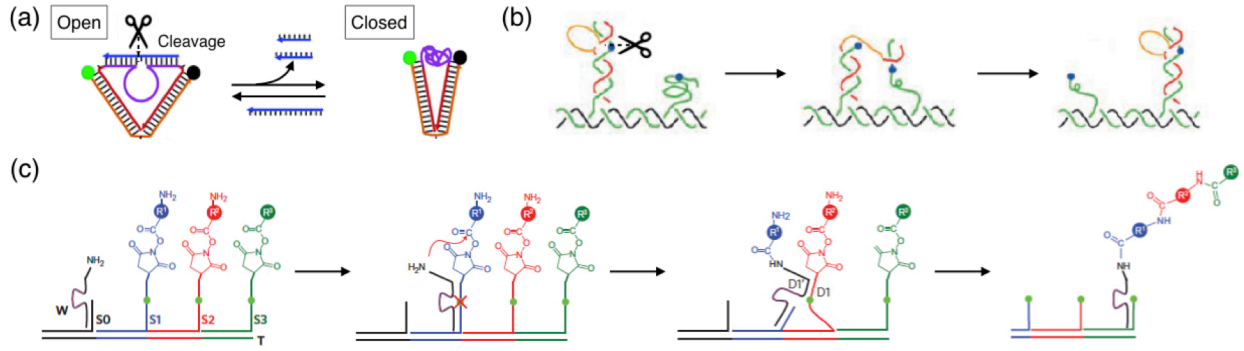

Figure 1-10. DNAzyme-based molecular machines. (a) An autonomous DNA molecular motor using an RNA-cleaving DNAzyme. Reproduced from ref. [47]. Copyright 2004 Wiley-VCH. (b) A DNA walker that moves along the DNA track fueled by cleavage of RNA substrates. Reproduced from ref. [48]. Copyright 2005 Wiley-VCH. (c) Autonomous multistep organic synthesis mediated by a DNA walker. Reprinted from ref. [50]. Copyright 2010 Nature Publishing Group.

Collectively, DNAzymes play essential roles in DNA-based nanotechnology and supramolecular chemistry. Regulation of DNAzyme activities allows for the development of stimulus-responsive DNAzymes, which would lead to novel applications in the fields of DNA supramolecular chemistry and nanotechnology.

1-3. Stimuli-responsive DNA systems

Toward functionalization of DNA materials, numerous stimuli-responsive DNA systems have been developed.[51] Regulation of DNA structures and functions by external stimuli can provide dynamic properties, thus allowing for the fabrication of DNA-based nanodevices and molecular machines.[52] Stimuli-responsive systems composed of natural DNA strands can be constructed by exploiting the strand displacement reaction,[14,15] self-assembly of high-order DNA structures,[53–55] and by inserting sequences of functional DNAs such as aptamers and DNAzymes.[23,56] Furthermore, chemical modification can impart responsiveness toward a variety of external stimuli.[57]

One of the most basic approaches is the use of oligonucleotides as external stimuli based on the strand displacement reactions.[14,15] For example, Seeman et al. developed stimuli-responsive DNA crystals by introducing a toehold region into each unit junction structure (Figure 1-11a).[58] By adding fluorophore-labeled strands, the crystal color changed through the strand displacement reaction. Gracias, Schulman et al. fabricated DNA hydrogels that swelled up by 100 fold in response to the addition of DNA strands (Figure 1-11b).[59] The strand displacement polymerization at the specific DNA crosslinks enabled the sequential shape changes of the hydrogel.

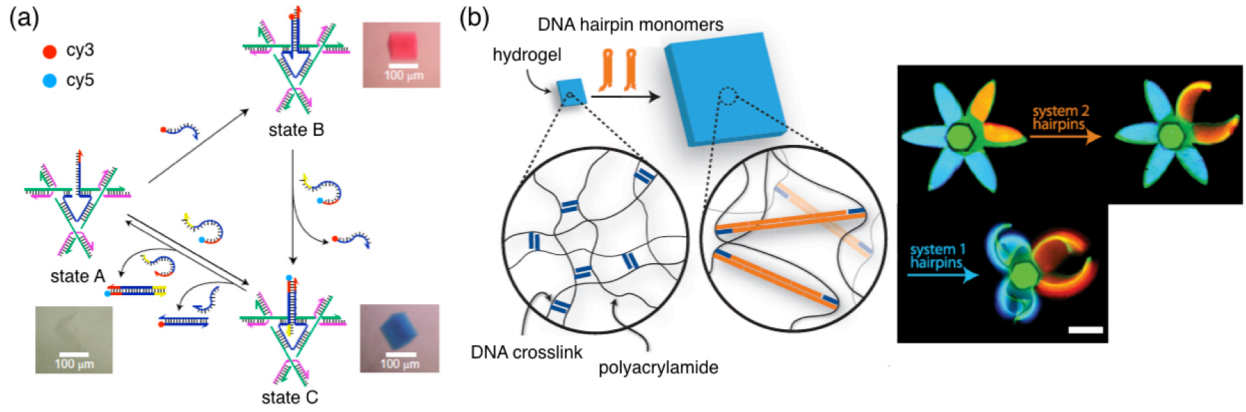

Figure 1-11. Stimulus-responsive DNA materials utilizing oligonucleotides as external stimuli. (a) A DNA crystal that changes its color in repose to additional oligonucleotides. Reprinted from ref. [58]. Copyright 2017 Nature Publishing Group. (b) A DNA hydrogel that drastically swells up upon addition of DNA hairpin strands. Reprinted from ref. [59]. Copyright 2017 American Association for the Advancement of Science.

Some DNA high-order structures, such as triplex[53] and i-motif,[54] are formed in a pH-dependent manner. Thus, natural DNA strands with a specific sequence can respond to pH

changes. Ricci et al. constructed DNA nanoswitches in response to different pH ranges (Figure 1-12a).[60] The pH responsiveness was tuned by changing the relative contents of C^+·G–C and T·A–T base triplets. Famulok et al. developed a prototype of proton-fueled DNA molecular machines by incorporating i-motif sequences into DNA rings (Figure 1-12b).[61] Folding into i-motif triggered dimerization of the DNA rings, thus realizing the pH-responsive switching motion.

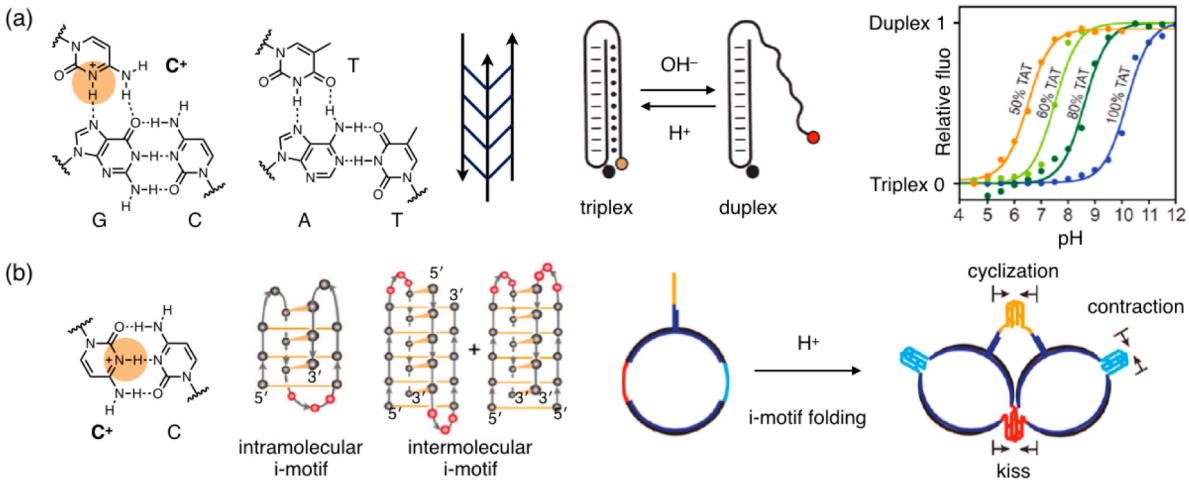

Figure 1-12. pH-Responsive DNA switches based on high-order DNA structures. (a) Triplex-based DNA nanoswitches that respond to different pH ranges. Reproduced from ref. [60]. Copyright 2014 American Chemical Society. (b) A pH-responsive DNA ring that forms a dimer through the i-motif formation. Reproduced from ref. [61]. Copyright 2013 American Chemical Society.

Aptamers, which bind to a specific target, have been extensively exploited for the development of stimulus-responsive DNA systems.[23,56] The incorporation of aptamer sequences can endow DNA molecules with responsiveness to various small molecules. Lu et al. fabricated a DNA-based

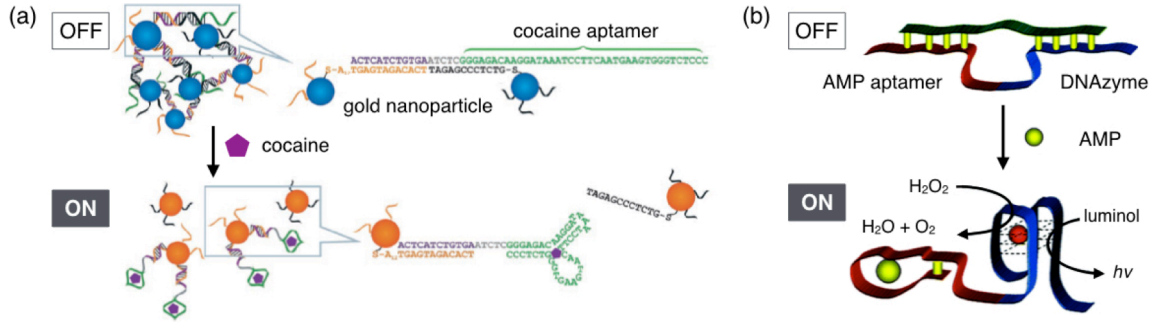

Figure 1-13. Aptamer-based DNA sensors in response to small molecules. (a) A cocaine-sensor using the gold nanoparticles functionalized with a DNA aptamer. Reproduced from ref. [62]. Copyright 2006 Wiley-VCH. (b) An aptamer–DNAzyme conjugate that detects adenosine monophosphate (AMP). Reproduced from ref. [63]. Copyright 2007 American Chemical Society.

colorimetric sensor by functionalizing gold nanoparticles with a cocaine aptamer (Figure 1-13a).[62] Upon binding to cocaine, the aptamer strands dissociated the aggregate of gold nanoparticles, resulting in the color change of the solution. Willner et al. synthesized a conjugate of a DNA aptamer and a DNAzyme for the detection of adenosine monophosphate (AMP) (Figure 1-13b).[63] The aptamer binding to AMP triggered the dissociation of the DNAzyme from a complementary strand, thus restoring its peroxidase-mimicking activity.

DNA molecules can also respond to macromolecules such as proteins. Church et al. developed a DNA transporter that releases molecular cargoes in response to antigens through the aptamer binding (Figure 1-14a).[64] Ricci et al. fabricated a DNA molecular machine that responds to an antibody (Figure 1-14b).[65] They attached antigens to the ends of DNA triplexes, which released a cargo DNA strand upon binding to an antibody.

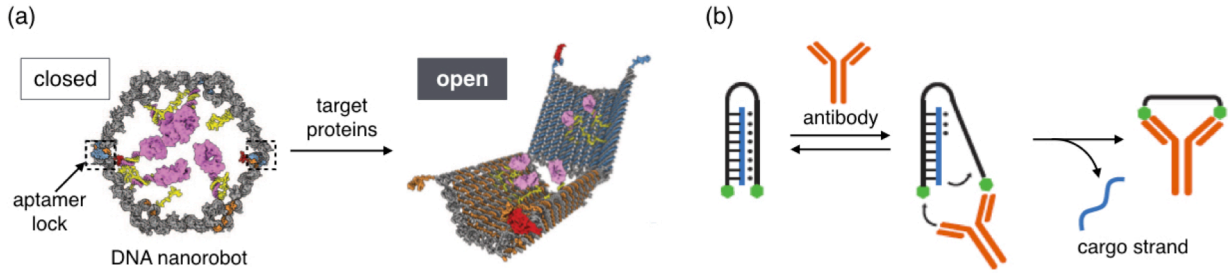

Figure 1-14. Protein-responsive DNA molecular machines. (a) A DNA transporter that can release molecular payloads in response to antigens. Reproduced from ref. [64]. Copyright 2012 American Association for the Advancement of Science. (b) A DNA nanomachine that can release a cargo DNA strand in response to antibody. Reproduced from ref. [65]. Copyright 2017 Nature Publishing Group.

Light has been often utilized as external stimuli to control DNA molecular systems.[66] As natural DNA molecules are not responsive to light, it is necessary to introduce unnatural functionalities for the construction of photo-responsive DNA systems. Asanuma, Komiyama et al. developed azobenzene-bearing nucleic acid monomer with a threoninol linker, which can control the hybridization of DNA duplexes through the *trans–cis* isomerization (Figure 1-15a).[67] Liang, Asanuma et al. utilized the azobenzene derivative for the development of a photo-responsive DNAzyme (Figure 1-15b).[68] Kuzyk, Liu et al. introduced the azobenzene into a DNA architecture with gold nanorods to control the plasmonic circular dichroism by light (Figure 1-15c).[69]

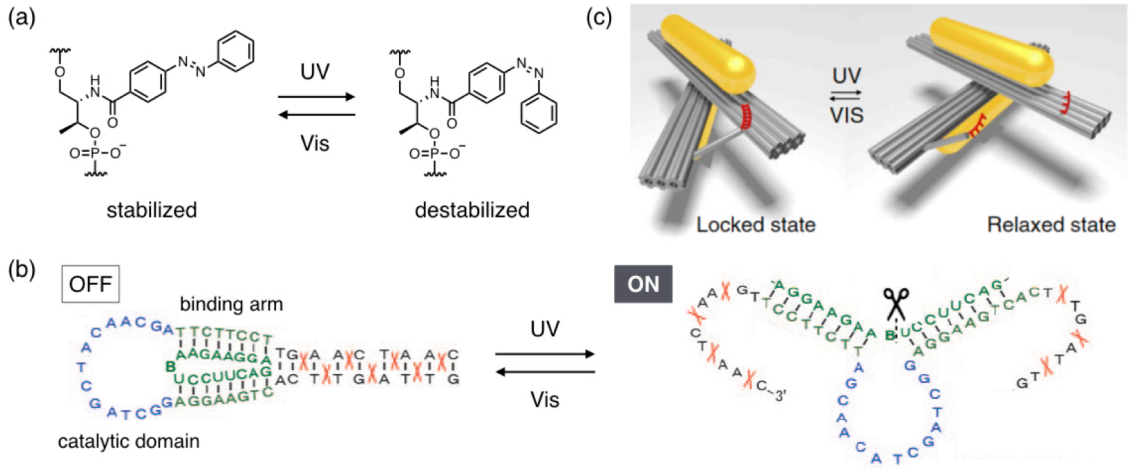

Figure 1-15. Photo-responsive DNA systems. (a) *Trans–cis* isomerization of the azobenzene moiety modified on DNA through a threoninol linker.[67] (b) A photo-responsive DNAzyme. The DNAzyme activity was regulated through the *trans–cis* isomerization of the azobenzene moieties. Reproduced from ref. [68]. Copyright 2010 Wiley-VCH. (c) A photo-responsive DNA plasmonic system using the azobenzene derivative. Reprinted from ref. [69]. Copyright 2016 Nature Publishing Group.

Metal-responsive DNA molecules have been developed by incorporating metal coordinating sites into oligonucleotides. The use of metal ions as external stimuli provides the following advantages. (i) Metal complexes form coordination bonds which are generally stronger than hydrogen bonds. Thus, the thermal stability of DNA structures can be controlled in a metal-dependent manner, allowing for the regulation of DNA functions. (ii) Reversibility of metal complexation can be utilized for the control of DNA system. The addition and removal of metal ions would regulate functions of DNA molecules in a reversible manner. (iii) Each metal ion can work as an external stimulus that binds to a ligand site with distinct affinity, stability, and kinetics. These properties also depend on the oxidation states of the metal ions. (iv) Some metal ions can offer responsiveness toward other stimuli such as light and redox agents.

Figure 1-16 shows examples of metal-responsive DNA supramolecules containing artificial ligand sites. Sleiman et al. incorporated terpyridine (tpy) and/or diphenylphenanthroline (dpp) ligands into DNA duplexes as a metal binding site (Figure 1-16a).[70] The ligands bind to metal ions inside the duplex with different affinity, and the DNA structures are thermally stabilized. Our group utilized a bipyridine-modified nucleotide (U_{bpy}) for the metal-dependent stabilization of three-way

junction structures,[71] which was applied to metal-triggered DNA structure conversion between duplexes and the junction structures (Figure 1-16b).[72] Ihara et al. demonstrated allosteric regulation of a peroxidase-mimicking activity of a G-quadruplex DNAzyme by metal complexation with terpyridine ligands (Figure 1-16c).[73] Clever et al. also controlled G-quadruplex structures and their thrombin binding ability through the metal complexation of pyridine ligands (Figure 1-16d).[74,75]

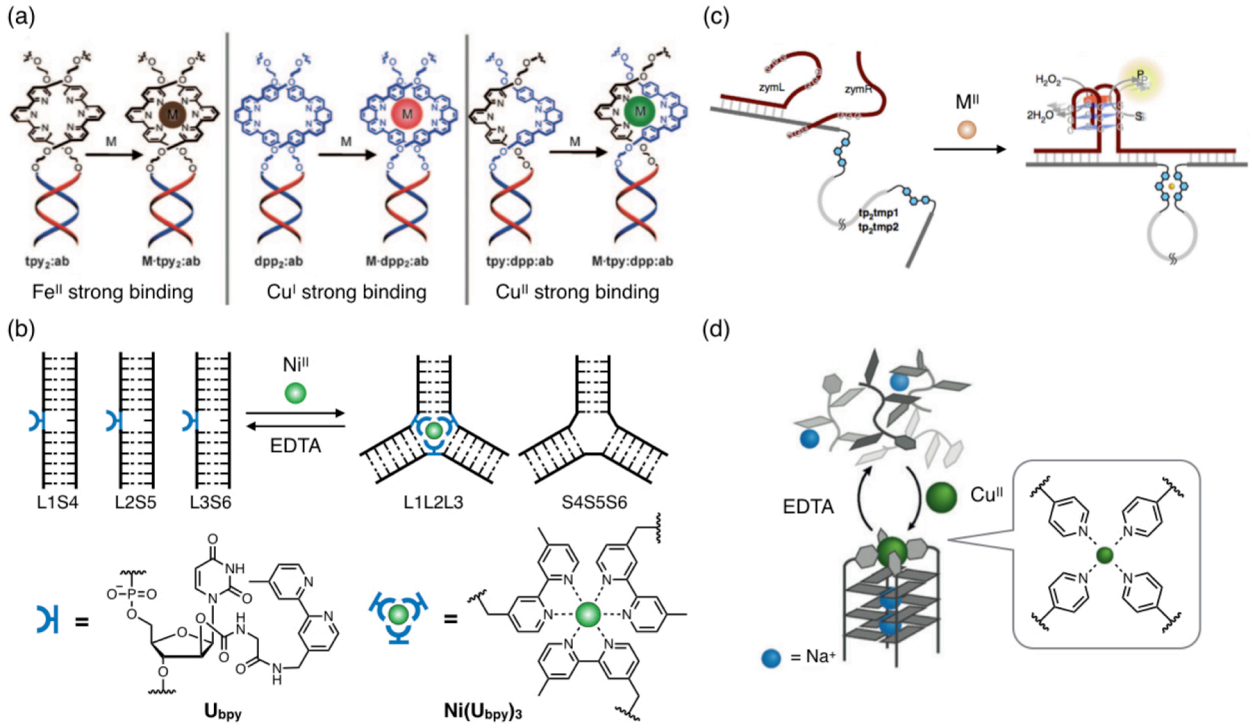

Figure 1-16. Metal-responsive DNA supramolecules. (a) Thermal stabilization of DNA duplexes containing terpyridine (tpy) and/or diphenylphenanthroline (dpp) with different metal affinity. Reproduced from ref. [70]. Copyright 2009 Wiley-VCH. (b) Metal-triggered DNA structure conversion between duplexes and three-way junctions. (c) Allosteric regulation of peroxidase-mimicking DNAzyme activity by metal complexation with tpy ligands. Reproduced from ref. [73]. Copyright 2015 Nature Publishing Group. (d) Cu^{II}-dependent formation of a pyridine-modified G-quadruplex. Reproduced from ref. [74]. Copyright 2013 Wiley-VCH.

Accordingly, metal-responsive DNA molecules are highly promising for the fabrication of sophisticated DNA-based systems. It is of great importance to develop versatile methodology to endow DNA molecules with metal-responsiveness.

1-4. Metal-mediated base pairing

As discussed in the section 1-3, the incorporation of metal cooridination sites is one of the most promising methods to develop stimulus-responsive DNA materials. Our group has firstly develoeped metal-mediated artificial base pairs,[76] which are composed of a pair of ligand-type nucleotides and a bridging metal ion.[77] Ligand-type nucleotides bind to a metal ion inside a DNA duplex, and the resulting metal-coordination bonding increases the thermal stability of the duplex. For example, unnatural ligand-type, hydroxypyridone (**H**) nucleotides form a Cu^{II}-mediated base pair (**H**–Cu^{II}–**H**) through 2:1 complexation with Cu^{II} ions in a square-planar geometry (Figure 1-17).[78] The formation of **H**–Cu^{II}–**H** base pair was confirmed by UV spectroscopy, duplex melting analysis, and electron paramagnetic resonance (EPR) measurement. A **H**–Cu^{II}–**H** base pair quantitatively forms at micromolar concentrations, which greatly stabilizes a DNA duplex and increases the melting temperature (T_m) by 13 °C in a typical case.

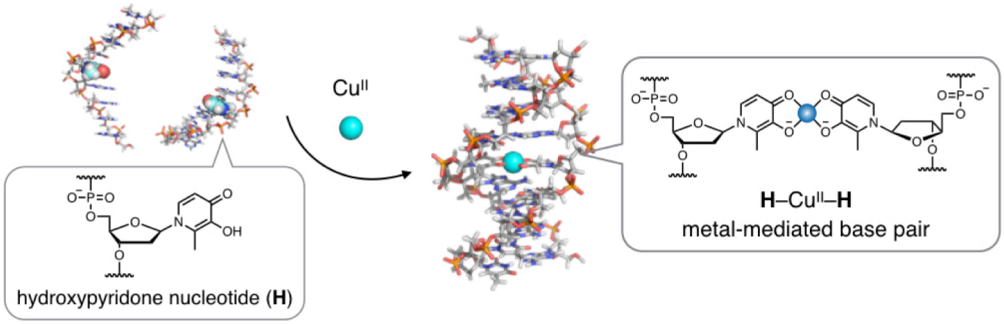

Figure 1-17. Cu^{II}-mediated hydroxypyridone (**H**) base pair (**H**–Cu^{II}–**H**). The formation of a **H**–Cu^{II}–**H** base pair stabilizes a DNA duplex, thus inducing the hybridization of DNA strands.

Many types of metal-mediated base pairs have been reported thus far with the use of various metal ions.[76] Shultz et al. developed a Cu^{II}-mediated heterobase pair with a pyridine (**Py**) nucleotide and a pyridine-2,6-dicarboxylate (**Dipic**) nucleotide as one of pioneering works (Figure

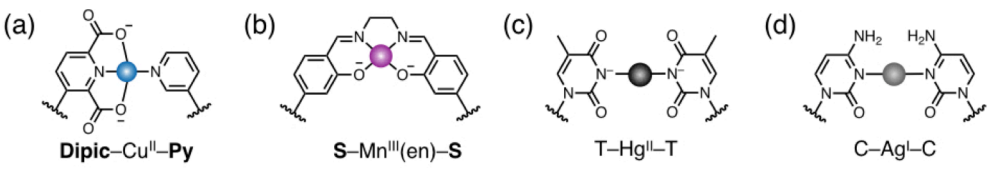

Figure 1-18. Chemical structures of metal-mediated base pairs. (a, b) Metal-mediated base pairs composed of unnatural ligand-type nucleotides. (c, d) Metal-mediated base pairs with natural nucleobases.

1-18a).[79] Carell et al. reported a Mn^{III}- or Cu^{II}-mediated salen base pair, which gretly stabilized a DNA duplex through metal complexation and crosslinking by enthylenediamine (en) (Figure 1-18b).[80] Natural pyrimidine nucleobases T and C can serve as a metal ligand to form a Hg^{II}- and a Ag^{I}-mediated base pairs, respectively (T–Hg^{II}–T[81] and C–Ag^{I}–C[82]; Figures 1-18c and 1-18d).

Metal-mediated base pairing provided attractive physicochemical properties especially when metal ions were arrayed inside a DNA duplex (Figure 1-19). Our group constructed a metal array with five Cu^{II} ions by using **H**–Cu^{II}–**H** base pairing, which exhibited ferromagnetic coupling (Figure 1-19a).[83] Carell et al. observed antiferromagnetic coupling between two Cu^{II} ions arrayed with **S**–Cu^{II}(en)–**S** base pairs (Figure 1-19b).[84] **H**–Cu^{II}–**H** base pairing was also exploited for controlling the electrical conductivity of DNA duplexes (Figure 1-19c).[85] It is expected that unique DNA materials will be developed from long metal arrays with the use of ligand-type nucleotides, including heterogeneous metal arrays[86] and arrays in the crystalline state.[87]

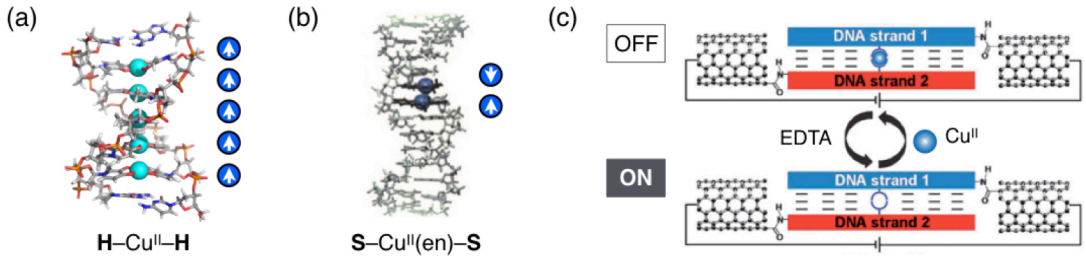

Figure 1-19. (a, b) Schematic representation of magnetic properties of Cu^{II} arrays assembled by metal mediated base pairs. Reproduced from ref. [83] and [84]. Copyright 2003 American Association for the Advancement of Science (a) and 2010 Wiley-VCH (b). (c) Control of the electrical conductivity of a DNA duplex mediated by **H**–Cu^{II}–**H** base pairing. Reproduced from ref. [85]. Copyright 2011 Wiley-VCH.

Metal-mediated base pairing can be also utilized for the control of DNA structures. Müller et al. demonstrated metal-dependent structure conversion of DNA strands between a duplex and hairpins by using Ag^{I}-mediated imidazole base pairs (**Im**–Ag^{I}–**Im**) (Figure 1-20a).[88] Luedtke et al. recently reported that the formation of T–Hg^{II}–C base pairs[89] can trigger B-to-A-form helical transition of DNA duplexes (Figure 1-20b).[90] Ligand-type nucleotides can be applied to the formation of high-order structures such as triplex by exploiting their coordination geometry (Figure 1-20c).[91,92]

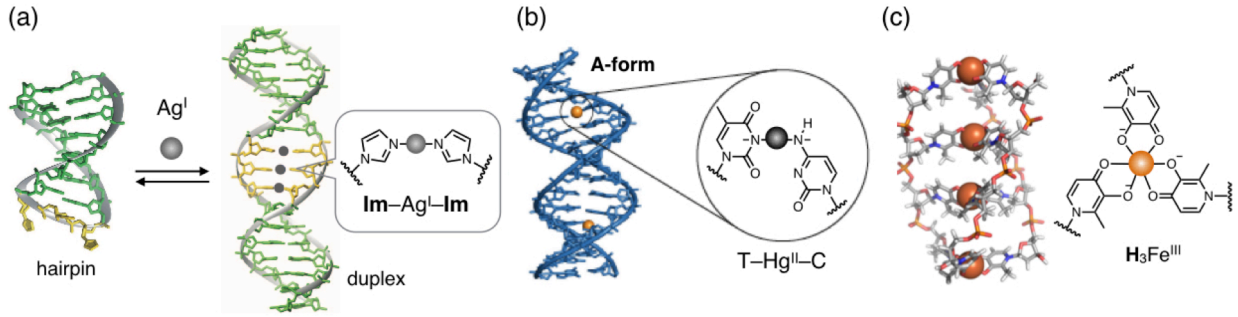

Figure 1-20. Control of DNA structures by utilizing metal-mediated base pairing. (a) Metal-dependent structure conversion by the formation of Ag^{I}-mediated imidazole base pairs. Reproduced from ref. [88]. Copyright 2010 Nature Publishing Group. (b) B-to-A-form helical transition of DNA duplexes induced by T–Hg^{II}–C base pairs. Reproduced from ref. [90]. Copyright 2019 Nature Publishing Group. (c) Formation of artificial triplex strands mediated by 3:1 hydroxypyridone–Fe^{III} complexes (**H**$_3$Fe^{III}). Reproduced from ref. [91]. Copyright 2009 Wiley-VCH.

The metal-induced hybridization of DNA duplexes and trasfromation of DNA structures would allow for the regulation of DNA functions with the use of metal-mediated base pairing, thus affording metal-responsive DNA materials. The metal-responsive functinal DNAs have been fabricated mainly by utilizing T–Hg^{II}–T and C–Ag^{I}–C base pairs (Figure 1-21).[93] Lu et al. developed a Hg^{II}-responsive DNAzyme by incorporating T–T mismatches into a reported DNAzyme (Figure 1-21a).[94] The formation of T–Hg^{II}–T base pairs restored the catalytically active structure, thus regulating the DNAzyme activity in a Hg^{II}-responsive manner. Willner et al. constructed a DNA catenane, which unidirectionally rotated by the formation of T–Hg^{II}–T base pairs (Figure 1-21b).[95] In a similar manner, various Hg^{II}- and Ag^{I}-responsive DNA materials have

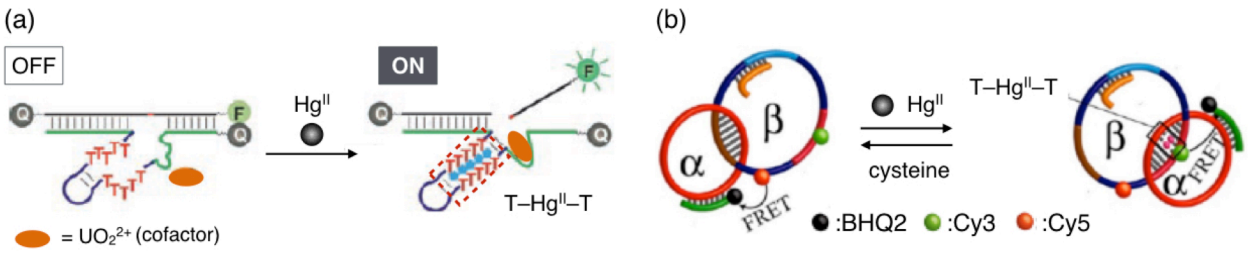

Figure 1-21. Metal-responsive functional DNAs utilizing T–Hg^{II}–T base pairing. (a) A Hg^{II}-responsive RNA-cleaving DNAzyme, whose activity was regulated by the formation of T–Hg^{II}–T base pairs. Reproduced from ref. [94]. Copyright 2007 Wiley-VCH. (b) A Hg^{II}-responsive DNA catenane. The rotation of the catenane was controlled by T–Hg^{II}–T base pairing. Reproduced from ref. [95]. Copyright 2013 American Chemical Society.

been developed by exploiting the natural pyrimidine bases as ligand sites, such as nanoswitches,[96] logic gates,[97] and molecular machines.[98]

The use of unnatural ligand-type nucleotides would provide novel functional DNAs that respond to diverse metal ions. In particular, by utilizing metal ions that rarely interact with natural nucleotides, metal-responsive DNA materials would be developed with a simple and rational design. However, such applications have been scarcely accomplished mainly because of the cumbersome process to prepare artificial ligand-bearing DNA strands with the basic solid-phase chemical synthesis. Therefore, new synthetic methods have been highly demanded for the preparation of DNA strands containing unnatural ligand-type nucleotides.

1-5. Enzymatic synthesis of artificial DNA strands

As well as the solid-phase chemical synthesis, enzymatic synthesis methods have been widely utilized to prepare natural DNA strands, such as DNA amplification by polymerase chain reaction (PCR)[99] and synthesis of long DNA strands by ligation reactions.[100] Artificial DNA strands have been also enzymatically synthesized with a careful design of unnatural nucleotides and a proper choice of enzymes.[101] Enzymatic reactions generally proceed under mild conditions, thus allowing for the incorporation of unnatural nucleotides incompatible with the chemical synthesis using several reactive agents. In addition, enzymatic synthesis provides easy access to long DNA strands, thus leading to novel applications of artificial nucleotides.

One of the approaches to enzymatically synthesized unnatural DNA strands is to develop artificial base pairs that can be replicated by DNA polymerases.[102] Benner et al. developed **P**–**Z** base pairing, which has a hydrogen bonding pattern different from Watson–Crick natural base pairs (Figure 1-22a).[103] The artificial base pair was replicated by DNA polymerases with high fidelity, thus serving as the third base pair. Hirao et al. and Romesberg et al. independently fabricated replicable base pairs that lack hydrogen bonding (Figures 1-22b and 1-22c).[104,105] These base pairs allowed for the functionalization of DNA molecules[106] and in vitro selection of novel aptamers.[107]

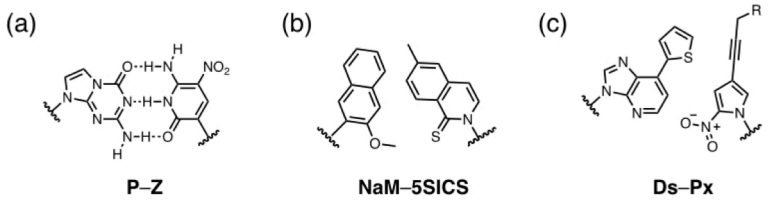

Figure 1-22. Artificial base pairs that can be replicated by DNA polymerases.

The polymerase replication of metal-mediated base pairs has been also investigated, and some promising candidates were reported thus far (Figure 1-23).[108–112] Urata et al. reported polymerase incorporation of T–Hg^{II}–T and T–Ag^{I}–C base pairs (Figure 1-23a).[108,109] T nucleotides were incorporated into the sites opposite T and C only in the presence of Hg^{II} and Ag^{I} ions, respectively, so as to form the metal-mediated base pairs. Carell et al. demonstrated polymerase replication of a Cu^{II}-mediated salen-type artificial base pair (**S**–Cu^{II}(en)–**S**) (Figure 1-23b).[110] A **S**–Cu^{II}(en)–**S**

base pair was fit well in the polymerase active site, thus incorporated with decent fidelity by a DNA polymerase. Switzer et al. reported the polymerase incorporation of a Cu^{II}-mediated base pair consisting of purine-2,6-dicarboxylate (**Pur^{DC}**) and pyridine (**Py**) unnatural nucleotides (**Pur^{DC}**–Cu^{II}–**Py**; Figure 1-23c).[111]

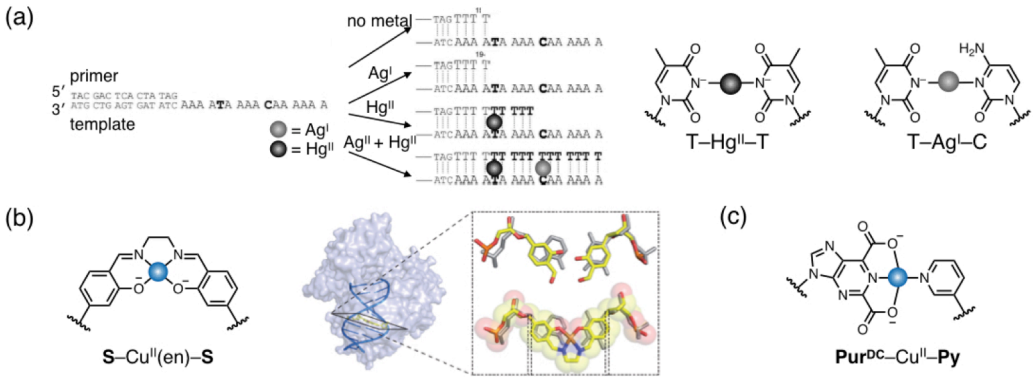

Figure 1-23. Polymerase incorporation of metal-mediated base pairs. (a) Polymerase incorporation of T–Hg^{II}–T and T–Ag^{I}–C base pairs. Reproduced from ref. [109]. Copyright 2014 Wiley-VCH. (b) Crystal structure of a Cu^{II}-mediated salen-type base pair (**S**–Cu^{II}(en)–**S**) in the polymerase active site. Reproduced from ref. [110]. Copyright 2011 Nature Publishing Group. (b) Chemical structure of a Cu^{II}-mediated heterobase pair, **Pur^{DC}**–Cu^{II}–**Py**.

Another strategy is chemical modification that can be accepted by enzymes (Figure 1-24). Modification of natural nucleobases is often accepted by DNA polymerases when they are attached to the position 7 or 8 of purines and the position 5 or 6 of pyrimidines at the major groove side (Figure 1-24a).[113] A variety of modified nucleotides have been incorporated by the polymerase synthesis.[114] For example, Hocek et al. reported that 2-nitrobenzyl-modified uracil nucleoside triphosphate (d**U^{NB}**TP) was efficiently introduced into DNA strands by a DNA polymerase (Figure 1-24b).[115] The photocaged **U^{NB}** nucleotides were deprotected inside a DNA duplex by light irradiation, thus allowing for the photo-responsive DNA cleavage by an endonuclease. Ligation reactions have been also exploited for the enzymatic synthesis of artificial DNA strands.[116-118] Hili, Liu et al. established ligase-mediated polymerization of short modified oligonucleotides (Figure 1-24c).[116,117] Their method enabled the polymerization of functionalized trimers[116] and pentamers[117] by T4 DNA ligase in accordance with template sequences.

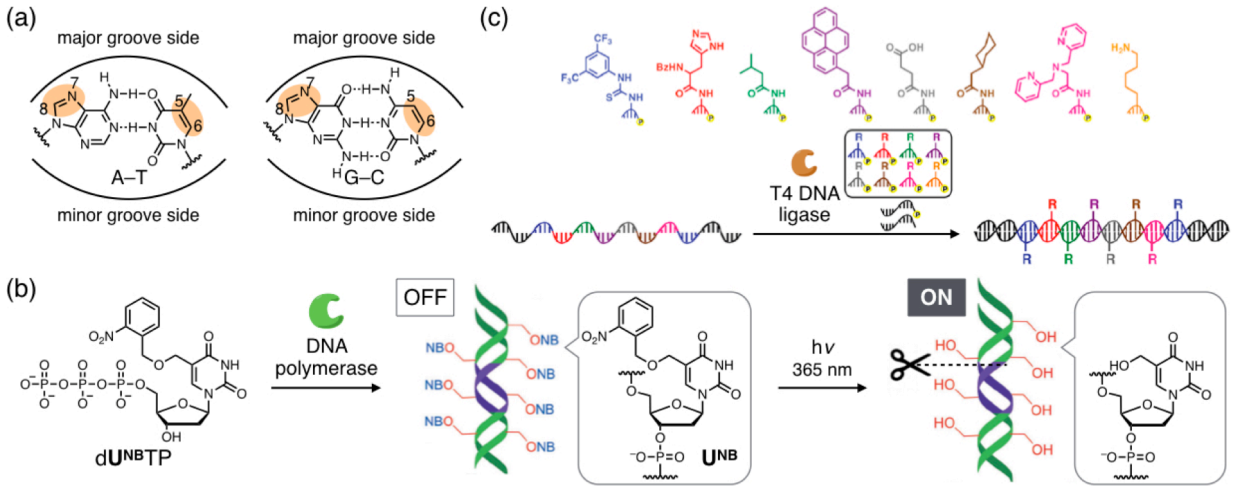

Figure 1-24. Enzymatic synthesis of modified DNA strands. (a) Possible modification sites of natural nucleobases (shown in orange). DNA polymerases tolerate modification at the major groove side. (b) Polymerase incorporation of 2-nitrobenzyl-modified nucleotides ($\mathbf{U}^{\mathbf{NB}}$), which afforded a photo-responsive DNA duplex. Reproduced from ref. [115]. Copyright 2014 Wiley-VCH. (c) Ligase-mediated polymerization of modified oligonucleotides. Reproduced from ref. [116]. Copyright 2013 American Chemical Society.

Our group has developed an enzymatic method to synthesize oligomers of hydroxypyridone (**H**) unnatural ligand-type nucleotides by a template-independent polymerase (Figure 1-25).[119] Terminal deoxynucleotidyl transferase (TdT) incorporated several hydroxypyridone nucleoside triphosphates (d**H**TP) to a primer strand. The resulting **H**-modified strands were assembled by the formation of **H**–Cu^{II}–**H** base pairs. This enzymatic method allowed for the post-synthetic modification of DNA strands to develop Cu^{II}-responsive materials.

Accordingly, enzymatic synthesis has provided powerful tools to prepare artificial DNA strands. It was expected that versatile synthetic methods for artificial ligand-bearing DNA strands can be developed by exploiting proper enzymes under specialized conditions.

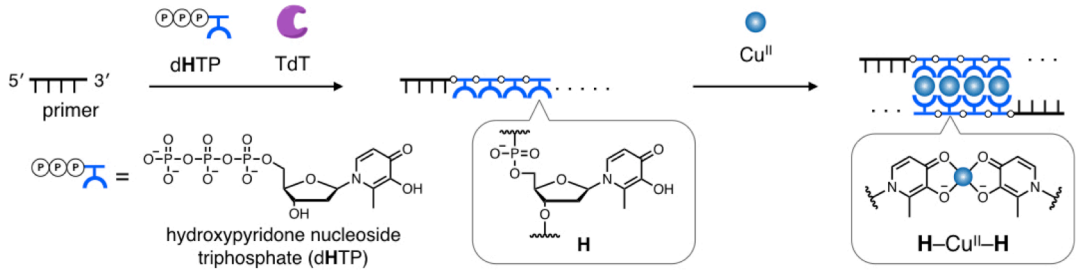

Figure 1-25. Enzymatic synthesis of artificial DNA strands containing unnatural ligand-type, hydroxypyridone (**H**) nucleotides by a template-independent polymerase (TdT). The ligand-bearing strands can be assembled by the formation of **H**–Cu^{II}–**H** base pairs.

1-6. The aim of this study

Metal-mediated artificial base pairs have gained much attention as functional units of DNA-based supramolecules and nanoarchitectures. Hg^{II}- and Ag^{I}-mediated base pairs consisting of natural pyrimidine bases (i.e. T–Hg^{II}–T and C–Ag^{I}–C) have been widely exploited for the fabrication of metal-responsive functional DNAs.[93–98] On the other hand, a variety of unnatural ligand-type nucleotides have been developed so far and have shown different metal affinities.[76] The unnatural nucleotides have the great potential for the development of metal-responsive DNA materials especially with the use of metal ions that rarely interfere with natural nucleobases other than Hg^{II} and Ag^{I} ions. Metallo-base pairs composed of artificial ligand-type nucleotides can be utilized for the metal-dependent regulation of DNA functions, thus imparting responsiveness toward diverse metal ions. However, such applications have been scarcely explored mainly because chemical synthesis of artificial ligand-bearing DNA strands is often cumbersome and time-consuming. The common chemical synthesis with the phosphoramidite chemistry uses several reactive agents including an acid, a base, and an oxidant. Thus, the synthetic method requires additional protecting groups at the metal coordinating sites of artificial nucleobases. Many byproducts are often generated during the deprotection, resulting in low yields and some troublesome purification processes. Accordingly, an alternative method to the chemical synthesis has been highly demanded for the preparation of DNA strands containing unnatural ligand-type nucleotides.

In this study, I aimed to develop enzymatic methods to synthesize artificial DNA strands containing hydroxypyridone (**H**) unnatural ligand-type nucleotides, which form a Cu^{II}-mediated base pair (**H**–Cu^{II}–**H**) (Figure 1-26a). Enzymatic reactions can proceed under mild conditions, thus requiring no protecting groups on artificial ligand-type nucleobases. Our group has previously established enzymatic synthesis of artificial **H**-bearing DNA strands by utilizing a template-independent DNA polymerase (Figure 1-25).[119] This synthetic method, however, can incorporate **H** nucleotides only into the 3′-terminus of DNA strands and cannot control the number of the

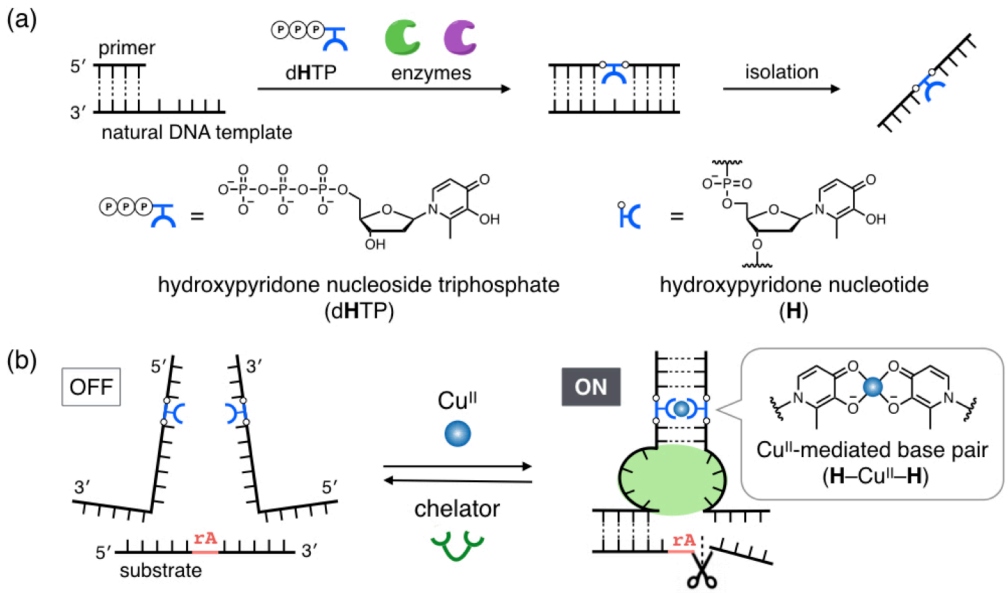

Figure 1-26. Schematic representation of enzymatic synthesis of Cu^{II}-responsive deoxyribozymes (DNAzymes) through the incorporation of hydroxypyridone (**H**) artificial ligand-type nucleotides. (a) Enzymatic synthesis of artificial DNA strands containing **H** nucleotides using natural DNA templates. (b) Development of Cu^{II}-responsive DNAzymes. The DNAzyme activities are regulated by the formation of a Cu^{II}-mediated **H**–Cu^{II}–**H** base pair.

nucleotides. In this research, I have developed enzymatic synthesis of artificial DNA strands containing **H** nucleotides at the prearranged internal positions with the use of natural DNA templates. Some enzymes with high tolerance were expected to incorporate even the artificial ligand-type nucleotides into the opposite site of natural nucleobases under specific conditions. The enzymatic methods can be performed with commercially available enzymes and standard biochemical equipment, thus allowing for the facile synthesis of artificial **H**-containing DNA strands with a defined sequence.

The enzymatic methods have been applied to the development of metal-responsive DNA supramolecules. In this study, I have developed Cu^{II}-responsive deoxyribozymes (DNAzymes) by employing **H**–Cu^{II}–**H** base pairing (Figure 1-26b). **H** nucleotides were incorporated into reported DNAzymes by the enzymatic methods. The formation of a **H**–Cu^{II}–**H** base pair would restore the catalytically active structures, thus regulating the DNAzyme activities. The catalytic activities would be regulated in a reversible manner by the addition and removal of Cu^{II} ions. The metal selectivity of **H**–Cu^{II}–**H** base pairing would allow for the Cu^{II}-specific activation of DNAzymes as

well as multimetal-dependent regulation of DNAzyme activities.

Chapter **2** describes the enzymatic synthesis of artificial ligand-bearing DNA strands. Four enzymatic methods have been established to synthesize artificial DNA strands containing **H** nucleotides.

Chapter **3** discusses the development of Cu^{II}-responsive split DNAzymes, whose activities are regulated through Cu^{II}-dependent hybridization of two strands by the formation of a **H**–Cu^{II}–**H** base pair.

Chapter **4** illustrates the development of Cu^{II}-responsive single-stranded DNAzymes based on the concept of allosteric regulation. The DNAzyme activities would be regulated through intrastrand conformational changes mediated by **H**–Cu^{II}–**H** base pairing.

Chapter **5** demonstrates multimetal-dependent regulation of DNAzyme activities. By exploiting multiple metal ions as external stimuli, I aimed at the orthogonal activation of two DNAzymes and construction of two types of AND-gate DNAzymes.

1-7. References

[1] E. T. Kool, *Annu. Rev. Biophys. Biomol. Struct.* **2001**, *30*, 1–22.

[2] N. C. Seeman, *J. Theor. Biol.* **1982**, *99*, 237–247.

[3] (a) N. C. Seeman, *Structural DNA Nanotechnology*; Cambridge University Press: Cambridge, 2016. (b) N. C. Seeman, H. F. Sleiman, *Nat. Rev. Mater.* **2017**, *3*, 17068. (c) *DNA in Supramolecular Chemistry and Nanotechnology*; E. Stulz, G. H. Clever, Eds.; Wiley-Blackwell: Chichester, 2015.

[4] J. Chen, N. C. Seeman, *Nature* **1991**, *350*, 631–633.

[5] P. W. K. Rothemund, *Nature* **2006**, *440,* 297–302.

[6] (a) F. Hong, F. Zhang, Y. Liu, H. Yan, *Chem. Rev.* **2017**, *117*, 12584–12640. (b) G. Tikhomirov, P. Petersen, L. Qian, *Nature* **2017**, *552*, 67–71. (c) L. L. Ong, N. Hanikel, O. K. Yaghi, C. Grun, M. T. Strauss, P. Bron, J. Lai-Kee-Him, F. Schueder, B. Wang, P. Wang, J. Y. Kishi, C. Myhrvold, A. Zhu, R. Jungmann, G. Bellot, Y. Ke, P. Yin, *Nature* **2017**, *552*, 72–77. (d) K. F. Wagenbauer, C. Sigl, H. Dietz, *Nature* **2017**, *552*, 78–83.

[7] J. J. Funke, H. Dietz, *Nat. Nanotechnol.* **2016**, *11*, 47−52.

[8] M. Langecker, V. Arnaut, T. G. Martin, J. List, S. Renner, M. Mayer, H. Dietz, F. C. Simmel, *Science* **2012**, *338*, 932−936.

[9] (a) F. A. Aldaye, A. L. Palmer, H. F. Sleiman, *Science* **2008**, *321*, 1795–1799. (b) C. K. McLaughlin, G. D. Hamblin, H. F. Sleiman, *Chem. Soc. Rev.* **2011**, *40*, 5647–5656. (c) M. R. Jones, N. C. Seeman, C. A. Mirkin, *Science* **2015**, *347*, 1260901.

[10] F. A. Aldaye, H. F. Sleiman, *Angew. Chem. Int. Ed.* **2006**, *45*, 2204–2209.

[11] F. A. Aldaye, H. F. Sleiman, *J. Am. Chem. Soc.* **2007**, *129*, 4130–4131.

[12] (a) C. A. Mirkin, R. L. Letsinger, R. C. Mucic, J. J. Storhoff, *Nature* **1996**, *382,* 607–609. (b) S. Y. Park, A. K. R. Lytton-Jean, B. Lee, S. Weigand, G. C. Schatz, C. A. Mirkin, *Nature* **2008**, *451*, 553–556.

[13] R. J. Macfarlane, B. Lee, M. R. Jones, N. Harris, G. C. Schatz, C. A. Mirkin, *Science* **2011**, *334*, 204–208.

[14] D. Y. Zhang, G. Seelig, *Nat. Chem.* **2011**, *3*, 103–113.

[15] F. C. Simmel, B. Yurke, H. R. Singh, *Chem. Rev.* **2019**, *119*, 6326−6369.

[16] B. Yurke, A. J. Turberfield, A. P. Mills Jr., F. C. Simmel, J. L. Neumann, *Nature* **2000**, *406*, 605–608.

[17] E. S. Andersen, M. Dong, M. M. Nielsen, K. Jahn, R. Subramani, W. Mamdouh, M. M. Golas, B. Sander, H. Stark, C. L. P. Oliveira, J. S. Pedersen, V. Birkedal, F. Besenbacher, K.

V. Gothelf, J. Kjems, *Nature* **2009**, *459*, 73–76.

[18] J.-S. Shin, N. A. Pierce, *J. Am. Chem. Soc.* **2004**, *126*, 10834–10835.

[19] (a) J. Bath, A. J. Turberfield, *Nat. Nanotechnol.* **2007**, *2*, 275–284. (b) H. Ramezani, H. Dietz, *Nat. Rev. Genet.* **2020**, *21*, 5–26.

[20] (a) G. Seelig, D. Soloveichik, D. Y. Zhang, E. Winfree, *Science* **2006**, *314*, 1585–1588. (b) D. Y. Zhang, A. J. Turberfield, B. Yurke, E. Winfree, *Science* **2007**, *318*, 1121–1125. (c) L. Qian, E. Winfree, J. Bruck, *Nature* **2011**, *475*, 368–372. (d) L. Qian, E. Winfree, *Science* **2011**, *332*, 1196–1201. (e) D. Woods, D. Doty, C. Myhrvold, J. Hui, F. Zhou, P. Yin, E. Winfree, *Nature* **2019**, *567*, 366–372.

[21] N. Srinivas, J. Parkin, G. Seelig, E. Winfree, D. Soloveichik, *Science* **2017**, *358*, eaal2052.

[22] (a) D. H. J. Bunka, P. G. Stockley, *Nat. Rev. Microbiol.* **2006**, *4*, 588–596. (b) L. C. Bock, L. C. Griffin, J. A. Latham, E. H. Vermaas, J. J. Toole, *Nature* **1992**, *355*, 564–566.

[23] J. Liu, Z. Cao, Y. Lu, *Chem. Rev.* **2009**, *109*, 1948–1998.

[24] (a) S. K. Silverman, *Trends Biochem. Sci.* **2016**, *41*, 595–609. (b) M. Hollenstein, *Molecules* **2015**, *20*, 20777–20804.

[25] R. R. Breaker, G. F. Joyce, *Chem. Biol.* **1994**, *1*, 223–229.

[26] D. S. Wilson, J. W. Szostak, *Annu. Rev. Biochem.* **1999**, *68*, 611–647.

[27] (a) M. Liu, D. Chang, Y. Li, *Acc. Chem. Res.* **2017**, *50*, 2273−2283. (b) R. R. Breaker, G. F. Joyce, *Chem. Biol.* **1995**, *2*, 655–660. (c) S. W. Santoro, G. F. Joyce, *Proc. Natl. Acad. Sci. U. S. A.* **1997**, *94*, 4262–4266. (d) K. Schlosser, Y. Li, *ChemBioChem* **2010**, *11*, 866–879.

[28] R. R. Breaker, G. M. Emilsson, D. Lazarev, S. Nakamura, I. J. Puskarz, A. Roth, N. Sudarsan, *RNA* **2003**, *9*, 949–957.

[29] (a) N. Carmi, L. A. Shultz, R. R. Breaker, *Chem. Biol.* **1996**, *3*, 1039–1046. (b) N. Carmi, S. R. Balkhi, R. R. Breaker, *Proc. Natl. Acad. Sci. U. S. A.* **1998**, *95*, 2233–2237. (c) J. Liu, Y. Lu, *J. Am. Chem. Soc.* **2007**, *129*, 9838−9839. (d) M. Wang, H. Zhang, W. Zhang, Y. Zhao, A. Yasmeen, L. Zhou, X. Yu, Z. Tang, *Nucleic Acids Res.* **2014**, *42*, 9262–9269.

[30] H. Gu, K. Furukawa, Z. Weinberg, D. F. Berenson, R. R. Breaker, *J. Am. Chem. Soc.* **2013**, *135*, 9121–9129.

[31] B. Cuenoud, J. W. Szostak, *Nature* **1995**, *375*, 611–614.

[32] P. Travascio, Y. Li, D. Sen, *Chem. Biol.* **1998**, *5*, 505–517.

[33] (a) Y. Xiao, V. Pavlov, T. Niazov, A. Dishon, M. Kotler, I. Willner, *J. Am. Chem. Soc.* **2004**, *126*, 7430–7431. (b) X. Cheng, X. Liu, T. Bing, Z. Cao, D. Shangguan, *Biochemistry* **2009**, *48*, 7817–7823. (c) J. Kosman, B. Juskowiak, *Anal. Chim. Acta* **2011**, *707*, 7–17.

[34] Y. Li, R. R. Breaker, *Proc. Natl. Acad. Sci. U. S. A.* **1999**. *96*, 2746–2751.

[35] B. M. Brandsen, A. R. Hesser, M. A. Castner, M. Chandra, S. K. Silverman, *J. Am. Chem. Soc.* **2013**, *135*, 16014–16017.

[36] M. Chandra, S. K. Silverman, *J. Am. Chem. Soc.* **2008**, *130*, 2936–2937.

[37] A. Ponce-Salvatierra, K. Wawrzyniak-Turek, U. Steuerwald, C. Höbartner, V. Pena, *Nature* **2016**, *529*, 231–234.

[38] H. Liu, X. Yu, Y. Chen, J. Zhang, B. Wu, L. Zheng, P. Haruehanroengra, R. Wang, S. Li, J. Lin, J. Li, J. Sheng, Z. Huang, J. Ma, J. Gan, *Nat. Commun.* **2017**, *8*, 2006.

[39] (a) L. Gong, Z. Zhao, Y.-F. Lv, S.-Y. Huan, T. Fu, X.-B. Zhang, G.-L. Shen, R.-Q. Yu, *Chem. Commun.* **2015**, *51*, 979–995. (b) K. Hwang, Q. Mou, R. J. Lake, M. Xiong, B. Holland, Y. Lu, *Inorg. Chem.* **2019**, *58*, 13696−13708. (c) Y. Xiang, Y. Lu, *Nat. Chem.* **2011**, *3*, 697–703. (d) P. Wu, K. Hwang, T. Lan, Y. Lu, *J. Am. Chem. Soc.* **2013**, *135*, 5254–5257. (e) S.-F. Torabi, P. Wu, C. E. McGhee, L. Chen, K. Hwang, N. Zheng, J. Cheng, Y. Lu, *Proc. Natl. Acad. Sci. U. S. A.* **2015**, *112*, 5903–5908.

[40] (a) H. Fan, X. Zhang, Y. Lu, *Sci. China Chem.* **2017**, *60*, 591–601. (b) H. Fan, Z. Zhao, G. Yan, X. Zhang, C. Yang, H. Meng, Z. Chen, H. Liu, W. Tan, *Angew. Chem. Int. Ed.* **2015**, *54*, 4801–4805.

[41] F. Praetorius, B. Kick, K. L. Behler, M. N. Honemann, D. Weuster-Botz, H. Dietz, *Nature* **2017**, *552*, 84–87.

[42] R. Orbach, B. Willner, I. Willner, *Chem. Commun.* **2015**, *51*, 4144−4160.

[43] (a) M. N. Stojanovic, T. E. Mitchell, D. Stefanovic, *J. Am. Chem. Soc.* **2002**, *124*, 3555–3561. (b) M. N. Stojanovic, D. Stefanovic, *J. Am. Chem. Soc.* **2003**, *125*, 6673–6676. (c) M. Stojanovic, D. Stefanovic, *Nat. Biotechnol.* **2003**, *21*, 1069–1074.

[44] H. Lederman, J. Macdonald, D. Stefanovic, M. N. Stojanovic, *Biochemistry* **2006**, *45*, 1194–1199.

[45] J. Elbaz, O. Lioubashevski, F. Wang, F. Remacle, R. D. Levine, I. Willner, *Nat. Nanotechnol.* **2010**, *5*, 417–422.

[46] F. Wang, C.-H. Lu, I. Willner, *Chem. Rev.* **2014**, *114*, 2881−2941.

[47] Y. Chen, M. Wang, C. Mao, *Angew. Chem. Int. Ed.* **2004**, *43*, 3554–3557.

[48] Y. Tian, Y. He, Y. Chen, P. Yin, C. Mao, *Angew. Chem. Int. Ed.* **2005**, *44*, 4355–4358.

[49] K. Lund, A. J. Manzo, N. Dabby, N. Michelotti, A. Johnson-Buck, J. Nangreave, S. Taylor, R. Pei, M. N. Stojanovic, N. G. Walter, E. Winfree, H. Yan, *Nature* **2010**, *465*, 206–210.

[50] Y. He, D. R. Liu, *Nat. Nanotechnol.* **2010**, *5*, 778–782.

[51] Z. Dai, H. M. Leung, P. K. Lo, *small* **2017**, *13*, 1602881.

[52] (a) Y. Krishnan, F. C. Simmel, *Angew. Chem. Int. Ed.* **2011**, *50*, 3124−3156. (b) X. Liu,

C.-H. Lu, I. Willner, *Acc. Chem. Res.* **2014**, *47*, 1673−1680. (c) F. Wang, X. Liu, I. Willner, *Angew. Chem. Int. Ed.* **2015**, *54*, 1098−1129.

[53] Y. Hu, A. Cecconello, A. Idili, F. Ricci, I. Willner, *Angew. Chem. Int. Ed.* **2017**, *56*, 15210–15233.

[54] Y. Dong, Z. Yang, D. Liu, *Acc. Chem. Res.* **2014**, *47*, 1853−1860.

[55] (a) J. T. Davis, G. P. Spada, *Chem. Soc. Rev.* **2007**, *36*, 296–313. (b) L. Stefan, D. Monchaud, *Nat. Rev. Chem.* **2019**, *3*, 650–668.

[56] (a) E. J. Cho, J.-W. Lee, A. D. Ellington, *Annu. Rev. Anal. Chem.* **2009**, *2*, 241–264. (b) J. L. Vinkenborg, N. Karnowski, M. Famulok, *Nat. Chem. Biol.* **2011**, *7*, 519–527.

[57] M. Madsen, K. V. Gothelf, *Chem. Rev.* **2019**, *119*, 6384–6458.

[58] Y. Hao, M. Kristiansen, R. Sha, J. J. Birktoft, C. Hernandez, C. Mao, N. C. Seeman, *Nat. Chem.* **2017**, *9*, 824–827.

[59] A. Cangialosi, C. Yoon, J. Liu, Q. Huang, J. Guo, T. D. Nguyen, D. H. Gracias, R. Schulman, *Science* **2017**, *357*, 1126–1130.

[60] A. Idili, A. Vallée-Bélisle, F. Ricci, *J. Am. Chem. Soc.* **2014**, *136*, 5836−5839.

[61] T. Li, M. Famulok, *J. Am. Chem. Soc.* **2013**, *135*, 1593−1599.

[62] J. Liu, Y. Lu, *Angew. Chem. Int. Ed.* **2006**, *45*, 90–94.

[63] D. Li, B. Shlyahovsky, J. Elbaz, I. Willner, *J. Am. Chem. Soc.* **2007**, *129*, 5804–5805.

[64] S. M. Douglas, I. Bachelet, G. M. Church, *Science* **2012**, *335*, 831–834.

[65] S. Ranallo, C. Prévost-Tremblay, A. Idili, A. Vallée-Bélisle, F. Ricci, *Nat. Commun.* **2017**, *8*, 15150.

[66] (a) Y. Kamiya, H. Asanuma, *Acc. Chem. Res.* **2014**, *47*, 1663−1672. (b) A. S. Lubbe, W. Szymanski, B. L. Feringa, *Chem. Soc. Rev.* **2017**, *46*, 1052−1079.

[67] H. Asanuma, T. Takarada, T. Yoshida, D. Tamaru, X. Liang, M. Komiyama, *Angew. Chem. Int. Ed.* **2001**, *40*, 2671–2673.

[68] M. Zhou, X. Liang, T. Mochizuki, H. Asanuma, *Angew. Chem. Int. Ed.* **2010**, *49*, 2167−2170.

[69] A. Kuzyk, Y. Yang, X. Duan, S. Stoll, A. O. Govorov, H. Sugiyama, M. Endo, N. Liu, *Nat. Commun.* **2016**, *7*, 10591.

[70] H. Yang, A. Z. Rys, C. K. McLaughlin, H. F. Sleiman, *Angew. Chem. Int. Ed.* **2009**, *48*, 9919–9923.

[71] J.-L. H. A. Duprey, Y. Takezawa, M. Shionoya, *Angew. Chem. Int. Ed.* **2013**, *52*, 1212–1216.

[72] Y. Takezawa, S. Yoneda, J.-L. H. A. Duprey, T. Nakama, M. Shionoya, *Chem. Sci.* **2016**, *7*,

3006–3010.

[73] T. Ihara, H. Ohura, C. Shirahama, T. Furuzono, H. Shimada, H. Matsuura, Y. Kitamura, *Nat. Commun*. **2015**, *6*, 6640.

[74] D. M. Engelhard, R. Pievo, G. H. Clever, *Angew. Chem. Int. Ed*. **2013**, *52*, 12843–12847.

[75] D. M. Engelhard, J. Nowack, G. H. Clever, *Angew. Chem. Int. Ed*. **2017**, *56*, 11640–11644.

[76] (a) Y. Takezawa, J. Müller, M. Shionoya, *Chem. Lett.* **2017**, *46*, 622–633. (b) Y. Takezawa, M. Shionoya, J. Müller, In *Comprehensive Supramolecular Chemistry II*; J. L. Atwood, Eds.; Elsevier Ltd.: Oxford, 2017; Vol. 4, pp 259–293. (c) Y. Takezawa, M. Shionoya, *Acc. Chem. Res.* **2012**, *45*, 2066–2076.

[77] K. Tanaka, M. Shionoya, *J. Org. Chem.* **1999**, *64,* 5002–5003.

[78] T. Tanaka, A. Tengeiji, T. Kato, N. Toyama, M. Shiro, M. Shionoya, *J. Am. Chem. Soc*. **2002**, *124*, 12494–12498.

[79] E. Meggers, P. L. Holland, W. B. Tolman, F. E. Romesberg, P. G. Schultz, *J. Am. Chem. Soc.* **2000**, *122*, 10714–10715.

[80] G. H. Clever, K. Polborn, T. Carell, *Angew. Chem. Int. Ed*. **2005**, *44*, 7204–7208.

[81] (a) S. Katz, *Biochim. Biophys. Acta* **1963**, *68*, 240–253. (b) Y. Miyake, H. Togashi, M. Tashiro, H. Yamaguchi, S. Oda, M. Kudo, Y. Tanaka, Y. Kondo, R. Sawa, T. Fujimoto, T. Machinami, A. Ono, *J. Am. Chem. Soc.* **2006**, *128*, 2172–2173.

[82] A. Ono, S. Cao, H. Togashi, M. Tashiro, T. Fujimoto, T. Machinami, S. Oda, Y. Miyake, I. Okamoto, Y. Tanaka, *Chem. Commun.* **2008**, *44*, 4825–4827.

[83] K. Tanaka, A. Tengeiji, T. Kato, N. Toyama, M. Shionoya, *Science* **2003**, *299*, 1212–1213.

[84] G. H. Clever, S. J. Reitmeier, T. Carell, O. Schiemann, *Angew. Chem. Int. Ed.* **2010**, *49*, 4927–4929.

[85] S. Liu, G. H. Clever, Y. Takezawa, M. Kaneko, K. Tanaka, X. Guo, M. Shionoya, *Angew. Chem. Int. Ed.* **2011**, *50*, 8886–8890.

[86] K. Tanaka, G. H. Clever, Y. Takezawa, Y. Yamada, C. Kaul, M. Shionoya, T. Carell, *Nat. Nanotechnol*. **2006**, *1*, 190–194.

[87] J. Kondo, Y. Tada, T. Dairaku, Y. Hattori, H. Saneyoshi, A. Ono, Y. Tanaka, *Nat. Chem*. **2017**, *9*, 956–960.

[88] S. Johannsen, N. Megger, D. Böhme, R. K. O. Sigel, J. Müller, *Nat. Chem.* **2010**, *2*, 229–234.

[89] O. P. Schmidt, A. S. Benz, G. Mata, N. W. Luedtke, *Nucleic Acids Res.* **2018**, *46*, 6470–6479.

[90] O. P. Schmidt, S. Jurt, S. Johannsen, A. Karimi, R. K. O. Sigel, N. W. Luedtke, *Nat.*

Commun. **2019**, *10*, 4818.

[91] Y. Takezawa, W. Maeda, K. Tanaka, M. Shionoya, *Angew. Chem. Int. Ed.* **2009**, *48*, 1081–1084.

[92] K. Tanaka, Y. Yamada, M. Shionoya, *J. Am. Chem. Soc.* **2002**, *124*, 8802–8803.

[93] Y. Tanaka, J. Kondo, V. Sychrovsky, J. Sebera, T. Dairaku, H. Saneyoshi, H. Urata, H. Torigoe, A. Ono, *Chem. Commun.* **2015**, *51*, 17343–17360.

[94] J. Liu, Y. Lu, *Angew. Chem. Int. Ed.* **2007**, *46*, 7587–7590.

[95] C.-H. Lu, A. Cecconello, J. Elbaz, A. Credi, I. Willner, *Nano Lett.* **2013**, *13*, 2303–2308.

[96] (a) S. Shimron, J. Elbaz, A. Henning, I. Willner, *Chem. Commun.* **2010**, *46*, 3250−3252. (b) J. M. Thomas, H.-Z. Yu, D. Sen, *J. Am. Chem. Soc.* **2012**, *134*, 13738−13748. (c) F. Wang, R. Orbach, I. Willner, *Chem. - Eur. J.* **2012**, *18*, 16030–16036. (d) A. Porchetta, A. Vallée-Bélisle, K. W. Plaxco, F. Ricci, *J. Am. Chem. Soc.* **2013**, *135*, 13238–13241.

[97] (a) R. Freeman, T. Finder, I. Willner, *Angew. Chem. Int. Ed.* **2009**, *48*, 7818−7821. (b) K. S. Park, C. Jung, H. G. Park, *Angew. Chem. Int. Ed.* **2010**, *49*, 9757–9760. (c) X. Zhu, H. Xu, X. Gao, X. Li, Q. Liu, Z. Lin, B. Qiu, G. Chen, *Chem. Commun.* **2011**, *47*, 9080–9082.

[98] Z.-G. Wang, J. Elbaz, I. Willner, *Nano Lett.* **2011**, *11*, 304–309.

[99] H. A. Erlich, D. Gelfand, J. J. Sninsky, *Science* **1991**, *252*, 1643–1651.

[100] S. Kosuri, G. M. Church, *Nat. Methods* **2014**, *11*, 499–507.

[101] J. Aschenbrenner, A. Marx, *Curr. Opin. Biotechnol.* **2017**, *48*, 187–195.

[102] D. A. Malyshev, F. E. Romesberg, *Angew. Chem. Int. Ed.* **2015**, *54*, 11930–11944.

[103] (a) J. A. Piccirilli, T. Krauch, S. E. Moroney, S. A. Benner, *Nature* **1990**, *343*, 33–37. (b) Z. Yang, F. Chen, J. B. Alvarado, S. A. Benner, *J. Am. Chem. Soc.* **2011**, *133*, 15105–15112.

[104] Y. J. Seo, G. T. Hwang, P. Ordoukhanian, F. E. Romesberg, *J. Am. Chem. Soc.* **2009**, *131*, 3246–3252.

[105] (a) M. Kimoto, R. Kawai, T. Mitsui, S. Yokoyama, I. Hirao, *Nucleic Acids Res.* **2009**, *37*, e14. (b) I. Hirao, T. Mitsui, M. Kimoto, S. Yokoyama, *J. Am. Chem. Soc.* **2007**, *129*, 15549–15555.

[106] Y. J. Seo, D. A. Malyshev, T. Lavergne, P. Ordoukhanian, F. E. Romesberg, *J. Am. Chem. Soc.* **2011**, *133*, 19878–19888.

[107] (a) K. Sefah, Z. Yang, K. M. Bradley, S. Hoshika, E. Jiménez, L. Zhang, G. Zhu, S. Shanker, F. Yu, D. Turek, W. Tan, S. A. Benner, *Proc. Natl. Acad. Sci. U. S. A.* **2014**, *111*, 1449–1454. (b) K. Matsunaga, M. Kimoto, I. Hirao, *J. Am. Chem. Soc.* **2017**, *139*, 324−334.

[108] (a) H. Urata, E. Yamaguchi, T. Funai, Y. Matsumura, S. Wada, *Angew. Chem. Int. Ed.* **2010**, *49*, 6516–6519. (b) T. Funai, Y. Miyazaki, M. Aotani, E. Yamaguchi, O. Nakagawa, S.

Wada, H. Torigoe, A. Ono, H. Urata, *Angew. Chem. Int. Ed.* **2012**, *51*, 6464–6466.

[109] T. Funai, J. Nakamura, Y. Miyazaki, R. Kiriu, O. Nakagawa, S. Wada, A. Ono, H. Urata, *Angew. Chem. Int. Ed.* **2014**, *53*, 6624–6627.

[110] C. Kaul, M. Müller, M. Wagner, S. Schneider, T. Carell, *Nat. Chem.* **2011**, *3*, 794–800.

[111] E.-K. Kim, C. Switzer, *ChemBioChem* **2013**, *14*, 2403–2407.

[112] (a) P. Röthlisberger, F. Levi-Acobas, I. Sarac, P. Marlière, P. Herdewijn, M. Hollenstein, *Org. Biomol. Chem.* **2017**, *15*, 4449–4455. (b) P. Röthlisberger, F. Levi-Acobas, I. Sarac, P. Marlière, P. Herdewijn, M. Hollenstein, *J. Inorg. Biochem.* **2019**, *191*, 154–163. (c) F. Levi-Acobas, P. Röthlisberger, I. Sarac, P. Marlière, P. Herdewijn, M. Hollenstein, *ChemBioChem* **2019**, *20*, 3032–3040.

[113] A. Hottin, A. Marx, *Acc. Chem. Res.* **2016**, *49*, 418−427.

[114] (a) M. Kuwahara, N. Sugimoto, *Molecules* **2010**, *15*, 5423–5444. (b) M. Hollenstein, *Molecules* **2012**, *17*, 13569–13591. (c) M. Hocek, *J. Org. Chem.* **2014**, *79*, 9914−9921.

[115] Z. Vaníková, M. Hocek, *Angew. Chem. Int. Ed.* **2014**, *53*, 6734−6737.

[116] R. Hili, J. Niu, D. R. Liu, *J. Am. Chem. Soc.* **2013**, *135*, 98–101.

[117] (a) C. Guo, C. P. Watkins, R. Hili, *J. Am. Chem. Soc.* **2015**, *137*, 11191–11196. (b) Z. Chen, P. A. Lichtor, A. P. Berliner, J. C. Chen, D. R. Liu, *Nat. Chem.* **2018**, *10*, 420–427.

[118] (a) D. Kestemont, M. Renders, P. Leonczak, M. Abramov, G. Schepers, V. B. Pinheiro, J. Rozenski, P. Herdewijn, *Chem. Commun.* **2018**, *54*, 6408–6411. (b) X. Liang, K. Fujioka, H. Asanuma, *Chem. - Eur. J.* **2011**, *17*, 10388–10396. (c) J. Riedl, Y. Ding, A. M. Fleming, C. J. Burrows, *Nat. Commun.* **2015**, *6*, 8807.

[119] T. Kobayashi, Y. Takezawa, A. Sakamoto, M. Shionoya, *Chem. Commun.* **2016**, *52*, 3762–3765.

Chapter 2.

Enzymatic Synthesis of Artificial Ligand-bearing DNA Strands

2-1. Introduction

Synthesis of DNA strands containing unnatural nucleotides is of great importance to expand the toolbox of DNA-based supramolecular chemistry and nanotechnology. The incorporation of unnatural nucleotides can impart stimuli-responsiveness to DNA molecules, thus allowing for the development of DNA-based smart materials such as nanodevices and molecular machines.[1] In general, artificial DNA strands bearing unnatural ligand-type nucleotides have been prepared by the chemical synthesis with the well-established phosphoramidite method (Figure 2-1). Nucleoside phosphoramidites are successively coupled on a solid support to afford an oligonucleotide with a desired sequence. The chemical synthesis also allows for introducing artificial ligand-type nucleotides with the same reaction cycle. It needs to use reactive agents including an acid (trichloroacetic acid), an activator (tetrazole), a base (e.g. aqueous ammonia), and an oxidant (iodine) to synthesize DNA strands. Metal coordinating functionalities in unnatural nucleotides are usually susceptible to these reagents. Thus, the additional protecting groups on the ligand sites are required for the chemical synthesis of artificial ligand-bearing DNA strands. Many byproducts are

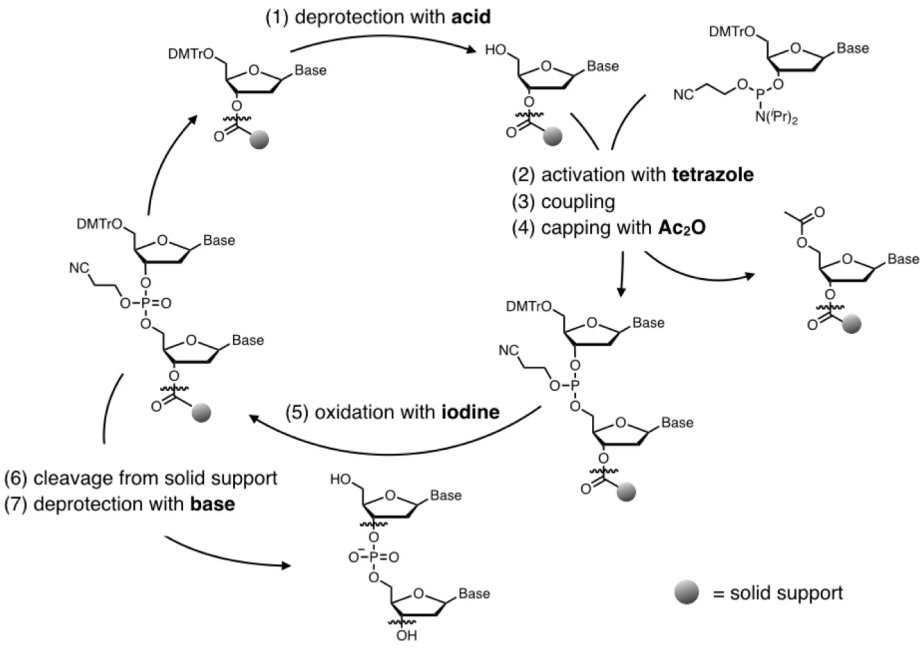

Figure 2-1. Chemical synthesis cycle of oligonucleotides with the phosphoramidite method. Reactive agents are highlighted in bold. DMTr = 4,4′-dimethoxytrityl.

often generated during the deprotection, which reduces yields of the artificial strands and make it difficult to purify the products. Accordingly, an alternative method to the cumbersome chemical synthesis has been demanded for the preparation of artificial ligand-bearing DNA strands.

As a new approach, I have focused on enzymatic synthesis of artificial ligand-bearing DNA strands. Table 2-1 summarizes the comparison between enzymatic synthesis and chemical synthesis. Enzymatic reactions can proceed under mild conditions without using reactive agents. Therefore, no protecting groups on artificial ligand-type nucleobases would be needed in the enzymatic synthesis. Moreover, enzymatic reactions can be performed with standard biochemical setups, leading to easier access to ligand-bearing DNA strands. Although the synthetic scale of enzymatic synthesis is smaller than that of chemical synthesis, it is sufficient for the application to nanotechnology and biotechnology. Thus, the enzymatic synthesis would be a powerful method to prepare artificial ligand-bearing DNA strands.

Table 2-1. Comparison between enzymatic synthesis and chemical synthesis

	Reaction condition	Metal coordinating ligand sites	Versatility	Synthetic scale
Enzymatic synthesis	Mild conditions without reactive agents	No protection	Available with standard setups	pmol ~ nmol
Chemical synthesis	Harsh conditions using an acid, a base, and an oxidant	Additional protecting groups	Need for the DNA chemical synthesizer	nmol ~ μmol

Our group has previously investigated enzymatic synthesis of artificial DNA strands containing unnatural ligand-type, hydroxypyridone (**H**)-bearing nucleotides with a template-independent DNA polymerase (Figure 2-2).[2] Terminal deoxynucleotidyl transferase (TdT) appended several

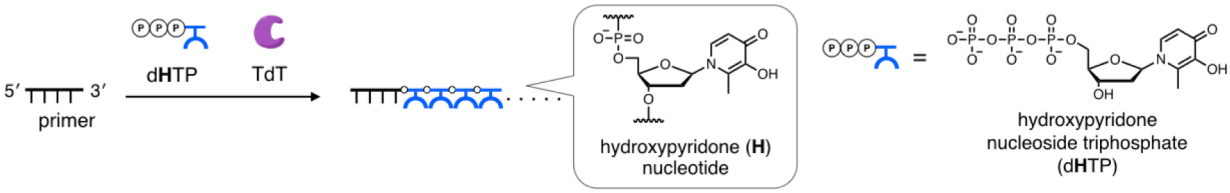

Figure 2-2. Schematic representation of template-independent enzymatic synthesis of DNA strands bearing hydroxypyridone (**H**) nucleotides with a terminal deoxynucleotidyl transferase (TdT).

hydroxypyridone nucleoside triphosphates (d**H**TP) to a primer strand without any protecting groups on the ligand sites. Thus, it allowed for the post-synthetic modification of DNA strands with **H** nucleotides. This enzymatic synthesis, however, incorporates ligand-type nucleotides only to the 3′-terminus and cannot control the number of the nucleotides. Therefore, an alternative enzymatic method has been required for the incorporation of ligand-type nucleotides at the internal positions of DNA strands with a defined sequence.

In this study, I have developed enzymatic synthesis of artificial ligand-bearing DNA strands with the use of natural DNA templates (Figure 2-3). Some enzymes were expected to tolerate even

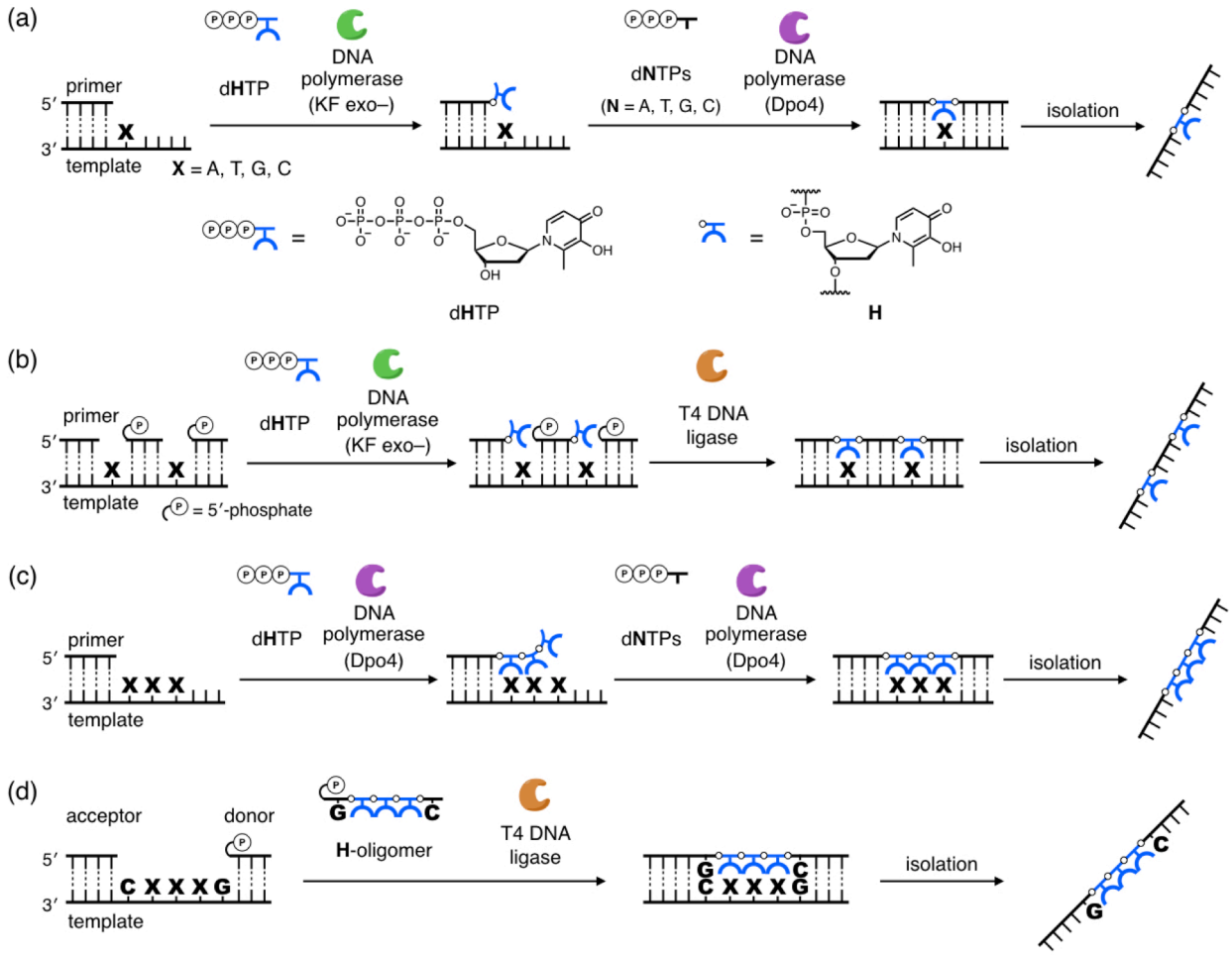

Figure 2-3. Schematic representation of enzymatic synthesis of DNA strands containing hydroxypyridone (**H**) nucleotides with natural DNA templates. (a) Polymerase synthesis of DNA strands containing one **H** nucleotide. (b) Enzymatic synthesis of DNA strands containing multiple **H** nucleotides by using a DNA polymerase and a DNA ligase. (c) Polymerase synthesis of DNA strands containing consecutive **H** nucleotides. (d) Enzymatic incorporation of a **H**-oligomer by using a DNA ligase.

unnatural ligand-type nucleotides, thus incorporating them into the opposite sites of template nucleobases. It would allow for the enzymatic synthesis of artificial DNA strands in accordance with template sequences. In this study, I have investigated the enzymatic methods to incorporate **H** unnatural ligand-type nucleotides, which form a Cu^{II}-mediated base pair (**H**–Cu^{II}–**H**) in a DNA duplex. I have developed the enzymatic synthesis of artificial **H**-containing DNA strands using d**H**TP as a substrate (Figures 2-3a–c). In addition, the enzymatic incorporation of **H**-oligomers has been also examined (Figures 2-3d).

To establish the enzymatic methods, I have utilized three types of enzymes; an exonuclease-deficient DNA polymerase, a lesion-bypass polymerase, and a DNA ligase. First, I have focused on a DNA polymerase that lacks proofreading activity. In general, DNA polymerases append a natural nucleotide to the 3′-end of a primer strand so that the incoming nucleotide forms a Watson–Crick base pair with the template nucleobase. Mismatched nucleotides can be incorporated with low efficiency although they are immediately removed by the proofreading activity of the polymerases. Many previous studies have shown that unnatural nucleotides can be incorporated by proofreading-deficient DNA polymerases.[3–6] Kool et al. reported that exonuclease-deficient Klenow fragment of DNA polymerase I (KF exo–) efficiently incorporated a difluorotoluene nucleotide into the opposite site of a template A (Figure 2-4a).[3] Other various unnatural nucleotides were also incorporated by KF exo– with a natural DNA template such as a pyrene nucleotide[4] (Figure 2-4b) and a dinitrobenzimidazole nucleotide (Figure 2-4c).[5] Kool et al. have shown that it is not necessary for DNA replication to form hydrogen bonding between incoming nucleotides and template nucleobases, and that the fitness of the base pairs in the active site is more important for the efficient incorporation of artificial nucleotides by a DNA polymerase.[6] Thus, I

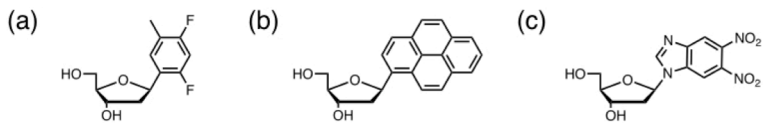

Figure 2-4. Unnatural nucleosides that were incorporated into the opposite site of natural nucleotides by KF exo–. (a) Difluorotoluene nucleoside. (b) Pyrene nucleoside. (c) Dinitrobenzimidazole nucleoside.

expected that KF exo– can also incorporate a **H** nucleotide, which has a base size comparable to a natural nucleotide, by using natural DNA strands as templates (see section **2-2**).

As the second enzyme, a lesion-bypass DNA polymerase has been exploited for the enzymatic synthesis of **H**-containing strands. Once a mismatched nucleotide is incorporated by a DNA polymerase, further primer extension gets much slower.[7] The inhibition of the further elongation of primer strands was also often observed after the incorporation of an unnatural nucleotide.[8] Thus, it is most likely that the primer extension is terminated after a **H** nucleotide is appended to the primer. I expected that a Y-family polymerase[9] that has a lesion bypass capacity would be suitable for the elongation after the **H** nucleotide. *Sulfolobus solfataricus* DNA Polymerase IV (Dpo4),[10] one of the Y-family polymerases, can extend DNA strands beyond variants such as a thymine–thymine dimer (Figure 2-5a), a cisplatin–guanine adduct (Figure 2-5b), and alkylated guanines (Figures 2-5c and 2-5d).[10,11] Kool et al. found that Dpo4 polymerase also accepts artificial pairs with a size-expanded nucleobase (Figure 2-5e).[12] Thus, Dpo4 polymerase would also extend a primer beyond a **H** nucleotide by incorporating subsequent natural nucleoside triphosphates (dNTPs) (Figure 2-3a, see section **2-2**). The high tolerance of Dpo4 polymerase would be also applicable to the consecutive incorporation of **H** nucleotides (Figure 2-3c, see section **2-4**).

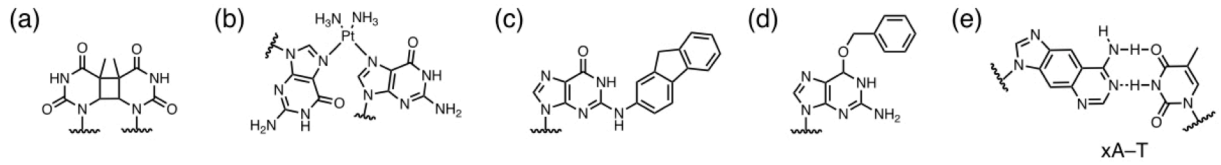

Figure 2-5. Chemical structures of variant nucleotides and an artificial base pair that can be bypassed by Dpo4 polymerase. (a) Thymine dimer. (b) Guanine–Pt^{II} complex. (c, d) Alkylated guanines. (e) Size expanded xA–T base pair.

I have also utilized a DNA ligase, which makes a phosphodiester bond between two DNA strands. A DNA ligase is involved in the base excision repair (BER) process,[13] which restores DNA lesions or damages in biological systems (Figure 2-6). After a DNA glycosylase and an AP endonuclease remove a damaged nucleotide, a DNA polymerase inserts dNTP into the resulting gap site. A DNA ligase finally seals the nick by making a phosphodiester bond. I expected that **H**

nucleotides can be also incorporated into gap sites by using a DNA polymerase and a DNA ligase in a manner similar to BER (Figure 2-3b). The successive primer extension and ligation reactions would incorporate multiple **H** nucleotides into distant positions of a single DNA strand (see section **2-3**).

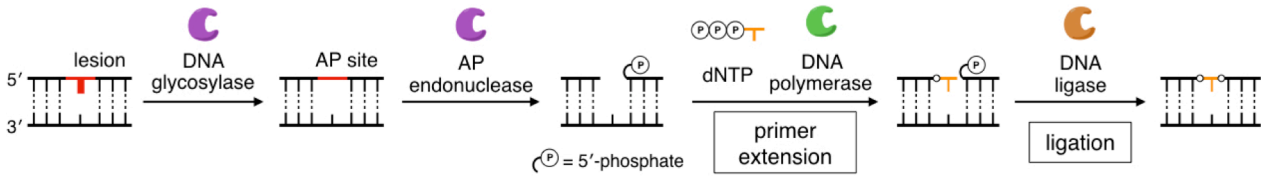

Figure 2-6. Schematic representation of base excision repair (BER) process.

For the ligation of **H**-bearing strands, I selected T4 DNA ligase, which is widely exploited in nucleic acid chemistry and DNA-based supramolecular chemistry. T4 DNA ligase shows high tolerance to mismatches[14] and some modifications.[15–21] It can make a phosphodiester bond not only in a DNA duplex but also in a hybrid DNA/RNA or RNA duplex.[15] Beardsley et al. found that T4 DNA ligase can ligate strands containing arabino nucleic acids (ANA) at the terminus.[16] Herdewijn et al. recently reported the ligation of xeno nucleic acids (XNA) by T4 DNA ligase under molecular crowding conditions (Figure 2-7a).[17] They succeeded in ligating 2′-methoxy RNA (2′-OMe RNA) duplexes and chimeric duplexes containing 2′-fluoroarabino nucleic acids (FANA), locked nucleic acids (LNA), or 1,5-dianhydrohexitol nucleic acids (HNA). I expected that T4 DNA ligase would also tolerate artificial **H**-bearing strands, thus affording artificial DNA strands containing **H** nucleotides (see section **2-3**).

Incorporation of **H**-oligomers by T4 DNA ligase has been also examined (Figure 2-3d). Hili, Liu et al. demonstrated ligase-mediated polymerization of short oligonucleotides modified with peptides (Figure 2-7b).[18–20] Their method allowed for the polymerization of peptide-modified trimers[18] and pentamers[19,20] by T4 DNA ligase according to the template sequences. I expected that short **H**-oligomers can be inserted into a DNA strand by T4 DNA ligase in a manner similar to their method (see section **2-5**).

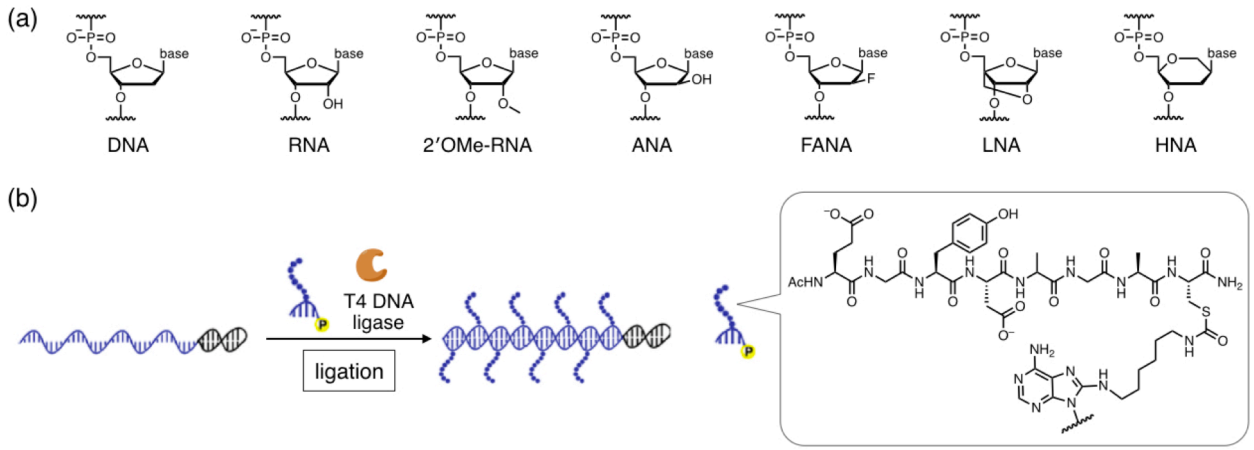

Figure 2-7. Enzymatic synthesis of modified nucleic acids through ligation by T4 DNA ligase. (a) Nucleic acids that can be ligated by T4 DNA ligase. (d) Ligase-mediated polymerization of peptide-modified oligonucleotides. Reproduced from ref. [19]. Copyright 2015 American Chemical Society.

Figure 2-8 shows a proposed mechanism of a ligation reaction by T4 DNA ligase.[22] T4 DNA ligase is first activated with adenosine triphosphate (ATP), which reacts with a lysine residue of the ligase to yield an adduct of an adenosine monophosphate (AMP) (step 1). T4 DNA ligase then binds to a DNA duplex and transfers AMP to a 5′-phosphate group (step 2). T4 DNA ligase catalyzes the nucleophilic attack of a hydroxy group at the 3′-end to the resulting adenylated phosphate, thus yielding a phosphodiester bond (step 3). Accordingly, T4 DNA ligase requires ATP as a cofactor for the ligation reaction. It should be noted that ATP can become a substrate of a DNA

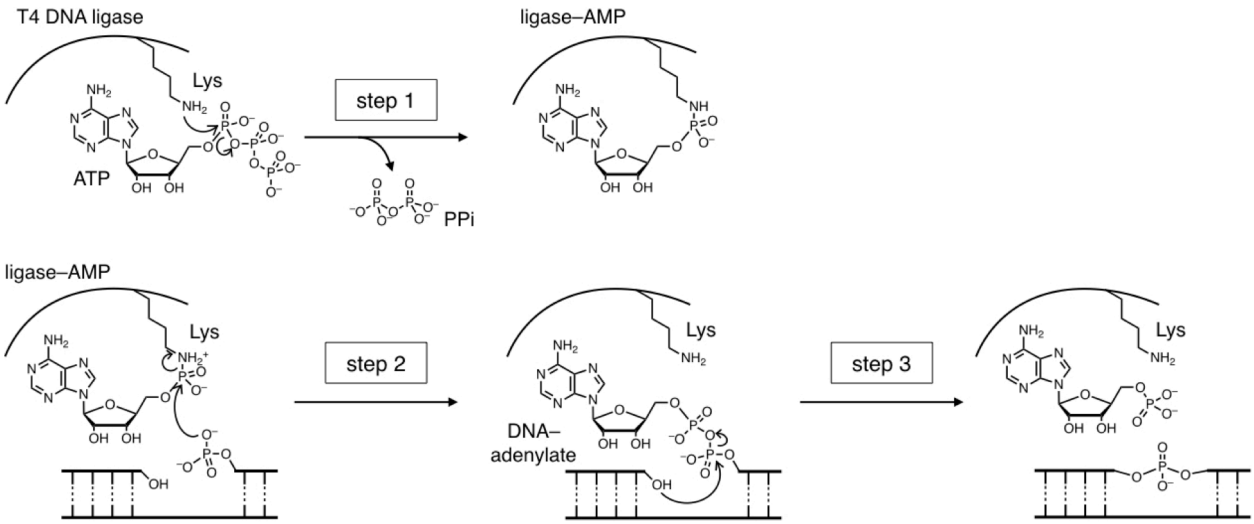

Figure 2-8. A proposed mechanism of a ligation reaction by T4 DNA ligase.

polymerase and would be appended to primers instead of artificial nucleotides of interests (i.e. d**H**TP in this study). To obtain **H**-containing strands by the successive primer extension and ligation (Figure 2-3b), the reaction conditions should be optimized so that the DNA polymerase selectively incorporates d**H**TP even in the presence of ATP.

In this chapter, I report the development of four enzymatic methods to synthesize artificial DNA strands possessing hydroxypyridone (**H**) nucleotides. Section **2-2** describes the polymerase synthesis of artificial DNA strands containing a **H** nucleotide (Figure 2-3a). Incorporation of d**H**TP and the subsequent dNTPs by the two DNA polymerases would afford **H**-bearing strands. Section **2-3** accounts for the enzymatic synthesis of DNA strands containing multiple **H** nucleotides by using a DNA polymerase and a DNA ligase (Figure 2-3b). KF exo– and T4 DNA ligase were employed for the incorporation of **H** nucleotides in a manner similar to BER process. Section **2-4** illustrates polymerase synthesis of artificial DNA strands possessing consecutive **H** nucleotides (Figure 2-3c). High tolerance of Dpo4 polymerase would enable the successive incorporation of **H** nucleotides. Section **2-5** describes an enzymatic method to incorporate **H**-oligomers by T4 DNA ligase (Figure 2-3d).

The enzymatic synthesis developed here would allow for the facile preparation of artificial ligand-bearing DNA strands without any protection on metal coordinating groups. The enzymatic methods can be carried out with commercially available enzymes and standard equipment. Thus, unnatural ligand-type, hydroxypyridone (**H**) nucleotides can be easily incorporated into DNA strands. The enzymatic synthesis would enable the fabrication of Cu^{II}-responsive functional DNAs based on **H**–Cu^{II}–**H** base pairing. Accordingly, this study would provide a powerful tool for developing metal-responsive DNA materials with the use of unnatural ligand-type nucleotides.

2-2. Polymerase synthesis of artificial DNA strands bearing a hydroxypyridone nucleotide

I first investigated polymerase synthesis of artificial DNA strands containing a hydroxypyridone (**H**) with a natural DNA template. As discussed in the section **2-1**, I expected that an unnatural **H** nucleotide can be incorporated into the opposite site of a natural nucleobase using a DNA polymerase that lacks the proofreading ability. Figure 2-9 represents a synthetic scheme of artificial DNA strands possessing a **H** nucleotide by a DNA polymerase. The polymerase synthesis consists of two primer extension reactions. In the first step, a DNA polymerase appends a **H** nucleotide to the primer in the presence of only a hydroxypyridone nucleoside triphosphate (d**H**TP) as a substrate. When natural nucleoside triphosphates (dNTPs) are added in the second step, the polymerase further extends the primer after a **H** nucleotide. As a result, the two-step primer extension with a natural DNA template affords a DNA strand containing a **H** nucleotide in the middle.

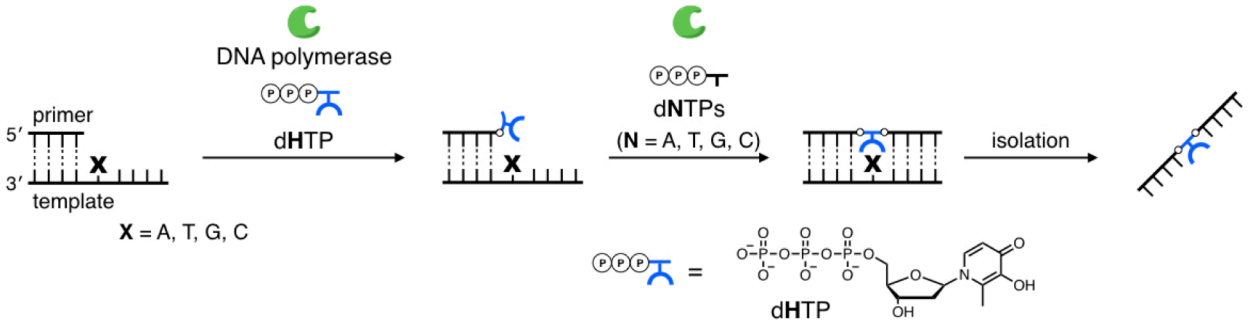

Figure 2-9. Schematic representation of polymerase synthesis of artificial DNA strands containing a hydroxypyridone (**H**) nucleotide.

The first primer extension to incorporate a **H** nucleotide was studied with a natural DNA template and a primer labeled with a FAM fluorophore (Figure 2-10). As an enzyme substrate, d**H**TP was synthesized through the procedure reported in the previous work.[2] To preclude the removal of the **H** nucleotide after the incorporation, I chose a proofreading-deficient Klenow fragment of DNA polymerase I (KF exo–), which lacks both 5′→3′ and 3′→5′ exonuclease activities. Because the polymerase incorporation of a **H** nucleotide was expected to proceed more

slowly than usual, I added polyethylene glycol (PEG), which has been reported to enhance polymerase activities by making a molecular crowding condition,[23] to a standard buffer for KF exo–. The primer extension reaction was performed in the presence of only d**H**TP (10 equiv) with template DNA strands having a different opposite natural nucleotide (Figure 2-10a). Figure 2-10b shows denaturing polyacrylamide gel electrophoresis (PAGE) analysis of the polymerase reaction after 2 h. The result shows that KF exo– recognized d**H**TP as a substrate, and one-base longer products were synthesized. The extension rate of the primer (R) was calculated from the band intensities as follows:

$$R\ (\%) = I_{n+1} / (I_n + I_{n+1}) \times 100,$$

where I_n and I_{n+1} are the band intensities of the unreacted primer and the extended one, respectively. Figure 2-10c shows the plots of the extension rates (R) against the reaction time. When the opposite base (X) was A or T, KF exo– almost quantitatively appended the **H** nucleotide to the primer after 2 h. When G or C was used as an opposite template nucleobase, the incorporation of d**H**TP was much less efficient. The elongated product was characterized by a matrix-assisted laser desorption/ionization time-of-flight (MALDI-TOF) mass analysis (Figure 2-11). The spectrum of the reaction mixture shows that the mass of the primer was increased by 303, which corresponds to the molecular weight of a **H** nucleotide (Figures 2-11a). The **H**-bearing DNA strand was isolated by denaturing PAGE and identified by MALDI-TOF mass spectrometry ($[M–H]^-$: calcd. 6372.3, found 6371.6; Figure 2-11b). Accordingly, the polymerase incorporation of a single **H** nucleotide was accomplished using a natural DNA template with A or T as the opposite base.

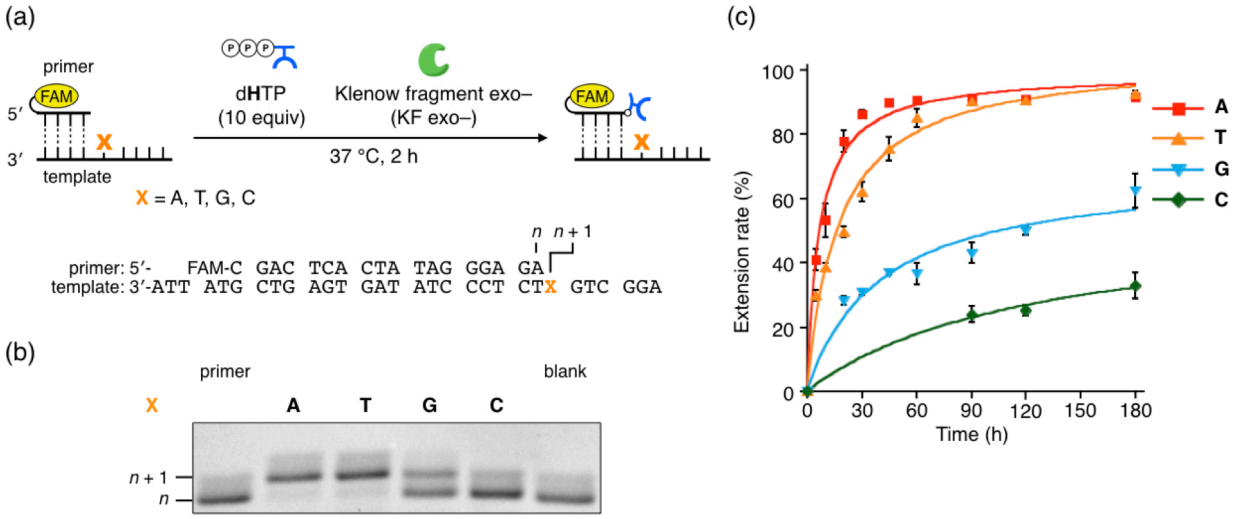

Figure 2-10. Polymerase incorporation of a hydroxypyridone-bearing nucleoside triphosphate (d**H**TP) with varying the opposite natural nucleotide (**X**). (a) Reaction scheme. [primer] = 1.0 μM, [template] = 1.5 μM, [d**H**TP] = 10 μM, [KF exo–] = 0.04 U μL^{-1} in 10 mM Tris–HCl (pH 7.9), 50 mM NaCl, 10 mM $MgCl_2$, 1 mM DTT, 6% PEG6000. 37 °C. (b) Denaturing PAGE analysis of the incorporation of a single **H** nucleotide after 2 h. The bands were detected by FAM fluorescence. (c) Time-course analysis of the incorporation of a **H** nucleotide. *N* = 3. Error bars indicate standard errors.

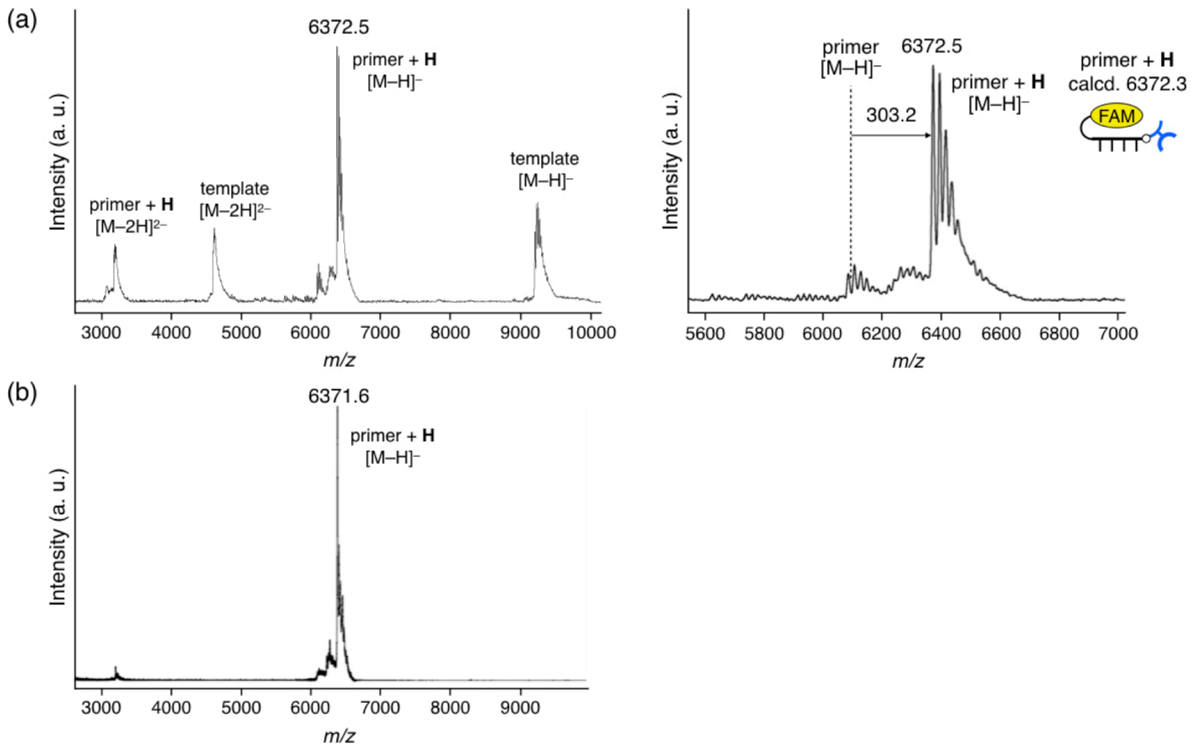

Figure 2-11. MALDI-TOF mass analysis of the products in the polymerase incorporation of d**H**TP. (a) A mass spectrum of the reaction mixture. A magnified spectrum is shown on the right. X = T. (b) A mass spectrum of the isolated product. X = A. Negative mode. Sodium adducts were also observed.

A and T were found to be the appropriate template bases for the incorporation of a **H** nucleotide. The same base selectivity was also observed when a natural nucleotide (dNTP) was incorporated into the opposite site of a template **H** nucleotide (Figure 2-12). The primer extension was examined in the presence of one of the dNTPs (10 equiv) with a template strand containing a **H** nucleotide (Figure 2-12a). The result showed that KF exo– appended dATP and dTTP more efficiently than dGTP and dCTP (Figrue 2-12b).

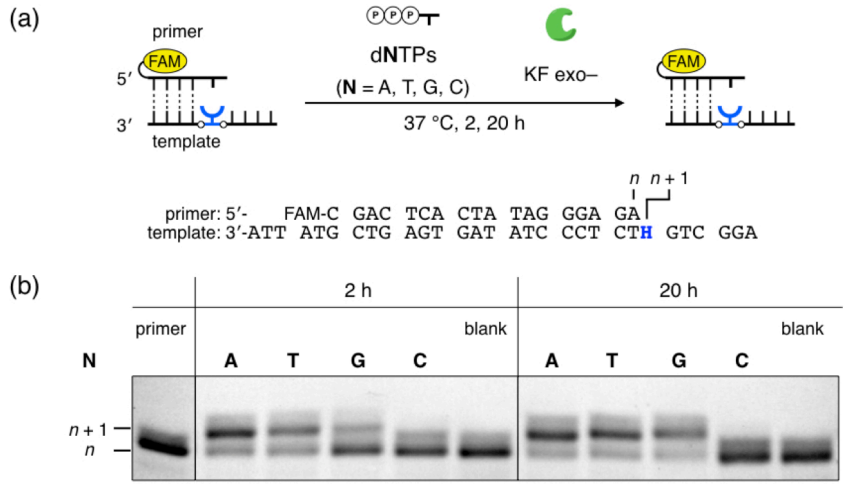

Figure 2-12. Polymerase incorporation of a natural nucleotide at the opposite site of **H** on the template. (a) Reaction scheme. [primer] = 1.0 μM, [template] = 1.5 μM, [dNTP] = 10 μM, [KF exo–] = 0.04 U μL^{-1} in 10 mM Tris–HCl (pH 7.9), 50 mM NaCl, 10 mM $MgCl_2$, 1 mM DTT, 6% PEG6000. 37 °C, 2 or 20 h. (b) Denaturing PAGE analysis. 20% gel, FAM detection. An A and a T nucleotides were incorporated more efficiently than the others.

This selectivity agrees well with the thermal stability of **H**–**X** pairs inside DNA duplexes (Figure 2-13). A thermal denaturation experiment was conducted with DNA duplexes containing a **H**–X, an A–T, or an A–A pair. The melting temperatures (T_m) of the duplexes were determined as the indexes of the thermal stability. The T_m values of the duplexes with a **H**–A or a **H**–T pair were higher than those with a **H**–G or a **H**–C. The result suggests that d**H**TP may be accommodated into the sites opposite A and T better than those opposite G and C, thus incorporated more efficiently.

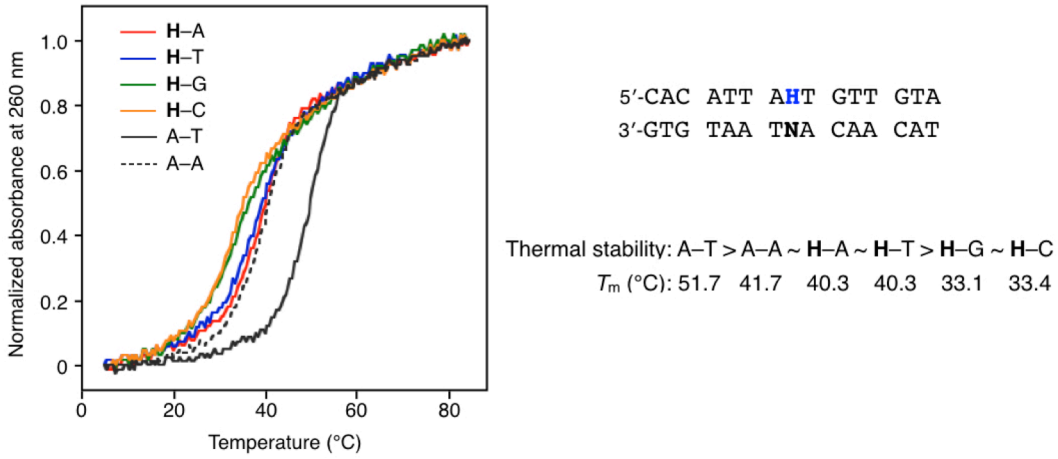

Figure 2-13. Melting analysis of DNA duplexes containing a **H**–N pair. N = A, T, G, C. [DNA duplex] = 1.0 μM in 50 mM Tris–HCl buffer (pH 7.5), 10 mM $MgCl_2$. 0.2 °C min^{-1}. All the samples were annealed before the measurements. Melting curves of DNA duplexes containing an A–T pair or an A–A mismatch pair are also shown.

The reaction rate of the incorporation of a **H** nucleotide into the opposite of A was compared with those of natural nucleotides (Figure 2-14a). Figure 2-14b shows the time-course of the primer extension reaction by KF exo– with d**H**TP or dNTP as a substrate. The incorporation of d**H**TP was much slower than that of dTTP, which forms a matched T–A pair with the A base on the template. Mismatched nucleotides (i.e. A, G, and C) were appended to the primer as slow as a **H** nucleotide.

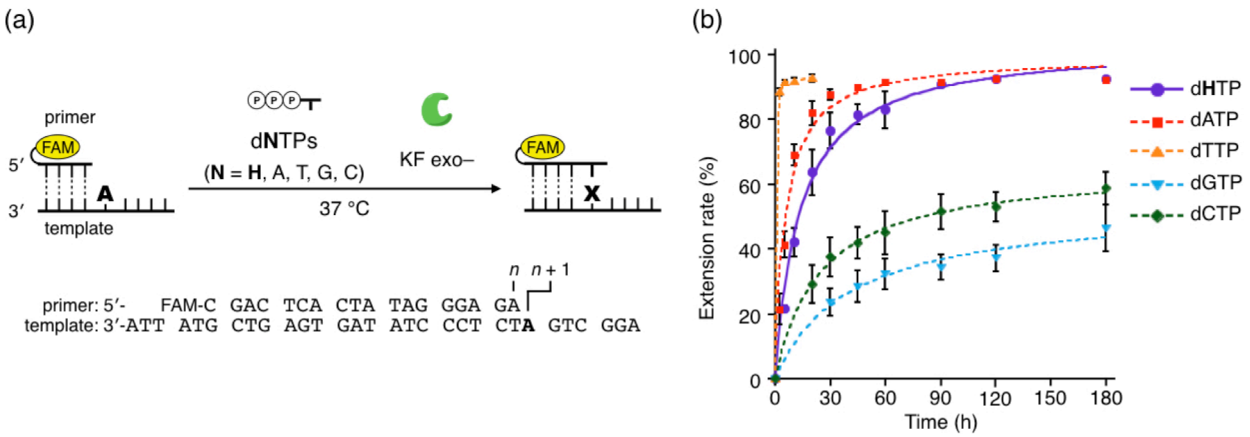

Figure 2-14. Time-course analysis of the polymerase incorporation of dNTPs (N = **H**, A, T, G and C) to the opposite site of A. [primer] = 1.0 μM, [template] = 1.5 μM, [dNTP] = 10 μM, [KF exo–] = 0.04 U $μL^{-1}$ in 10 mM Tris–HCl (pH 7.9), 50 mM NaCl, 10 mM $MgCl_2$, 1 mM DTT, 6% PEG6000. 37 °C. *N* = 3. Error bars indicate standard errors.

These results validate that d**H**TP was incorporated as a result of the misrecognition by the DNA polymerase in a manner similar to the incorporation of mismatched nucleotides.

The sequence-dependency of the polymerase incorporation of a **H** nucleotide was then investigated with different natural DNA templates. First, a base pair at the primer terminus was varied to examine all the four combinations (Figure 2-15a; Y–Z = A–T, T–A, G–C, or C–G). Denaturing PAGE analysis showed that KF exo– incorporated d**H**TP regardless of the terminus base pair (Figure 2-15b). Next, the downstream template nucleotide was changed to check if the second **H** nucleotide would be inserted or not (Figure 2-16a; Y = A, T, G, or C). The result showed that a single **H** nucleotide was incorporated in all the cases, and further elongation did not occur even after 20 h (Figure 2-16b). Even with templates possessing consecutive AA or TT bases, more than one **H** nucleotide were not appended to the primer. Accordingly, these results suggest that the polymerase method can incorporate a single **H** nucleotide into any sequences.

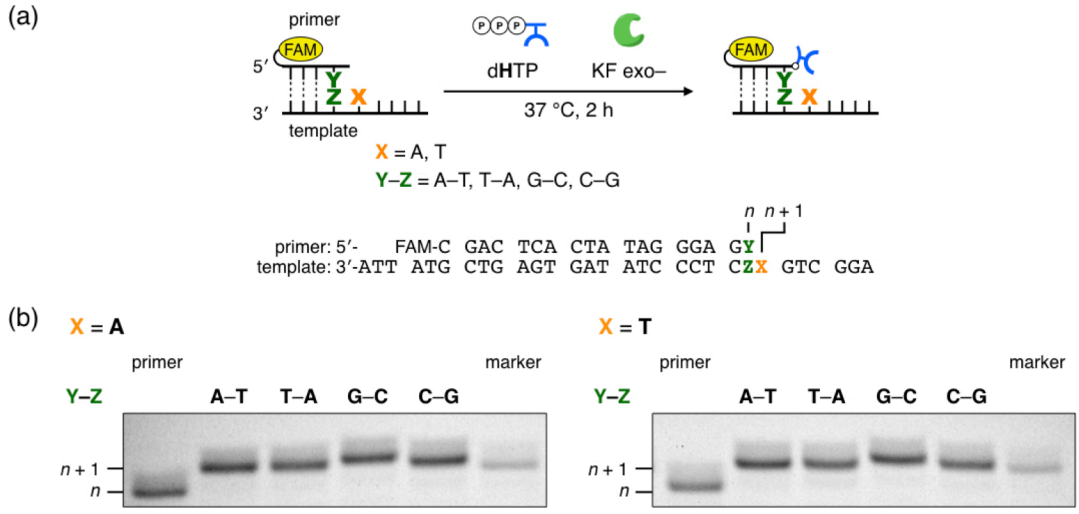

Figure 2-15. Polymerase incorporation of a **H** nucleotide with varying the primer terminus base pair. (a) Reaction scheme. [primer] = 1.0 μM, [template] = 1.5 μM, [d**H**TP] = 10 μM, [KF exo–] = 0.04 U μL^{-1} in 10 mM Tris–HCl (pH 7.9), 50 mM NaCl, 10 mM $MgCl_2$, 1 mM DTT, 6% PEG6000. 37 °C, 2 h. (b) Denaturing PAGE analysis. 20% gel, FAM detection.

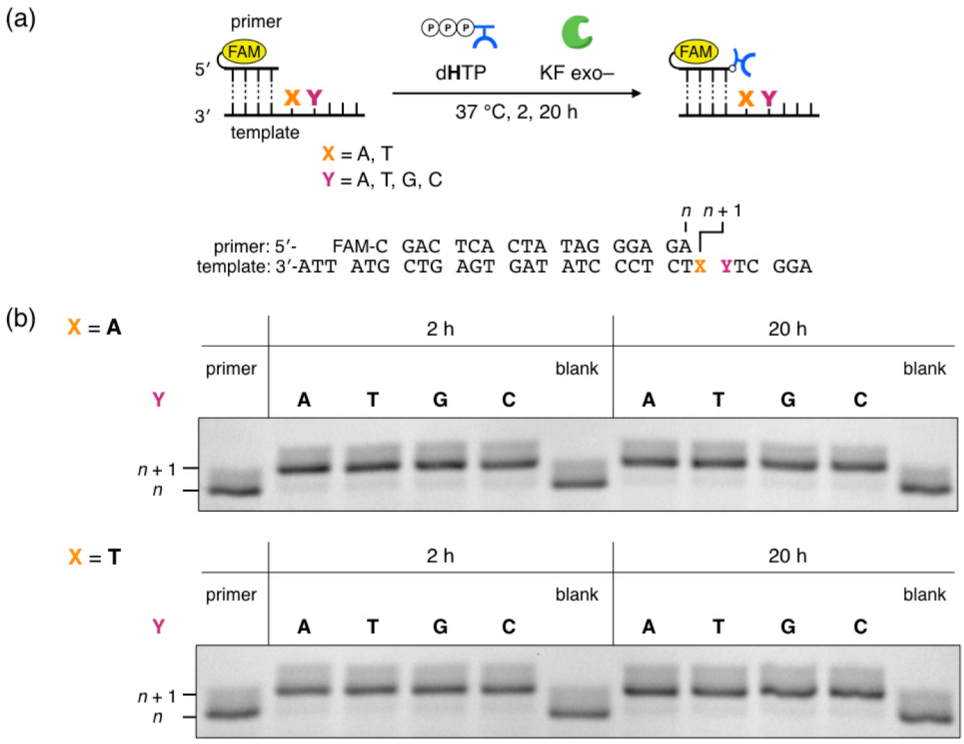

Figure 2-16. Polymerase incorporation of a **H** nucleotide with varying the downstream template nucleotides. (a) Reaction scheme. [primer] = 1.0 μM, [template] = 1.5 μM, [d**H**TP] = 10 μM, [KF exo–] = 0.04 U μL^{-1} in 10 mM Tris–HCl (pH 7.9), 50 mM NaCl, 10 mM $MgCl_2$, 1 mM DTT, 6% PEG6000. 37 °C, 2 or 20 h. (b) Denaturing PAGE analysis. 20% gel, FAM detection.

The second primer extension to introduce natural nucleotides (dNTPs) was subsequently investigated with a primer strand possessing a **H** nucleotide at the 3′-end (Figure 2-17a). However, even after 20 h, KF exo– hardly extended the primer in the presence of dNTPs (Figure 2-17b). This is presumably because the **H**–X pair at the primer terminus behaved as a mismatch pair, thus inhibiting the further primer elongation.[7,8] To overcome this problem, *Sulfolobus solfataricus* DNA Polymerase IV (Dpo4), one of the Y-family polymerases that has a lesion bypass ability,[10] was examined for the second extension reaction as a more tolerant polymerase. Dpo4 polymerase was found to efficiently extend the **H**-bearing primer by bypassing the **H**–X mismatch, thus yielding a full-length product (Figure 2-17b).

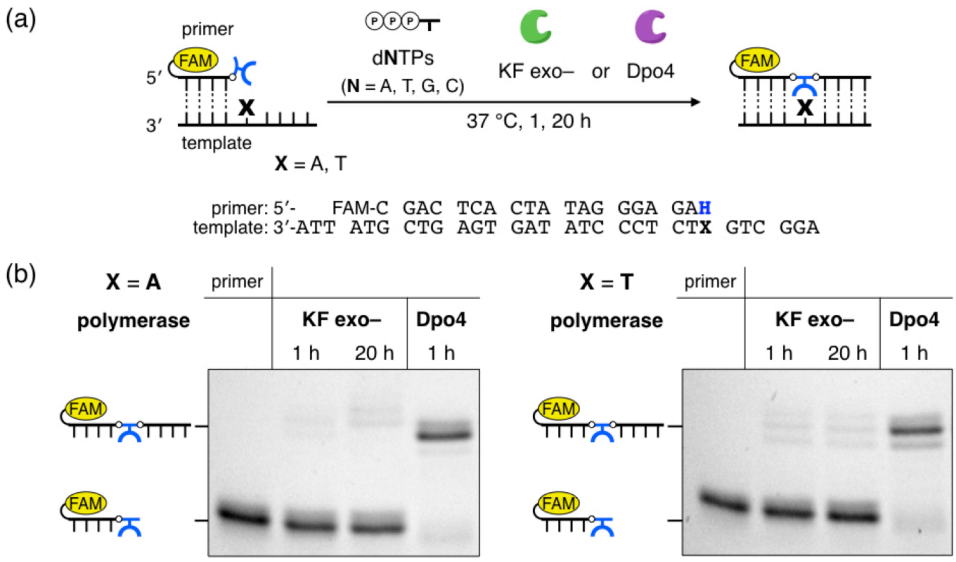

Figure 2-17. Enzymatic elongation of DNA strands after the **H** nucleotide. (a) Reaction scheme. [**H**-bearing strand] = 1.0 μM, [template] = 1.5 μM, [dNTPs] = 100 μM each, [KF exo–] = 0.04 U μL^{-1} or [Dpo4] = 0.02 U μL^{-1} in 10 mM Tris–HCl (pH 7.9), 50 mM NaCl, 10 mM $MgCl_2$, 1 mM DTT, 6% PEG6000. 37 °C, 1 or 20 h. (b) Denaturing PAGE analysis. 20% gel, FAM detection.

The incorporation of d**H**TP in the first step was also examined with the use of Dpo4 polymerase (Figure 2-18a). The primer extension was conducted at the optimal temperature for Dpo4 polymerase (55 °C) in the buffer used in the previous experiments (Figure 2-18b) as well as in an optimal buffer for Dpo4 (Figure 2-18c). Denaturing PAGE analysis of 2-h reactions showed that little d**H**TP was incorporated regardless of the opposite natural nucleobases (Figures 2-18b and 2-18c). After 20 h, the primer extension proceeded with low efficiency, and some two-base longer products were observed. These results indicate that Dpo4 polymerase introduced d**H**TP much more slowly than KF exo– and was not able to control the number of **H** nucleotides, showing the necessity of KF exo– in the first step. Therefore, both KF exo– and Dpo4 are required for the polymerase synthesis of **H**-containing DNA strands.

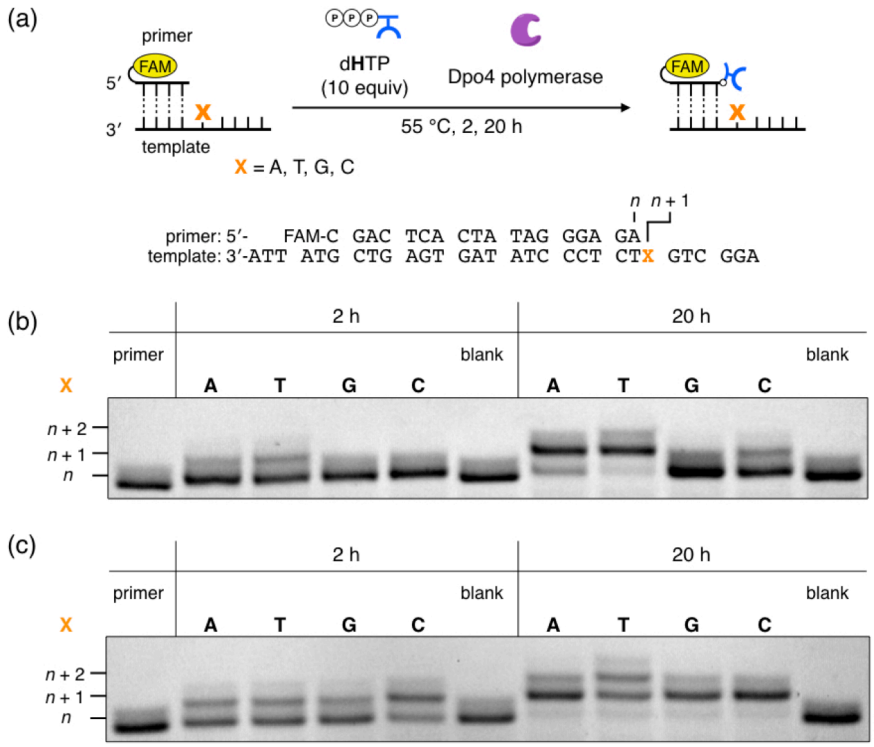

Figure 2-18. Enzymatic incorporation of a **H** nucleotide by Dpo4 polymerase. (a) Reaction scheme. [primer] = 1.0 μM, [template] = 1.5 μM, [d**H**TP] = 10 μM, [Dpo4] = 0.04 U μL^{-1}. (b) A reaction in the buffer used for KF exo– (10 mM Tris–HCl (pH 7.9), 50 mM NaCl, 10 mM $MgCl_2$, 1 mM DTT, 6% PEG6000). (c) A reaction in an optimal buffer for Dpo4 (20 mM Tris–HCl (pH 8.8), 10 mM $(NH_4)_2SO_4$, 10 mM KCl, 2 mM $MgSO_4$, 0.1% Triton® X-100, 6% PEG6000), 55 °C, 2 or 20 h. Denaturing PAGE analysis. 20% gel, FAM detection.

Based on these results, the two-step primer extesnion was designed to synthesize artificial DNA strands possessing a **H** nucleotide by using the two polymerases (Figrue 2-19a). KF exo– firstly incorporates d**H**TP into a site opposite A or T, and Dpo4 polymerase subsequently introduces natural nucleotides to afford a full-length product. Just before Dpo4 and dNTPs were added, the reaction mixture was heated to deactivate KF exo– because the polymerase has a terminal transferase (TdT) activity to append an extra nucleotide to the product.[24] Denaturing PAGE analysis showed that each step progressed in an almost quantitative manner (Figure 2-19b). Although Dpo4 polymerase also has a weaker TdT activity,[25] the one-base longer byproduct was hardly observed after 1 h. The product was isolated by denaturing PAGE and identified by MALDI-TOF mass spectrometry ($[M–H]^-$: calcd. 8186.5, found 8187.0; Figure 2-19c). This result

verifies that the polymerase synthesis can yield artificial **H**-bearing DNA strands without intermediate purification.

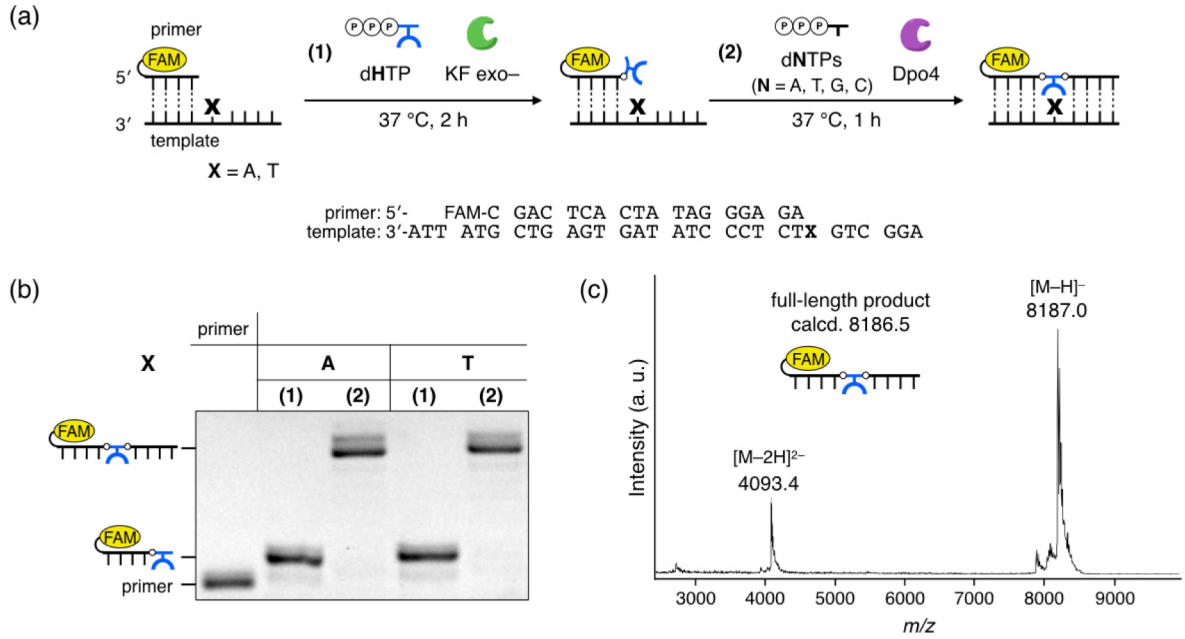

Figure 2-19. Enzymatic synthesis of DNA strands containing a hydroxypyridone (**H**) nucleotide. (a) Reaction scheme. (1st step) [primer] = 2.0 μM, [template] = 3.0 μM, [d**H**TP] = 20 μM, [KF exo–] = 0.08 U μL^{-1}. 37 °C, 2 h. (2nd step) [primer] = 1.0 μM, [template] = 1.5 μM, [d**H**TP] = 10 μM, [dNTPs] = 100 μM each, [Dpo4] = 0.02 U μL^{-1}. 37 °C, 1 h. In 10 mM Tris–HCl (pH 7.9), 50 mM NaCl, 10 mM $MgCl_2$, 1 mM DTT, 6% PEG6000. The reactions were carried out by the sequential addition of the corresponding triphosphates and the polymerases without purification of the intermediate. (b) Denaturing PAGE analysis. 20% gel, FAM detection. (c) MALDI-TOF mass analysis of the product. Negative mode.

The sequence of the full-length product was first confirmed by a stepwise extension experiment (Figure 2-20a). The primer extension reactions in the second step were conducted by adding some of the four natural nucleotides. When only dCTP was added, the one-base longer product was predominantly yielded (Figure 2-20b). This indicates that a cytidine nucleotide was incorporated after the **H** nucleotide via the formation of a C–G base pair, and no further elongation took place due to the lack of the other natural nucleotides. In the same manner, the primers were extended as far as correct nucleotides can be incorporated. Accordingly, it was proved that Dpo4 polymerase appended natural nucleotides to the primer in accordance with the template sequence.

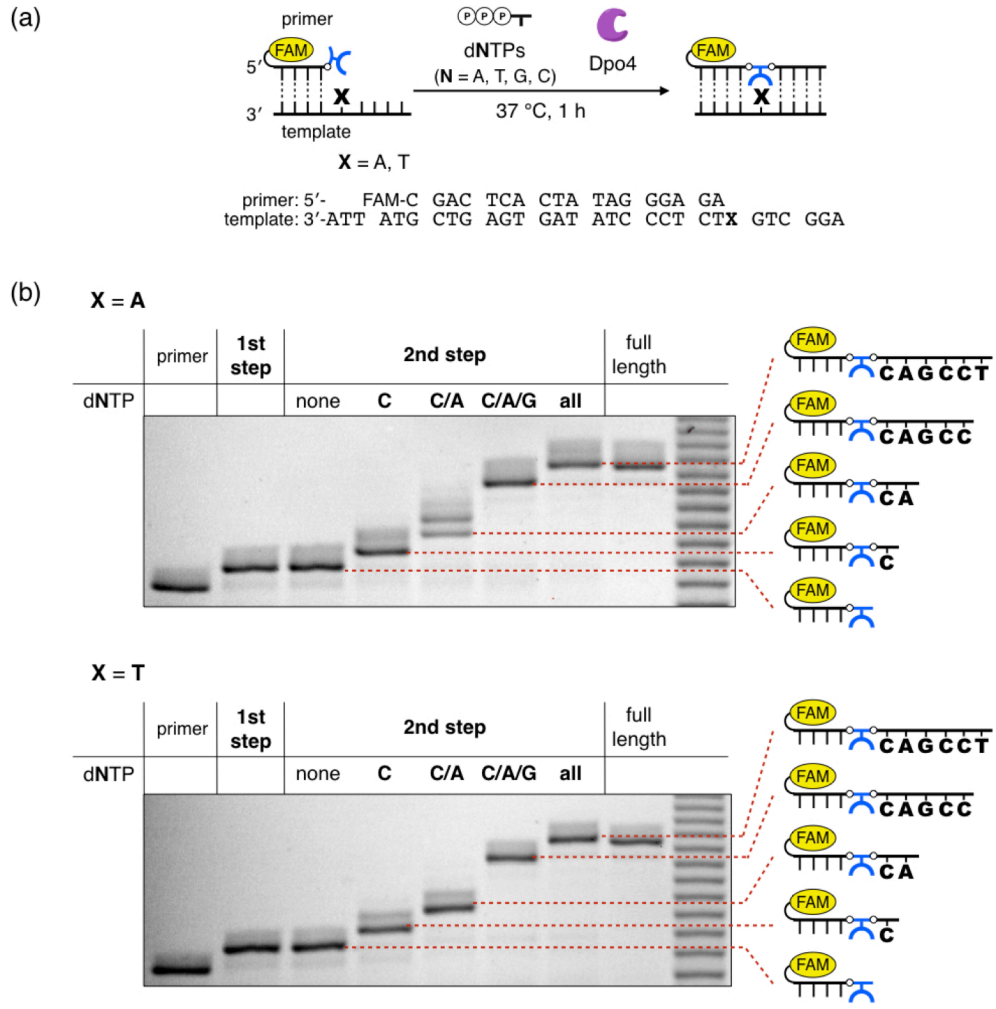

Figure 2-20. Stepwise extension of DNA strands after the **H** nucleotide by Dpo4 polymerase. (a) Reaction scheme. [primer] = 1.0 μM, [template] = 1.5 μM, [d**H**TP] = 10 μM, [dNTPs] = 100 μM each, [Dpo4] = 0.02 U μL^{-1} in 10 mM Tris–HCl (pH 7.9), 50 mM NaCl, 10 mM $MgCl_2$, 1 mM DTT, 6% PEG6000. 37 °C, 1 h. (b) Denaturing PAGE analysis. 20% gel, FAM detection.

MALDI-TOF mass analysis of the digested product further supports the accuracy of the sequence (Figure 2-21). The full-length product was hydrolyzed from the 3′-end by phosphodiesterase I. The digested sample was subsequently analyzed by MALDI-TOF mass spectrometry.[26] The mass differences between the successive peaks in the spectrum agreed well with the molecular weights of the nucleotides in the desired sequence. The result validates that the polymerase synthesis can afford artificial **H**-containing DNA strands with high fidelity of the sequence.

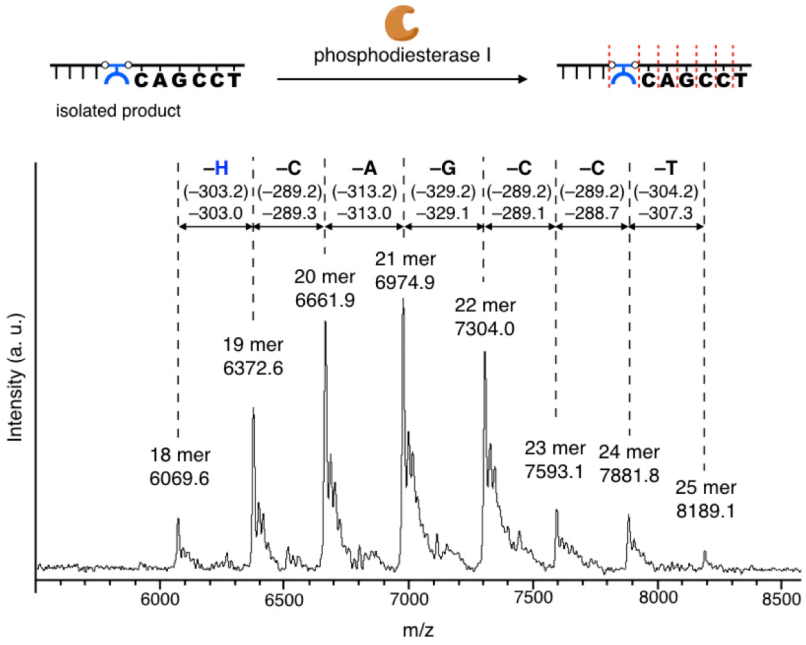

Figure 2-21. MALDI-TOF mass analysis of the full-length product after enzymatic digestion by phosphodiesterase I. Negative mode. Sodium adducts were also observed. Calculated mass is shown in the parenthesis.

To demonstrate the versatility of the synthetic procedure with the two polymerases, the two-step primer extension reactions were performed with DNA templates having different sequences. As shown in Figure 2-15, the incorporation of d**H**TP in the first step quantitatively proceeded regardless of the primer terminus base pair. When the downstream template nucleotide was varied, the polymerase reactions yielded the full-length product in all the cases (Figure 2-22; X = A or T, Y = A, T, G, or C). Next, I examined if a correct nucleotide is incorporated after the **H** nucleotide for all the eight sequences (Figure 2-23). The second primer extension was carried out by adding one of the four dNTPs. Denaturing PAGE analysis showed that the primer was not elongated in the presence of only mismatched nucleotides. In contrast, when the correct nucleotide was added, Dpo4 efficiently extended the primer. Accordingly, Dpo4 polymerase appended correct natural nucleotides to the **H**-bearing primer with all the eight templates. The results indicate that the polymerase synthesis can afford artificial DNA strands with a desired sequence regardless of the downstream template nucleotides. Taken all together, the two-step primer extension is capable of incorporating a **H** nucleotide into a DNA strand for all sequence combinations (5′-N**H**N′-3′, N, N′ =

A, T, G, or C). Accordingly, **H**-bearing DNA strands with desired sequences can be obtained by the enzymatic synthesis with natural complementary template strands.

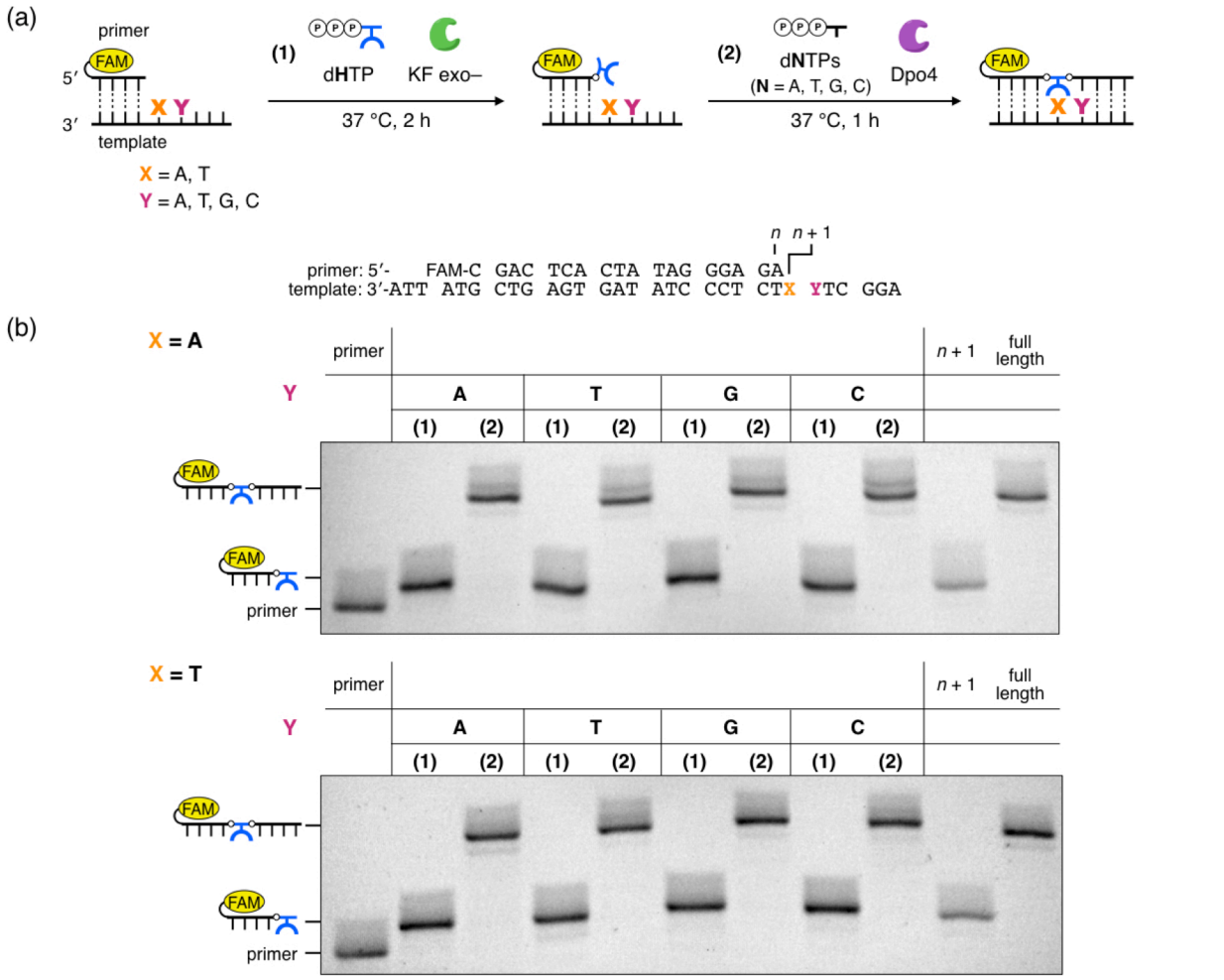

Figure 2-22. Enzymatic synthesis of DNA strands containing a hydroxypyridone (**H**) nucleotide. (a) Reaction scheme. (1st step) [primer] = 2.0 μM, [template] = 3.0 μM, [d**H**TP] = 20 μM, [KF exo–] = 0.08 U μL^{-1}. 37 °C, 2 h. (2nd step) [primer] = 1.0 μM, [template] = 1.5 μM, [d**H**TP] = 10 μM, [dNTPs] = 100 μM each, [Dpo4] = 0.02 U μL^{-1}. 37 °C, 1 h. In 10 mM Tris–HCl (pH 7.9), 50 mM NaCl, 10 mM $MgCl_2$, 1 mM DTT, 6% PEG6000. (b) Denaturing PAGE analysis. 20% gel, FAM detection.

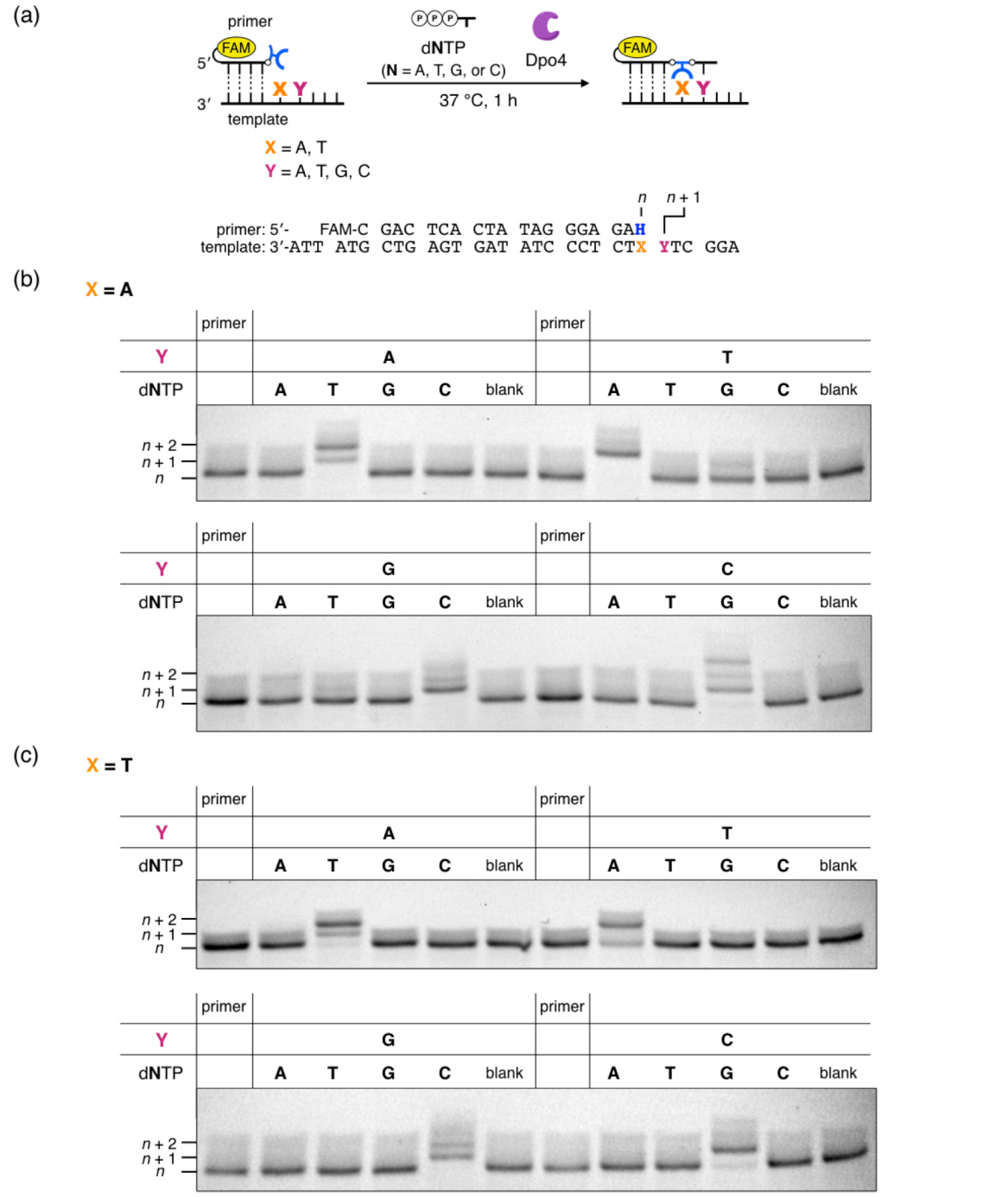

Figure 2-23. Polymerase incorporation of natural nucleotides after a hydroxypyridone (**H**) nucleotide. (a) Reaction scheme. [primer (**H**-bearing strand)] = 1.0 μM, [template] = 1.5 μM, [dNTP] = 100 μM, [Dpo4] = 0.02 U μL^{-1}. 37 °C, 1 h. In 10 mM Tris–HCl (pH 7.9), 50 mM NaCl, 10 mM $MgCl_2$, 1 mM DTT, 6% PEG6000. (b, c) Denaturing PAGE analysis. 20% gel, FAM detection. In some cases the further elongation was observed because natural nucleotides were incorporated after the matched base pair.

Although the unnatural triphosphate is needed for the enzymatic reaction, the two-step primer extension can afford artificial DNA strands containing a **H** nucleotide with commercially available polymerases and general equipment. Importantly, the reactions can be performed by the sequential addition of the triphosphates and polymerases without purification of the intermediate. Therefore, the polymerase synthesis developed here allows for the facile preparation of artificial DNA strands bearing ligand-type nucleotides.

第 2 章以降の節(3–7)は 5 年以内に 5 年以内に論文誌で刊行予定のため、非公開。

2-8. References

[1] (a) Y. Krishnan, F. C. Simmel, *Angew. Chem. Int. Ed.* **2011**, *50*, 3124−3156. (b) X. Liu, C.-H. Lu, I. Willner, *Acc. Chem. Res.* **2014**, *47*, 1673−1680. (c) F. Wang, X. Liu, I. Willner, *Angew. Chem. Int. Ed.* **2015**, *54*, 1098−1129.

[2] T. Kobayashi, Y. Takezawa, A. Sakamoto, M. Shionoya, *Chem. Commun.* **2016**, *52*, 3762–3765.

[3] S. Moran, R. X.-F. Ren, E. T. Kool, *Proc. Natl. Acad. Sci. U. S. A.* **1997**, *94*, 10506–10511.

[4] T. J. Matray, E. T. Kool, *Nature* **1999**, *399*, 704–708.

[5] K. Kincaid, J. Beckman, A. Zivkovic, R. L. Halcomb, J. W. Engels, R. D. Kuchta, *Nucleic Acids Res.* **2005**, *33*, 2620–2628.

[6] (a) E. T. Kool, *Biopolymers* **1998**, *48*, 3–17. (b) E. T. Kool, J. C. Morales, K. M. Guckian, *Angew. Chem. Int. Ed.* **2000**, *39*, 990–1009. (c) E. T. Kool, *Annu. Rev. Biophys. Biomol. Struct.* **2001**, *30*, 1–22. (d) E. T. Kool, *Annu. Rev. Biochem.* **2002**, *71*, 191–219.

[7] J. Petruska, M. F. Goodman, M. S. Boosalis, L. C. Sowers, C. Cheong, I. Tinoco, Jr., *Proc. Natl. Acad. Sci. U. S. A.* **1988**, *85*, 6252−6256.

[8] (a) M.-J. Guo, S. Hildbrand, C. J. Leumann, L. W. McLaughlin, M. J. Waring, *Nucleic Acids Res.* **1998**, *26*, 1863–1869. (b) S. Matsuda, A. A. Henry, P. G. Schultz, F. E. Romesberg, *J. Am. Chem. Soc.* **2003**, *125*, 6134–6139. (c) S. Matsuda, A. M. Leconte, F. E. Romesberg, *J. Am. Chem. Soc.* **2007**, *129*, 5551–5557. (d) A. M. Leconte, G. T. Hwang, S. Matsuda, P. Capek, Y. Hari, F. E. Romesberg, *J. Am. Chem. Soc.* **2008**, *130*, 2336–2343.

[9] (a) J. E. Sale, A. R. Lehmann, R. Woodgate, *Nat. Rev. Mol. Cell Biol.* **2012**, *13*, 141–152. (b) P. J. Rothwell, G. Waksman, *Adv. Protein Chem.* **2005**, *71*, 401–440.

[10] F. Boudsocq, S. Iwai, F. Hanaoka, R. Woodgate, *Nucleic Acids Res.* **2001**, *29*, 4607−4616.

[11] (a) H. L. Gahlon, W. B. Schweizer, S. J. Sturla, *J. Am. Chem. Soc.* **2013**, *135*, 6384−6387. (b) H. L. Gahlon, M. L. Boby, S. J. Sturla, *ACS Chem. Biol.* **2014**, *9*, 2807−2814.

[12] (a) H. Lu, S. R. Lynch, A. H. F. Lee, E. T. Kool, *ChemBioChem* **2009**, *10*, 2530−2538. (b) H. Lu, A. T. Krueger, J. Gao, H. Liu, E. T. Kool, *Org. Biomol. Chem.* **2010**, *8*, 2704−2710.

[13] (a) T. Lindahl, R. D. Wood, *Science* **1999**, *286*, 1897–1905. (b) S. S. David, V. L. O'Shea, S. Kundu, *Nature* **2007**, *447*, 941–950.

[14] (a) D. Y. Wu, R. B. Wallace, *Gene*, **1989**, *76*, 245–254. (b) R. C. Alexander, A. K. Johnson, J. A. Thorpe, T. Gevedon, S. M. Testa, *Nucleic Acids Res.* **2003**, *31*, 3208–3216.

[15] (a) K. Kleppe, J. H. van de Sande, H. G. Khorana, *Proc. Natl. Acad. Sci. U. S. A.* **1970**, *67*, 68–73. (b) M. J. Engler, C. C. Richardson, In *The Enzymes*; P. D. Boyer, Eds.; Academic

Press: New York, 1982; Vol. XV, pp 3–29.

[16] T. Mikita, G. P. Beardsley, *Biochemistry*, **1988**, *27*, 4698–4705.

[17] D. Kestemont, M. Renders, P. Leonczak, M. Abramov, G. Schepers, V. B. Pinheiro, J. Rozenski, P. Herdewijn, *Chem. Commun.* **2018**, *54*, 6408–6411.

[18] R. Hili, J. Niu, D. R. Liu, *J. Am. Chem. Soc.* **2013**, *135*, 98–101.

[19] C. Guo, C. P. Watkins, R. Hili, *J. Am. Chem. Soc.* **2015**, *137*, 11191–11196.

[20] (a) D. Kong, Y. Lei, W. Yeung, R. Hili, *Angew. Chem. Int. Ed.* **2016**, *55*, 13164–13168. (b) D. Kong, W. Yeung, R. Hili, *J. Am. Chem. Soc.* **2017**, *139*, 13977−13980. (c) Z. Chen, P. A. Lichtor, A. P. Berliner, J. C. Chen, D. R. Liu, *Nat. Chem.* **2018**, *10*, 420–427.

[21] (a) X. Liang, K. Fujioka, H. Asanuma, *Chem. - Eur. J.* **2011**, *17*, 10388–10396. (b) J. Riedl, Y. Ding, A. M. Fleming, C. J. Burrows, *Nat. Commun.* **2015**, *6*, 8807. (c) Y. Oda, J. Chiba, F. Kurosaki, Y. Yamade, M. Inouye, *ChemBioChem* **2019**, *20*, 1945–1952.

[22] (a) I. R. Lehnman, *Science* **1974**, *186*, 790–797. (b) J. M. Pascal, *Curr. Opin. Struct. Biol.* **2008**, *18*, 96–105. (c) S. Shuman, *J. Biol. Chem.* **2009**, *284*, 17365–17369.

[23] (a) Y. Sasaki, D. Miyoshi, N. Sugimoto, *Biotechnol. J.* **2006**, *1*, 440–446. (b) S. Nakano, D. Miyoshi, N. Sugimoto, *Chem. Rev.* **2014**, *114*, 2733−2758.

[24] G. Hu, *DNA Cell Biol.* **1993**, *12*, 763–770.

[25] A. Vaisman, H. Ling, R. Woodgate, W. Yang, *EMBO J.* **2005**, *24*, 2957–2967.

[26] C. M. Castleberry, C.-W. Chou, P. A. Limbach, In *Current Protocols in Nucleic Acid Chemistry*; John Wiley & Sons: New York, 2008; Vol. 33, pp 10.1.1−10.1.21.

[27] D. Sasaki, *Master's thesis* (Bioinorganic Chemistry Laboratory, Department of Chemistry, Graduate School of Science, The University of Tokyo), 2015.

[28] (a) K. Tanaka, A. Tengeiji, T. Kato, N. Toyama, M. Shionoya, *Science* **2003**, *299*, 1212–1213. (b) S. Liu, G. H. Clever, Y. Takezawa, M. Kaneko, K. Tanaka, X. Guo, M. Shionoya, *Angew. Chem. Int. Ed.* **2011**, *50*, 8886–8890.

[29] (a) Y. Takezawa, J. Müller, M. Shionoya, *Chem. Lett.* **2017**, *46*, 622–633. (b) Y. Takezawa, M. Shionoya, J. Müller, In *Comprehensive Supramolecular Chemistry II*; J. L. Atwood, Eds.; Elsevier Ltd.: Oxford, 2017; Vol. 4, pp 259–293. (c) Y. Takezawa, M. Shionoya, *Acc. Chem. Res.* **2012**, *45*, 2066–2076.

[30] (a) C. Kaul, M. Müller, M. Wagner, S. Schneider, T. Carell, *Nat. Chem.* **2011**, *3*, 794–800. (b) E.-K. Kim, C. Switzer, *ChemBioChem* **2013**, *14*, 2403–2407. (c) P. Röthlisberger, F. Levi-Acobas, I. Sarac, P. Marlière, P. Herdewijn, M. Hollenstein, *Org. Biomol. Chem.* **2017**, *15*, 4449–4455. (d) P. Röthlisberger, F. Levi-Acobas, I. Sarac, P. Marlière, P. Herdewijn, M. Hollenstein, *J. Inorg. Biochem.* **2019**, *191*, 154–163. (e) F. Levi-Acobas, P. Röthlisberger, I.

Sarac, P. Marlière, P. Herdewijn, M. Hollenstein, *ChemBioChem* **2019**, *20*, 3032–3040.

[31] T. Tanaka, A. Tengeiji, T. Kato, N. Toyama, M. Shiro, M. Shionoya, *J. Am. Chem. Soc.* **2002**, *124*, 12494–12498.

[32] C. C. Richardson, *Proc. Natl. Acad. Sci. U. S. A.* **1965**, *54*, 158−165.

[33] J. H. Eastberg, J. Pelletier, B. L. Stoddard, *Nucleic Acids Res.* **2004**, *32*, 653–660.

[34] B. H. Pheiffer, S. B. Zimmerman, *Nucleic Acids Res.* **1983**, *11*, 7853–7871.

[35] K. Shi, T. E. Bohl, J. Park, A. Zasada, S. Malik, S. Banerjee, V. Tran, N. Li, Z. Yin, F. Kurniawan, K. Orellana, H. Aihara, *Nucleic Acids Res.* **2018**, *46*, 10474–10488.

[36] (a) M. Kuwahara, N. Sugimoto, *Molecules* **2010**, *15*, 5423–5444. (b) M. Hollenstein, *Molecules* **2012**, *17*, 13569–13591. (c) M. Hocek, *J. Org. Chem.* **2014**, *79*, 9914−9921.

[37] (a) D. A. Malyshev, F. E. Romesberg, *Angew. Chem. Int. Ed.* **2015**, *54*, 11930–11944. (b) J. A. Piccirilli, T. Krauch, S. E. Moroney, S. A. Benner, *Nature* **1990**, *343*, 33–37. (c) I. Hirao, T. Mitsui, M. Kimoto, S. Yokoyama, *J. Am. Chem. Soc.* **2007**, *129*, 15549–15555. (d) D. A. Malyshev, Y. J. Seo, P. Ordoukhanian, F. E. Romesberg, *J. Am. Chem. Soc.* **2009**, *131*, 14620–14621.

[38] Y. Takezawa, K. Tanaka, M. Yori, S. Tashiro, M. Shiro, M. Shionoya, *J. Org. Chem.* **2008**, *73*, 6092–6098.

[39] Y. Takezawa, W. Maeda, K. Tanaka, M. Shionoya, *Angew. Chem. Int. Ed.* **2009**, *48*, 1081–1084.

Chapter 3.

Development of Cu^{II}-responsive Split DNAzymes

3-1. Introduction

In **chapter 2**, I have established the facile synthetic methods of artificial ligand-bearing DNA strands with the use of enzymes. These enzymatic methods offer a powerful tool for developing metal-responsive functional DNAs based on metal-mediated base pairing. Accordingly, unnatural ligand-type, hydroxypyridone (**H**) nucleotides can be easily incorporated into DNA strands to impart Cu^{II} responsiveness to known functional DNA molecules. In this study, I have chosen deoxyribozymes (DNAzymes) as a target functional DNA molecule. DNAzymes are catalytically active DNA strands that can catalyze various reactions, and have been utilized as key components of diverse DNA-based supramolecules and nanomachines.[1] I have applied the enzymatic methods to develop metal-responsive DNAzymes. The activity of DNAzymes can be regulated by the formation of a **H**–Cu^{II}–**H** base pair. As DNAzymes have been widely used for constructing DNA-based biosensors, logic gates, and molecular machines,[2] the development of stimulus-responsive DNAzymes has been highly demanded for the construction of sophisticated DNA-based molecular systems.

One of the methods to endow DNAzymes with responsiveness to specific external stimuli is the use of split DNAzymes. Parent DNAzymes are separated into several strands, and the external stimuli induce the association of the split strands to restore the original catalytic activities.[3–15] For example, Kolpashchikov developed a split DNAzyme that responds to DNA analytes.[3] A known RNA-cleaving DNAzyme was divided into two halves, and the addition of a DNA strand induced the reconstruction of the catalytically active DNAzyme structure, leading to the cleavage of an RNA substrate. Willner et al. utilized the split DNAzymes as subunits of DNA logic gates, in which the DNAzymes cleaved substrates in response to appropriate input DNA strands (Figure 3-1a).[4] Willner et al. fabricated peroxidase-mimicking split DNAzymes, which were activated by the addition of an input oligonucleotide.[5] Kolpashchikov and Zhou et al. independently exploited the split DNAzymes for discriminating single nucleotide polymorphisms (SNPs) (Figure 3-1b).[6] Hybridization of split DNAzymes can be triggered not only by oligonucleotides but also by other

stimuli such as small molecules,[7,8] pH changes,[9] and light.[10,11] Willner et al. also developed Hg^{II}-responsive split DNAzymes by using a Hg^{II}-mediated thymine base pair (T–Hg^{II}–T)[16].[8,12] Thus, split DNAzymes offer a compelling platform for developing stimulus-responsive DNA systems.

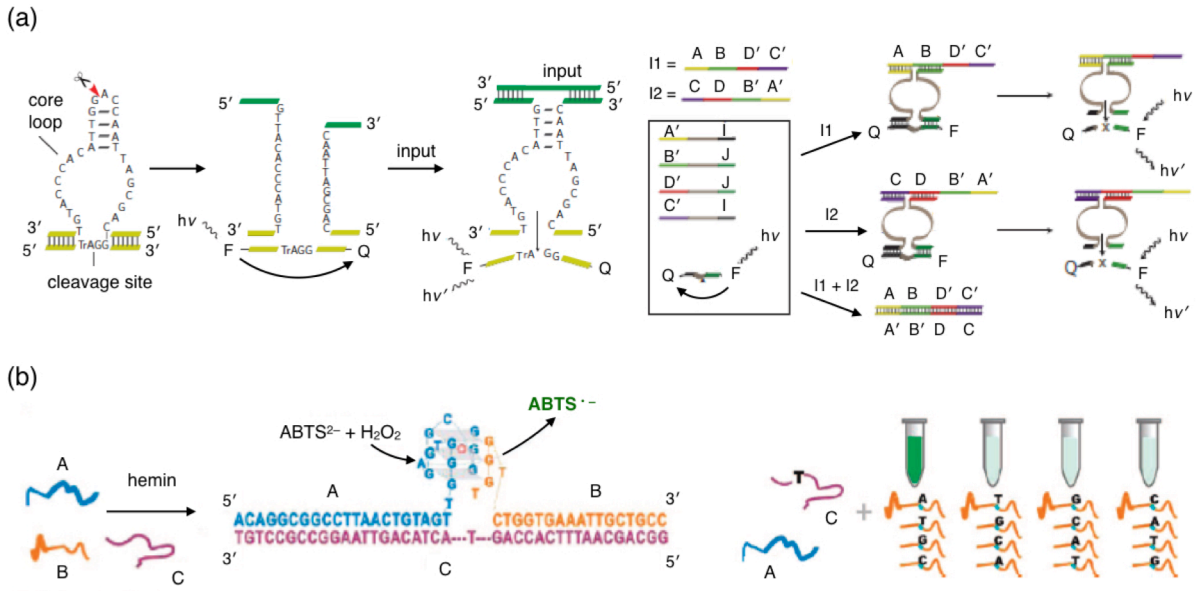

Figure 3-1. Examples of stimulus-responsive split DNAzymes. (a) RNA-cleaving DNAzyme as a subunit of DNA-based logic gates. The addition of input DNA strands induced the association of the split DNAzymes, leading to output fluorescence signals. Reproduced from ref. [4a]. Copyright 2010 Nature Publishing Group. (b) Colorimetric SNP analysis by using a split G-quadruplex peroxidase-mimicking DNAzyme. A specific DNA analyte restored the active DNAzyme structure, thus allowing SNP discrimination. Reproduced from ref. [6b]. Copyright 2008 American Chemical Society.

In this chapter, I describe the development of split-type Cu^{II}-responsive DNAzymes that can be activated by the formation of a metal-mediated **H**–Cu^{II}–**H** base pair. **H**–Cu^{II}–**H** base pairing greatly increases the thermal stability of DNA duplexes (ΔT_m = +13 °C in a typical case) and can trigger association of DNA strands in a Cu^{II}-responsive manner.[17] I expected that this Cu^{II}-induced DNA hybridization can be utilized for the regulation of catalytic activities of split DNAzymes. By incorporating **H** nucleotides into known split DNAzymes, the DNAzyme activities would be modulated through hybridization of the split strands triggered by **H**–Cu^{II}–**H** base pairing. As a consequence, Cu^{II}-responsive DNAzymes can be constructed with a **H**–Cu^{II}–**H** base pair.

Figure 3-2 represents a design strategy of Cu^{II}-responsive split DNAzymes. A reported DNAzyme is divided into two strands, and a **H** nucleotide is incorporated into a stem site of each split strand (Figure 3-2a). The formation of a **H**–Cu^{II}–**H** base pair would induce the hybridization of the two strands. As a result, a catalytically active DNAzyme structure is reconstructed, and thus its catalytic activity is restored (Figure 3-2b). To fabricate Cu^{II}-responsive DNAzymes, DNA strands containing a **H** nucleotide at different positions were prepared by the polymerase synthesis described in the section **2-2**. The enzymatic method would facilitate the screening of DNA sequence variations, leading to the development of a DNAzyme that responds to Cu^{II} ions with a large on–off contrast. Owing to the reversible complexation of **H**–Cu^{II}–**H**, the activity of the **H**-modified DNAzyme would be reversibly regulated by the addition and removal of Cu^{II} ions. It was also expected that redox reactions of Cu^{II} ions can be utilized for the modulation of the DNAzyme activity.

As the split design presented here is grounded on the hybridization of DNA strands induced by metal-meidated base pairing, this strategy would be applied for the regulation not only of DNAzyme activties but also of other DNA functions and structures. Accordingly, this study would provide the basis for the construction of metal-responsive DNA systems.

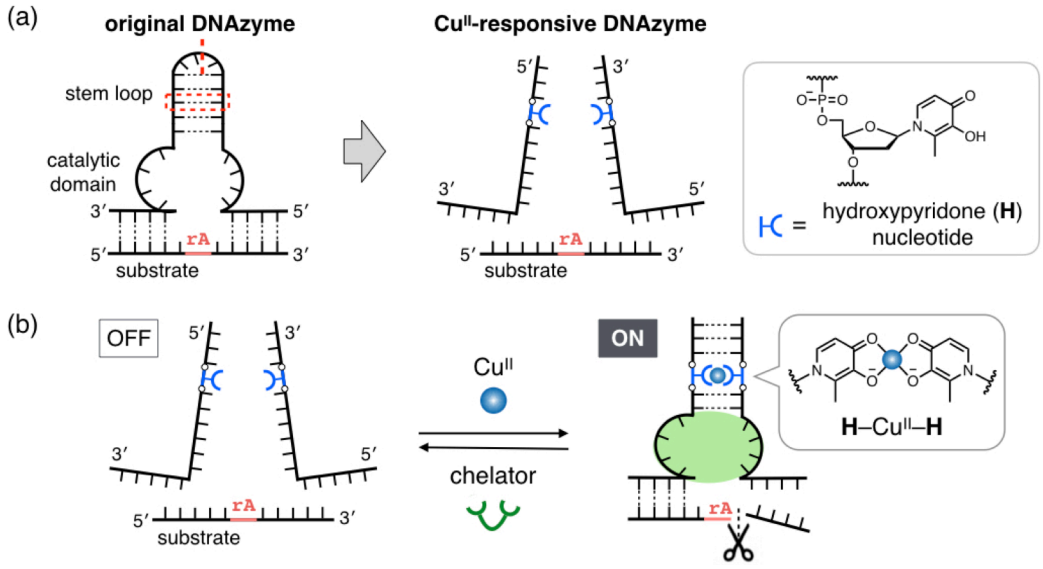

Figure 3-2. (a) Development of Cu^{II}-responsive split DNAzymes through the incorporation of hydroxypyridone (**H**) nucleotides. (b) Cu^{II}-dependent regulation of the activity of split DNAzymes by the formation of a **H**–Cu^{II}–**H** base pair. "rA" in the substrate strand represents an adenosine ribonucleotide.

3-2. Design and synthesis of Cu^{II}-responsive split DNAzymes

As a proof-of-concept, I selected a reported RNA-cleaving DNAzyme (E5 DNAzyme)[18] and converted it into a Cu^{II}-responsive split DNAzyme by incorporating hydroxypyridone (**H**) nucleotides as a Cu^{II}-binding site (Figure 3-3). E5 DNAzyme, reported by Breaker and Joyce in 1995, cleaves RNA substrates as well as DNA strands containing a ribonucleotide at the cleavage site in the presence of Mg^{II} ions as a cofactor. It is composed of a variable stem–loop, a catalytic domain, and a substrate-binding site. E5 DNAzyme is known to be separable into two strands, thus utilized in many previous studies.[3,4,7,9,10,12,13] Its catalytic activity can be restored by the hybridization of the two split strands triggered by external stimuli such as oligonucleotides,[3,4] small molecules,[7] pH changes,[9] and light.[10] In my design, the DNAzyme was split into two strands and a **H**–**H** mismatch pair was introduced in the stem region. In the absence of Cu^{II} ions, the split strands would be dissociated, and the DNAzyme would not cleave an RNA substrate. It was expected that only in the presence of Cu^{II} ions the catalytically active structure is reconstructed through the Cu^{II}-specific formation of a **H**–Cu^{II}–**H** base pair.

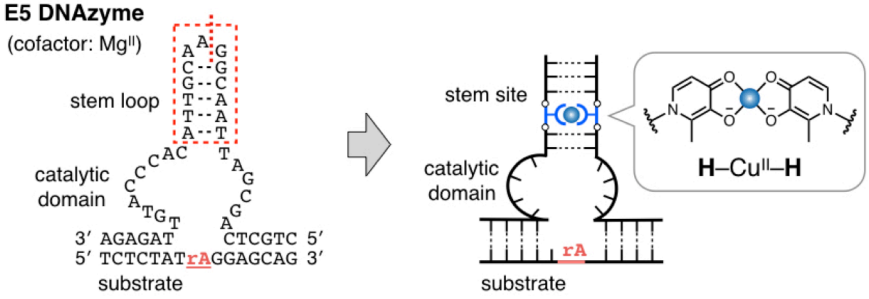

Figure 3-3. Design of Cu^{II}-responsive split DNAzymes. **H**: hydroxypyridone ligand-type nucleotide, rA: adenosine ribonucleotide.

I prepared several split DNAzymes to find out an appropriate stem length and the optimal position of the **H**–**H** pair. To achieve the regulation of the DNAzyme activity, the thermal stability of the stem duplex should be tuned so that the split strands are associated when Cu^{II} ions are added. The stem length and the **H**–**H** position were expected to have a large influence on the thermal stability of the stem duplex. The position of the artificial base pair is also crucial for retaining the

catalytically active structure of the DNAzyme. The sequences of the DNAzymes for screening are shown in Figure 3-4 and Table 3-1. A **H**–**H** mismatch pair was incorporated into the different positions of the stem region (A1–B1, A2–B2, A3–B3, and A7–B7), and the stem lengths were varied as 5, 8, and 11 base pairs (A5bp–B11bp, A3–B11bp, and A11bp–B11bp, respectively).

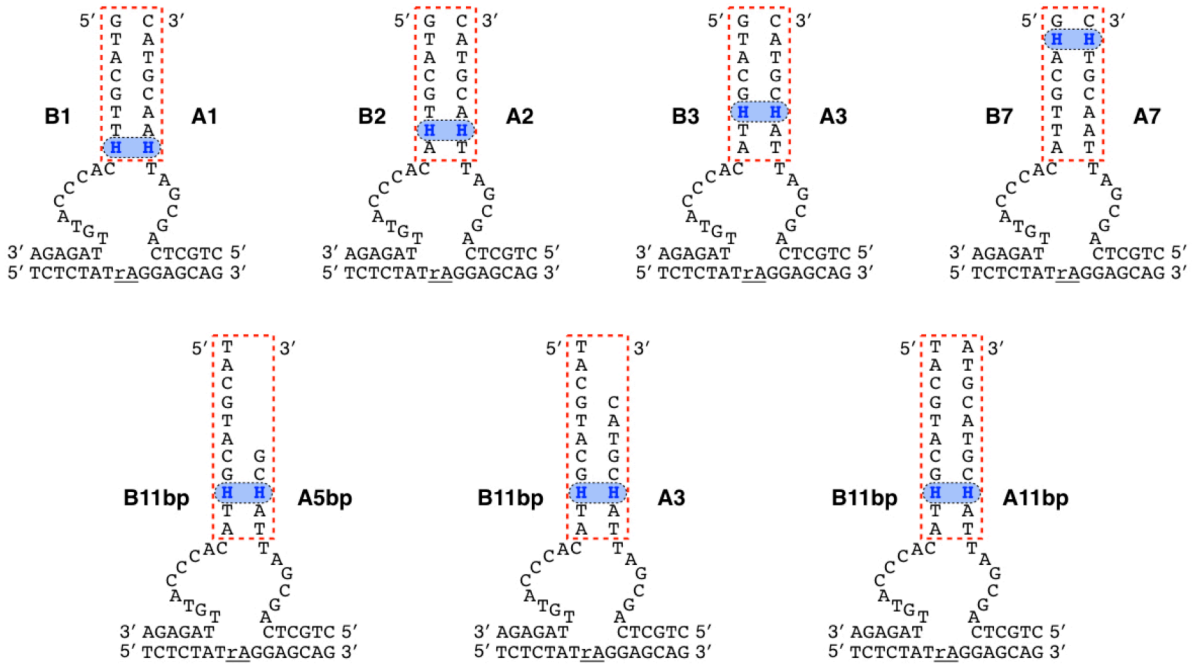

Figure 3-4. Design of **H**-containing DNA strands for Cu^{II}-responsive DNAzymes. The sequences are listed in Table 3-1.

All the **H**-bearing DNA strands were prepared by the enzymatic synthesis using the two DNA polymerases (see section **2-2** for the details). The two-step primer extension yielded the artificial DNA strands containing one **H** nucleotide. Because too short DNA strands do not function as primers for the polymerase synthesis, DNA strands possessing a **H** nucleotide near the 5′-end were synthesized with longer primer strands. After the polymerase reactions, the extra 5′-terminus was cut off by a nicking endonuclease (Nt. AlwI). The recognition sequence of Nt. AlwI was embedded into the extra overhang as shown in Table 3-2. As the endonuclease recognizes only the 5′-side of the cleavage site (i.e. the extra 5′-region), DNA strands containing a **H** nucleotide can be synthesized without any sequence limitation. Figure 3-5 represents a typical result of the enzymatic synthesis of a **H**-modified DNAzyme strand. Both the incorporation of a **H** nucleotide (step 1) and

the further elongation (step 2) progressed almost quantitatively. The cleavage of the extra 5′-terminus (step 3) afforded a product in over 80% yield. The desired **H**-modified DNAzyme strands were successfully purified by standard denaturing PAGE, gel filtration, and isopropanol precipitation. They were characterized by MALDI-TOF mass spectrometry (Figure3-5c, Table 3-1).

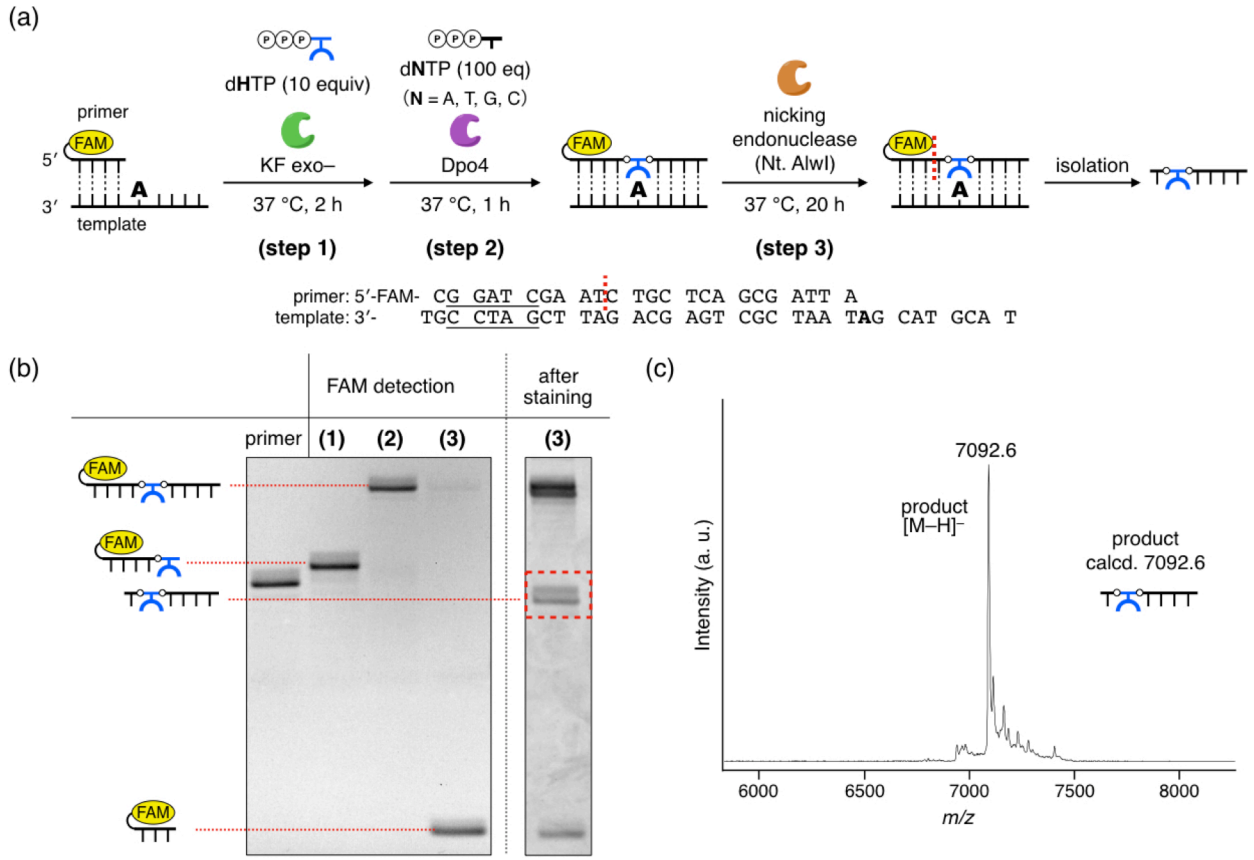

Figure 3-5. Enzymatic synthesis of **H**-containing DNA strands for Cu^{II}-responsive split DNAzymes. (a) Synthetic scheme. The extra 5′-region was cleaved by a nicking endonuclease (Nt. AlwI) in Step 3. (b) A typical result of the enzymatic synthesis (A11bp). Denaturing PAGE. (c) MALDI-TOF MS analysis of the product. Negative mode. Sodium adducts were also observed. (Step 1) [primer] = 2.0 μM, [template] = 3.0 μM, [d**H**TP] = 20 μM, [KF exo–] = 0.08 U μL^{-1} in 10 mM Tris–HCl (pH 7.9), 50 mM NaCl, 10 mM $MgCl_2$, 1.0 mM DTT, 6% PEG6000. 37 °C, 2 h. (Step 2) [primer] = 1.0 μM, [template] = 1.5 μM, [d**H**TP] = 10 μM, [dNTPs] = 100 μM each, [Dpo4] = 0.02 U μL^{-1} in 10 mM Tris–HCl (pH 7.9), 50 mM NaCl, 10 mM $MgCl_2$, 1.0 mM DTT, 6% PEG6000. 37 °C, 1 h. (Step 3) [primer] = 2.0 μM, [template] = 3.0 μM, [Nt. AlwI] = 0.2 U μL^{-1} in 50 mM AcOK, 20 mM Tris–acetate (pH 7.9), 10 mM $Mg(AcO)_2$, 0.1 mg mL^{-1} BSA. 37 °C, 20 h.

Table 3-1. Sequences of **H**-containing DNA strands for Cu^{II}-responsive DNAzymes

Name	Sequence[a] (5′ to 3′)	$[M–H]^-$	Calcd.[b]	Obs.[c]
A1	p-CTGCTCAGCGAT**H**AACGTAC	$C_{195}H_{247}N_{72}O_{121}P_{20}$	6155.0	6154.7
A2	p-CTGCTCAGCGATT**H**ACGTAC	$C_{195}H_{248}N_{69}O_{123}P_{20}$	6146.0	6146.0
A3	p-CTGCTCAGCGATTA**H**CGTAC	$C_{195}H_{248}N_{69}O_{123}P_{20}$	6146.0	6146.6
A7	CTGCTCAGCGATTAACGT**H**C	$C_{195}H_{247}N_{69}O_{120}P_{19}$	6066.0	6067.0
A5bp	p-CTGCTCAGCGATTA**H**CG	$C_{166}H_{211}N_{59}O_{105}P_{17}$	5239.4	5238.8
A11bp	p-CTGCTCAGCGATTA**H**CGTACGTA	$C_{225}H_{285}N_{81}O_{141}P_{23}$	7092.6	7092.6
B1	p-GTACGTT**H**CACCCATGTTAGAGA	$C_{226}H_{285}N_{83}O_{140}P_{23}$	7116.6	7118.7
B2	p-GTACGT**H**ACACCCATGTTAGAGA	$C_{226}H_{284}N_{86}O_{138}P_{23}$	7125.6	7127.2
B3	p-GTACG**H**TACACCCATGTTAGAGA	$C_{226}H_{284}N_{86}O_{138}P_{23}$	7125.6	7126.7
B7	p-G**H**ACGTTACACCCATGTTAGAGA	$C_{226}H_{284}N_{86}O_{138}P_{23}$	7125.6	7125.4
B11bp	p-TACGTACG**H**TACACCCATGTTAGAGA	$C_{255}H_{321}N_{96}O_{156}P_{26}$	8032.2	8032.6

a “p” stands for a 5′-phosphate group. *b* Calculated molecular mass for $[M–H]^-$. *c* Mass observed in MALDI-TOF MS analysis.

Table 3-2. Primers and templates used for synthesizing **H**-containing DNA strands

Target		Sequence[a] (5′ to 3′)
A1	primer	FAM-C*GG ATC* GAA T^CT GCT CAG CGA T
	template	GTA CGT T**A**A TCG CTG AGC AGA TTC *GAT CC*G T
A2	primer	FAM-C*GG ATC* GAA T^CT GCT CAG CGA TT
	template	GTA CGT **T**AA TCG CTG AGC AGA TTC *GAT CC*G T
A3	primer	FAM-C*GG ATC* GAA T^CT GCT CAG CGA TTA
	template	GTA CG**A** TAA TCG CTG AGC AGA TTC *GAT CC*G T
A7	primer	CTG CTC AGC GAT TAA CGT
	template	CTC TG**T** ACG TTA ATC GCT GAG CAG ATT C*GA TCC* GT
A5bp	primer	FAM-C*GG ATC* GAA T^CT GCT CAG CGA TTA
	template	CG**A** TAA TCG CTG AGC AGA TTC *GAT CC*G T
A11bp	primer	FAM-C*GG ATC* GAA T^CT GCT CAG CGA TTA
	template	TAC GTA CG**A** TAA TCG CTG AGC AGA TTC *GAT CC*G T
B1	primer	FAM-TTC ACC *GGA TC*G AAT^ GTA CGT T
	template	TCT CTA ACA TGG GTG **T**AA CGT ACA TTC *GAT CC*G GTG AAA
B2	primer	FAM-TTC ACC *GGA TC*G AAT^ GTA CGT
	template	TCT CTA ACA TGG GTG T**A**A CGT ACA TTC *GAT CC*G GTG AAA
B3	primer	FAM-TTC ACC *GGA TC*G AAT^ GTA CG
	template	TCT CTA ACA TGG GTG TA**A** CGT ACA TTC *GAT CC*G GTG AAA
B7	primer	FAM-TTC ACC *GGA TC*G AAT^ G
	template	TCT CTA ACA TGG GTG TAA CGT **A**CA TTC *GAT CC*G GTG AAA
B11bp	primer	FAM-C*GG ATC* GAA T^TA CGT ACG
	template	TCT CTA ACA TGG GTG TA**A** CGT ACG TAA TTC *GAT CC*G G

a The recognition sites for the nicking endonuclease (Nt. AlwI) are shown in italic, and the nicking sites are indicated by "^". The incorporation sites for a **H** nucleotide on the template strands are shown in bold.

3-3. Sequence investigation of a Cu^{II}-responsive split DNAzyme

To find out a Cu^{II}-responsive DNAzyme, the RNA-cleaving activity of each **H**-modified DNAzyme was evaluated in the absence and in the presence of equimolar Cu^{II} ions. The reaction was performed with one equivalent of a substrate labeled with a FAM fluorophore, and the substrate cleavage was analyzed by denaturing PAGE. The fraction of the cleaved substrate was calculated from the band intensities (Figures 3-6, 3-7, and 3-8).

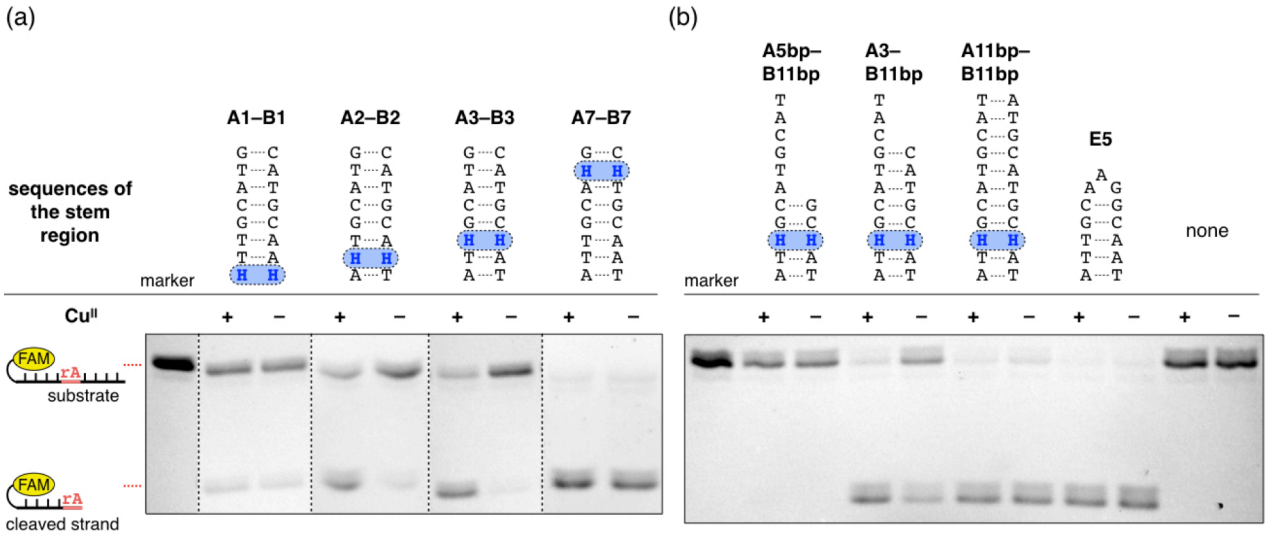

Figure 3-6. Denaturing PAGE analysis of the RNA-cleaving activity of the modified DNAzymes containing a **H**–**H** base pair. (a) DNAzymes containing a **H**–**H** base pair at different positions. (b) DNAzymes containing a **H**–**H** pair with different stem lengths. [DNAzyme] = 1.0 μM, [substrate] = 1.0 μM, [$CuSO_4$] = 0 or 1.0 μM in 10 mM HEPES (pH 7.0), 1.0 M NaCl, 10 mM $MgCl_2$. 25 °C, 3 h. FAM detection.

The stem length was first fixed to 8 base pairs, and the position of the **H**–**H** pair was changed (Figure 3-7). A DNAzyme possessing a **H**–**H** pair next to the catalytic domain (**A1**–**B1**) showed a rather low activity (less than 30% cleavage) even in the presence of Cu^{II} ions. The **H**–Cu^{II}–**H** base pair formed close to the catalytic domain was likely to distort the catalytically active structure because its C1′–C1′ distance (12.7 Å in a DNA analogue[19]) is longer than that of natural Watson–Crick base pairs (10.7 Å). The incorporation of unnatural nucleotides may have also disrupted the intrinsic interactions necessary for the folding of the DNAzyme tertiary structure. A DNAzyme possessing a **H**–**H** pair near the stem terminus (**A7**–**B7**) exhibited an activity comparable to the original E5 DNAzyme (around 90% cleavage) both in the absence and in the presence of Cu^{II} ions.

This may result from the thermal stability of the stem duplex having a **H**–**H** mismatch, which is high enough to be hybridized even under the Cu^{II}-free condition. Among the sequences tested, a DNAzyme containing a **H**–**H** pair at the third position (**A3**–**B3**) showed the highest turn-on ratio (4.8).

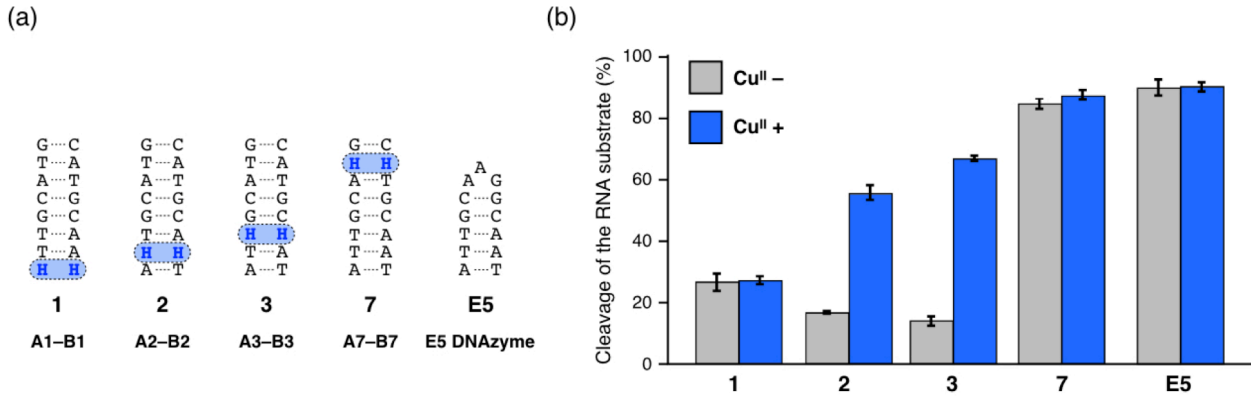

Figure 3-7. RNA-cleaving activity of modified DNAzymes containing a **H**–**H** base pair at the different positions in the stem. (a) Sequences of the stem region of the DNAzymes. (b) RNA-cleaving activity. [DNAzyme] = 1.0 μM, [substrate] = 1.0 μM, [$CuSO_4$] = 0 or 1.0 μM in 10 mM HEPES (pH 7.0), 1.0 M NaCl, 10 mM $MgCl_2$. 25 °C, 3 h. *N* = 3. Error bars indicate standard errors.

Next, the stem length was altered from 5 to 11 base pairs with the position of the **H**–**H** pair fixed at the third position (Figure 3-8). A DNAzyme with a shorter stem (**A5bp**–**B11bp**) did not cleave the substrate even in the presence of Cu^{II} ions. This 5-base-pair (bp) duplex is not thermally stable enough to associate the split DNAzyme strands in response to Cu^{II} ions. In contrast, a DNAzyme with a longer stem (**A11bp**–**B11bp**) exhibited an RNA-cleaving activity comparable to E5 DNAzyme both in the presence and in the absence of Cu^{II} ions. This result can be attributed to the high stability of the 11-bp stem duplex even with a **H**–**H** mismatch pair. The activity of the DNAzyme with an 8-bp stem (**A3**–**B11bp**) was efficiently regulated in response to Cu^{II} ions through the hybridization of the split strands mediated by **H**–Cu^{II}–**H** base pairing.

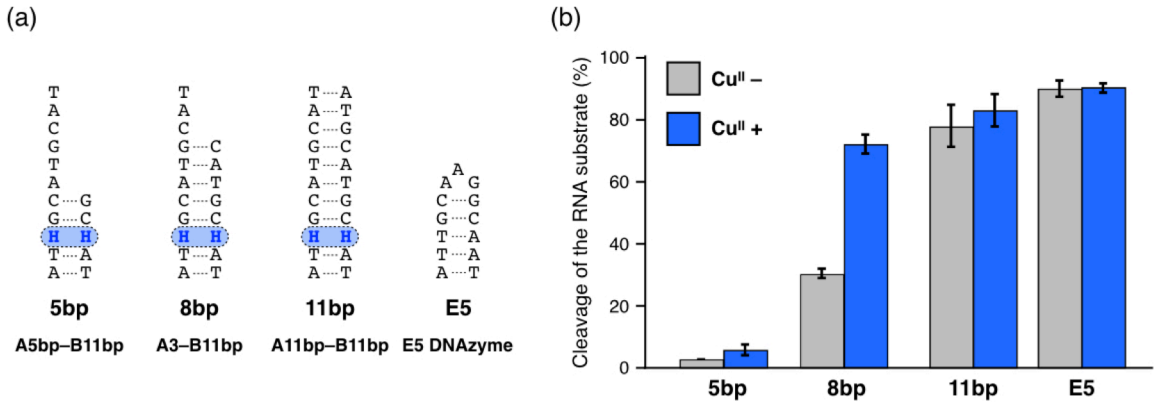

Figure 3-8. RNA-cleaving activity of the modified DNAzymes containing a **H**–**H** base pair with different stem lengths. (a) Sequences of the stem region of the DNAzymes. (b) RNA-cleaving activity. [DNAzyme] = 1.0 μM, [substrate] = 1.0 μM, [$CuSO_4$] = 0 or 1.0 μM in 10 mM HEPES (pH 7.0), 1.0 M NaCl, 10 mM $MgCl_2$. 25 °C, 3 h. *N* = 3. Error bars indicate standard errors.

Taken all together, the highest turn-on ratio was observed with a DNAzyme containing a **H**–**H** pair at the third position in the 8-bp stem (**A3**–**B3**), which is hereafter referred to as split **H**-DNAzyme (Figure 3-9). In the presence of one equivalent of Cu^{II} ions, the activity of the split **H**-DNAzyme was enhanced five-fold, which is acceptable for further application to develop DNA-based systems such as logic gates and molecular machines.

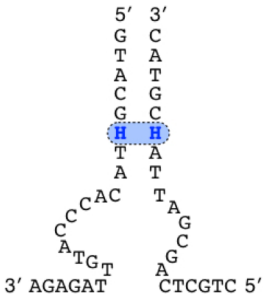

Figure 3-9. Sequence of the most active Cu^{II}-responsive split DNAzyme (split **H**-DNAzyme).

3-4. Activity assay of the Cu^{II}-responsive split DNAzyme

The catalytic activity of the split **H**-DNAzyme was further evaluated with an excess amount of the RNA substrate ([substrate]/[**H**-DNAzyme] = 10). Figure 3-10 shows the time-course analysis of the RNA-cleaving reactions by the split **H**-DNAzyme and the original E5 DNAzyme. Apparent first-order rate constants (k_{obs}) were estimated from the initial velocities. The result showed that the split **H**-DNAzyme catalytically cleaved the excess amount of the substrate. The initial rate of the RNA-cleaving reaction in the presence of Cu^{II} ions (k_{obs} = 0.16 ± 0.01 h^{-1}) was 5.5-times higher than that in the absence of Cu^{II} (0.029 ± 0.004 h^{-1}). This result supports that the activity of the split **H**-DNAzyme was regulated in a Cu^{II}-dependent manner. The rate of the RNA-cleaving reaction catalyzed by the split **H**-DNAzyme (k_{obs} = 0.16 ± 0.01 h^{-1}) was slightly decreased from that of the original E5 DNAzyme (0.23 ± 0.01 h^{-1}). This is possibly due to the slight distortion of the catalytically active structure by a **H**–Cu^{II}–**H** artificial base pair. The addition of Cu^{II} ions neither changed the activity of the original E5 DNAzyme (black and gray lines), nor caused substrate cleavage without DNAzymes (blue line). Therefore, the Cu^{II}-induced acceleration of the reaction was attributed to the enhancement of the catalytic activity of the **H**-DNAzyme itself.

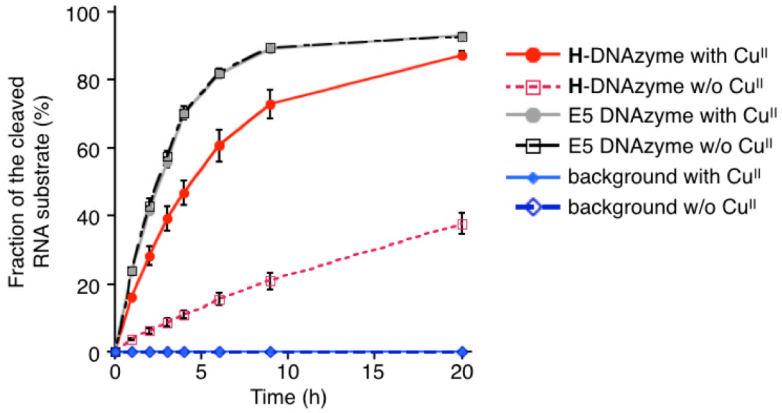

Figure 3-10. RNA-cleaving activity of the split **H**-DNAzyme and the original E5 DNAzyme in the absence and in the presence of one equivalent of Cu^{II} ions. [DNAzyme] = 1.0 μM, [substrate] = 10 μM, [$CuSO_4$] = 0 or 1.0 μM in 10 mM HEPES (pH 7.0), 1.0 M NaCl, 10 mM $MgCl_2$. 25 °C. *N* = 3. Error bars indicate standard errors.

Next, the activity of the split **H**-DNAzyme was assessed at different concentrations of Cu^{II} ions (Figure 3-11). The addition of more than one equivalent of Cu^{II} ions did not enhance the DNAzyme activity. It shows that an equimolar amount of Cu^{II} ions is enough to activate the split **H**-DNAzyme. This result agrees with the previous observation that a **H**–Cu^{II}–**H** base pair formed almost quantitatively within a duplex even at micromolar concentrations.[17] These results confirmed that the quantitative formation of a **H**–Cu^{II}–**H** base pair associated the split strands, resulting in the reconstruction of the active DNAzyme structure.

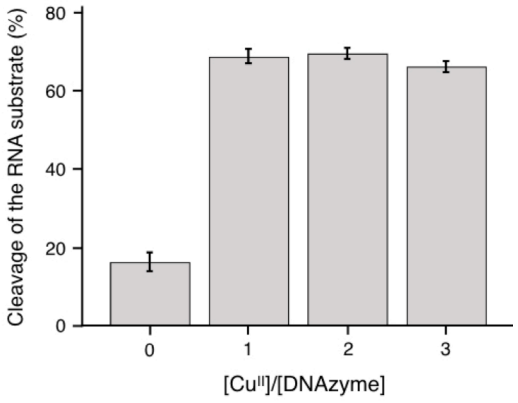

Figure 3-11. RNA-cleaving activity of the split **H**-DNAzyme at different concentrations of Cu^{II} ions. [**H**-DNAzyme] = 1.0 μM, [substrate] = 1.0 μM, [$CuSO_4$] = 0, 1.0, 2.0, or 3.0 μM in 10 mM HEPES (pH 7.0), 1.0 M NaCl, 10 mM $MgCl_2$. 25 °C, 3 h. *N* = 4. Error bars indicate standard errors.

To verify the Cu^{II}-triggered association of the split **H**-DNAzyme, the melting temperature (T_m) of the stem duplex was roughly estimated under the reaction condition (Table 3-3). The thermal stability of the 8-bp stem duplex possessing a **H**–**H** pair was estimated by the melting temperatures (T_m) of 15-bp DNA duplexes possessing a T–T, a C–G, a **H**–**H**, or a **H**–Cu^{II}–**H** base pair and 8-bp stem duplexes possessing a T–T or a C–G pair instead of a **H**–**H** pair. Assuming that the differences in the T_m values are the same as the 15-bp duplexes and the 8-bp stems, the thermal stability was estimated as follows,

T_m(8-bp, **H**–**H**) = T_m(8-bp, T–T) + {T_m(15-bp, **H**–**H**) – T_m(15-bp, T–T)},

T_m(8-bp, **H**–Cu^{II}–**H**) = T_m(8-bp, C–G) + {T_m(15-bp, **H**–Cu^{II}–**H**) – T_m(15-bp, C–G)}.

The estimated T_m values of the stem in the split **H**-DNAzyme were 16.5 °C and 41.7 °C in the

absence and in the presence of Cu^{II} ions, respectively. This result corroborates that the formation of a **H**–Cu^{II}–**H** base pair triggers the hybridization of the stem duplex to restore the catalytically active structure of the split **H**-DNAzyme.

Table 3-3. Melting temperatures of DNA duplexes under the condition for the DNAzyme reaction[a]

X–Y	T–T	**H**–**H**	C–G	**H**–Cu^{II}–**H**
15-bp[b]	46.6 ± 0.6	47.4 ± 0.8	57.9 ± 0.8	65.2 ± 0.5
8-bp stem[c]	15.7 ± 1.5	(16.5)[d]	34.4 ± 0.7	(41.7)[d]

a Averages of three runs are shown with standard errors. [DNA duplex] = 2.0 μM, [$CuSO_4$] = 0 or 2.0 μM (1.0 equiv) in 10 mM HEPES (pH 7.0), 1.0 M NaCl, 10 mM $MgCl_2$. 0.2 °C min^{-1}. *b* (5′-CAC ATT A**X**T GTT GTA-3′)·(3′-GTG TAA T**Y**A CAA CAT-5′). *c* (5′-GTA CG**X** TA-3′)·(3′-CAT GC**Y** AT-5′). *d* These T_m values were roughly estimated as follows: T_m(8-bp, **H**–**H**) = T_m(8-bp, T–T) + {T_m(15-bp, **H**–**H**) – T_m(15-bp, T–T)}, T_m(8-bp, **H**–Cu^{II}–**H**) = T_m(8-bp, C–G) + {T_m(15-bp, **H**–Cu^{II}–**H**) – T_m(15-bp, C–G)}.

It should be noted that the DNAzyme activity was regulated through the incorporation of only a single **H**–Cu^{II}–**H** base pair. The formation of one **H**–Cu^{II}–**H** base pair significantly raises the thermal stability of DNA duplexes (ΔT_m = +18 °C under the reaction condition), thus inducing the Cu^{II}-responsive DNA hybridization efficiently. In addition, Cu^{II} ions specifically bind to **H** nucleotides without interfering natural nucleobases, resulting in the selective formation of the active structure. Therefore, **H**–Cu^{II}–**H** base pairing is more suited for the development of metal-responsive functional DNAs than widely utilized Hg^{II}- and Ag^{I}-mediated base pairs consisting of natural pyrimidine bases (i.e. T−Hg^{II}−T[16] and C−Ag^{I}−C[20]).[21] To validate the superiority, two split DNAzymes were prepared by replacing a **H**–**H** pair in the **H**-DNAzyme with a T–T and a C–C pairs (Figure 3-12a). They would be activated by the formation of a T−Hg^{II}−T and a C−Ag^{I}−C base pairs, respectively. The DNAzyme activities, however, were not increased by the addition of equimolar Hg^{II} or Ag^{I} ions, while the split **H**-DNAzyme was activated by adding Cu^{II} ions under the same condition (Figure 3-12b). This result shows that T−Hg^{II}−T and C−Ag^{I}−C base pairing cannot induce the association of the split DNAzymes possibly due to the smaller stabilization effect (ΔT_m = 2–9 °C)[22] than that by **H**–Cu^{II}–**H**. This is also because Hg^{II} and Ag^{I} ions were likely to bind to the DNAzyme and the substrate strands in an unspecific manner. The result agreed with the precedent

studies that needed to use multiple T−Hg^{II}−T and C−Ag^{I}−C base pairs for the regulation of DNAzyme activities.[8,12–14]

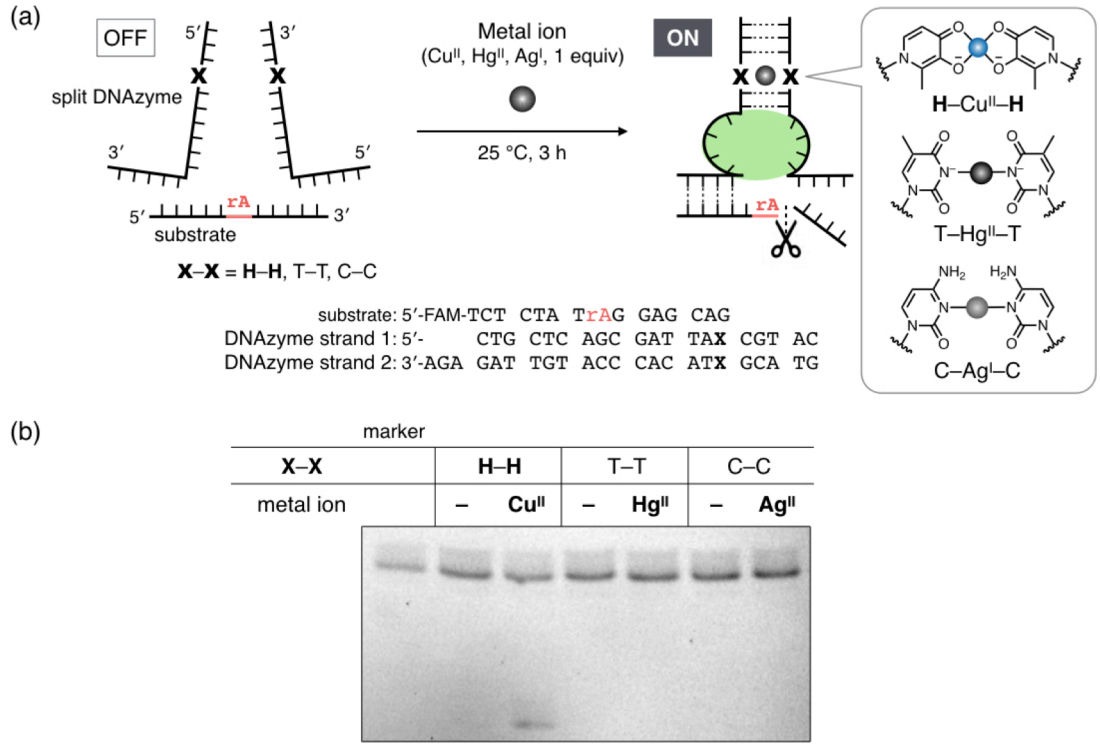

Figure 3-12. RNA-cleaving activity of the split DNAzymes containing a H–H, a T–T, or a C–C base pair in the absence and in the presence of one equivalent of metal ions. (a) Reaction scheme. [DNAzyme] = 1.0 μM, [substrate] = 1.0 μM, [metal ion] = 0 or 1.0 μM in 10 mM HEPES (pH 7.0), 1.0 M $NaNO_3$, 10 mM $Mg(NO_3)_2$. 25 °C, 3 h. (b) Denaturing PAGE analysis. FAM detection.

3-5. Metal selectivity of the Cu^{II}-responsive split DNAzyme

The metal selectivity of the split **H**-DNAzyme was then studied. Figure 3-13 shows the fraction of the cleaved RNA substrate in the presence of one equivalent of various transition metal ions. For the experiments with Hg^{II} and Ag^{I} ions, chloride ions in the buffer were replaced by nitrate ions. Among metal ions tested, only Cu^{II} ions enhanced the catalytic activity while the other metal ions did not have any influence on the cleavage reaction.

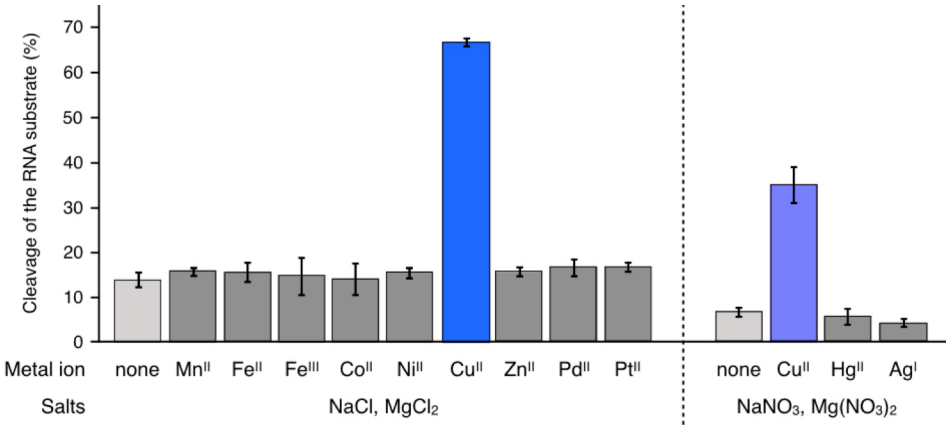

Figure 3-13. Metal selectivity of the split **H**-DNAzyme. [DNAzyme] = 1.0 μM, [substrate] = 1.0 μM, [metal ions] = 1.0 μM (1.0 equiv) in 10 mM HEPES (pH 7.0), 1.0 M NaCl, 10 mM $MgCl_2$. 25 °C, 3 h. *N* = 3. For the experiments with Hg^{II} and Ag^{I} ions, NaCl and $MgCl_2$ in the buffer were replaced by $NaNO_3$ and $Mg(NO_3)_2$, respectively. Error bars indicate standard errors.

This excellent metal specificity is fairly consistent with the selective formation of a **H**–Cu^{II}–**H** base pair in a DNA duplex. Figure 3-14 shows the melting profiles of a 15-bp duplex containing a **H**–**H** pair in the presence of the metal ions discussed above. The addition of one equivalent of Cu^{II} ions greatly stabilized the duplex (ΔT_m = +13 °C) through the formation of a **H**–Cu^{II}–**H** base pair. In the cases with most of the other metal ions except Fe^{II} ions, the thermal stability of the duplex was not changed at all, thus showing the high metal selectivity of a **H**–**H** pair.

It should be noted that Fe^{II} ions increased the thermal stability of the DNA duplex while it did not activate the **H**-DNAzyme. Fe^{II} ions form a 3:1 octahedral complex in general, which would severely distort the DNAzyme structure upon binding to **H** nucleotides. No activation of the DNAzyme can be also ascribed to the weaker binding of Fe^{II} ions, which is inferred from the

non-sigmoidal melting curve. It was previously reported that **H** nucleotides can form 3:1 complexes with Fe^{III} ions to provide triple-stranded DNA helices, but only at a high concentration (50 μM).[23] The previous finding is compatible with the results that Fe^{III} ions did not enhance the DNAzyme activity or stabilize the **H**-containing duplex.

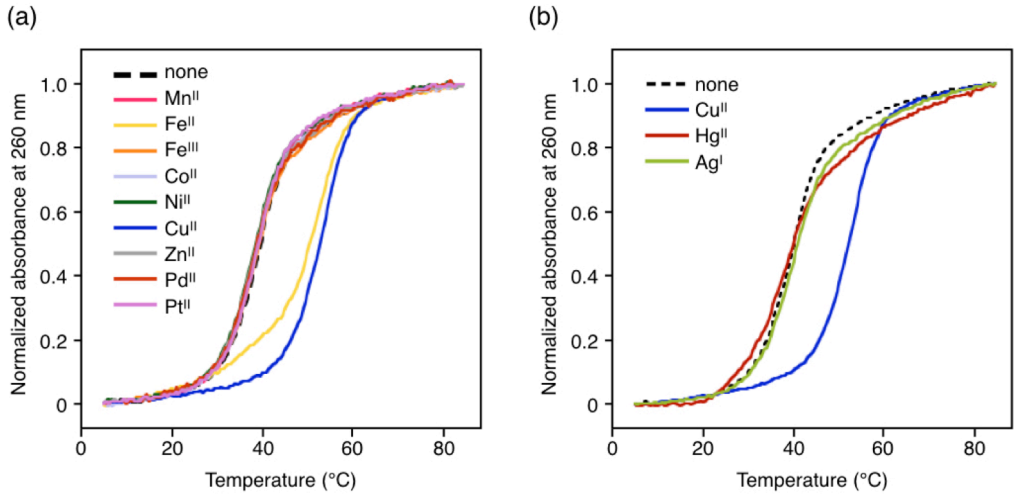

Figure 3-14. Melting analysis of DNA duplexes containing a **H**–**H** pair in the presence of various metal ions. Duplex sequence: (5′-CAC ATT A**H**T GTT GTA-3′)·(3′-GTG TAA T**H**A CAA CAT-5′). [DNA duplex] = 2.0 μM, [metal ions] = 2.0 μM (1.0 equiv) in 10 mM HEPES (pH 7.0), 100 mM NaCl (a) or $NaNO_3$ (b). 0.2 °C min^{-1}. All the samples were annealed before the measurement.

More importantly, the split **H**-DNAzyme was activated neither by Hg^{II} nor Ag^{I} ions, which are widely exploited for the formation of T–Hg^{II}–T and C–Ag^{I}–C base pairs. This result suggests that the Cu^{II}-responsive **H**-DNAzyme can be regulated in an orthogonal manner with Hg^{II}- or Ag^{I}-responsive DNA systems using T–Hg^{II}–T and C–Ag^{I}–C base pairs. The multimetal-dependent regulation of DNAzyme activities will be discussed in **chapter 5**.

3-6. Cu^{II}-dependent regulation of the DNAzyme activity

The regulation of the DNAzyme activity was examined by the addition and removal of Cu^{II} ions. Figure 3-15a represents the result of the Cu^{II}-induced activation of the split **H**-DNAzyme. The RNA-cleaving reaction was initiated without Cu^{II} ions. After 1 h, equimolar Cu^{II} ions were added to the reaction mixture to activate the DNAzyme (blue line). The DNAzyme activity was instantly increased to almost the same level as observed when the reaction started with Cu^{II} ions. This result indicates that the fast formation of a **H**–Cu^{II}–**H** base pair enabled the quick activation of the split **H**-DNAzyme under an isothermal condition. Next, deactivation of the split DNAzyme was demonstrated by removing Cu^{II} ions with the use of a natural Cu^{II}-binding peptide, Gly-His-Lys (GHK),[24] as a chelator (K_a = 7 × 10^{14} M).[25] The addition of one equivalent of GHK rapidly diminished the catalytic activity (Figure 3-15b, green line). The activity decrease was ascribed to the disassembly of the two split strands via the dissociation of the **H**–Cu^{II}–**H** base pair caused by the removal of Cu^{II} ions. Moreover, the iterative switching of the DNAzyme activity was accomplished

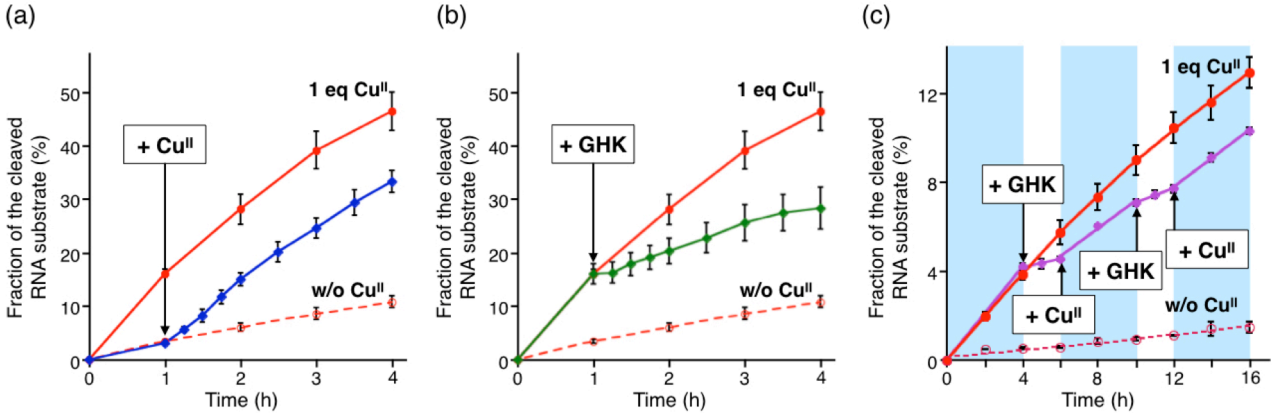

Figure 3-15. Regulation of the RNA-cleaving activity of the split **H**-DNAzyme by the addition and removal of Cu^{II} ions. (a) Activation of the split **H**-DNAzyme by adding one equivalent of Cu^{II} ions. (b) Deactivation of the split **H**-DNAzyme by removing Cu^{II} ions. The reaction was initiated in the presence of 1.0 equivalent of Cu^{II} ions. After 1 h, 1.0 equivalent of a Cu^{II}-binding tripeptide, Gly-His-Lys (GHK), was added to remove Cu^{II} ions. (c) Repetitive switching of the activity of **H**-DNAzyme by the alternate addition of Cu^{II} ions and a GHK peptide. In this experiment, a two-base shorter strand (5′-CTC TAT rAGG AGC A-3′) was used as a substrate. [DNAzyme] = 1.0 μM, [substrate] = 10 μM in 10 mM HEPES (pH 7.0), 1.0 M NaCl, 10 mM $MgCl_2$. 25 °C. *N* = 3. The activities of the **H**-DNAzyme in the presence and in the absence of Cu^{II} ions are also shown as a red solid line and a red dashed line, respectively. Error bars indicate standard errors.

by the alternate addition and removal of Cu^{II} ions (Figure 3-15c). A two-base shorter substrate strand was used to suppress the DNAzyme activity in the absence of Cu^{II} ions, leading to a larger on–off ratio (ca. 10). The result shows that the second addition of one equivalent of Cu^{II} ions revived the split **H**-DNAzyme (purple line). In a consequence, the DNAzyme activity was repetitively switched by the alternate addition of Cu^{II} ions and the Cu^{II}-binding peptide.

The DNAzyme activity was also modulated based on the redox reactions of Cu^{II} ions. Redox reactions of metal ions have been widely utilized for controlling structures of polymers[26] and supramolecules[27] and dynamics of molecular machines.[28] The redox chemistry has also attracted much attention in the field of DNA-based supramolecular chemistry[29–31] and recently applied to regulate the thermal stability of a DNA duplex possessing a Cu^{I}-mediated base pair.[32] Accordingly, the redox-dependent activity of the split **H**-DNAzyme was assayed by using ascorbate and hypochlorite as a reductant and an oxidant, respectively. First, the deactivation of the split **H**-DNAzyme was examined by reducing Cu^{II} ions (Figure 3-16a). When sodium ascorbate (Asc) was added to a mixture of the **H**-DNAzyme and Cu^{II} ions, the RNA-cleaving activity was immediately decreased to the level observed under the Cu^{II}-free condition. The addition of the reductant presumably triggered the dissociation of the **H**–Cu^{II}–**H** base pair, resulting in the deactivation of the split **H**-DNAzyme. Figure 3-16b shows the reactivation of the DNAzyme by the addition of the oxidant. The reaction was initiated in the presence of both Cu^{II} ions and ascorbate to retain the off-state activity. Upon the addition of an excess amount of hypochlorite, the DNAzyme activity was significantly increased possibly due to the oxidation of Cu^{I} ions. Furthermore, the iterative switching of the catalytic activity was demonstrated by the successive addition of the reductant and the oxidant (Figure 3-16c, green line). It should be noted that the addition of the reductant and the oxidant did not have any effects on the activity of the original E5 DNAzyme, and no substrate cleavage was observed without DNAzyme strands (Figures 3-16d, 3-16e, and 3-16f). Although it cannot be excluded that the disproportionation of Cu^{I} ions occurred to some degree, these results suggest the potential for redox-dependent regulation of DNAzyme activities via **H**–Cu^{II}–**H** base pairing.

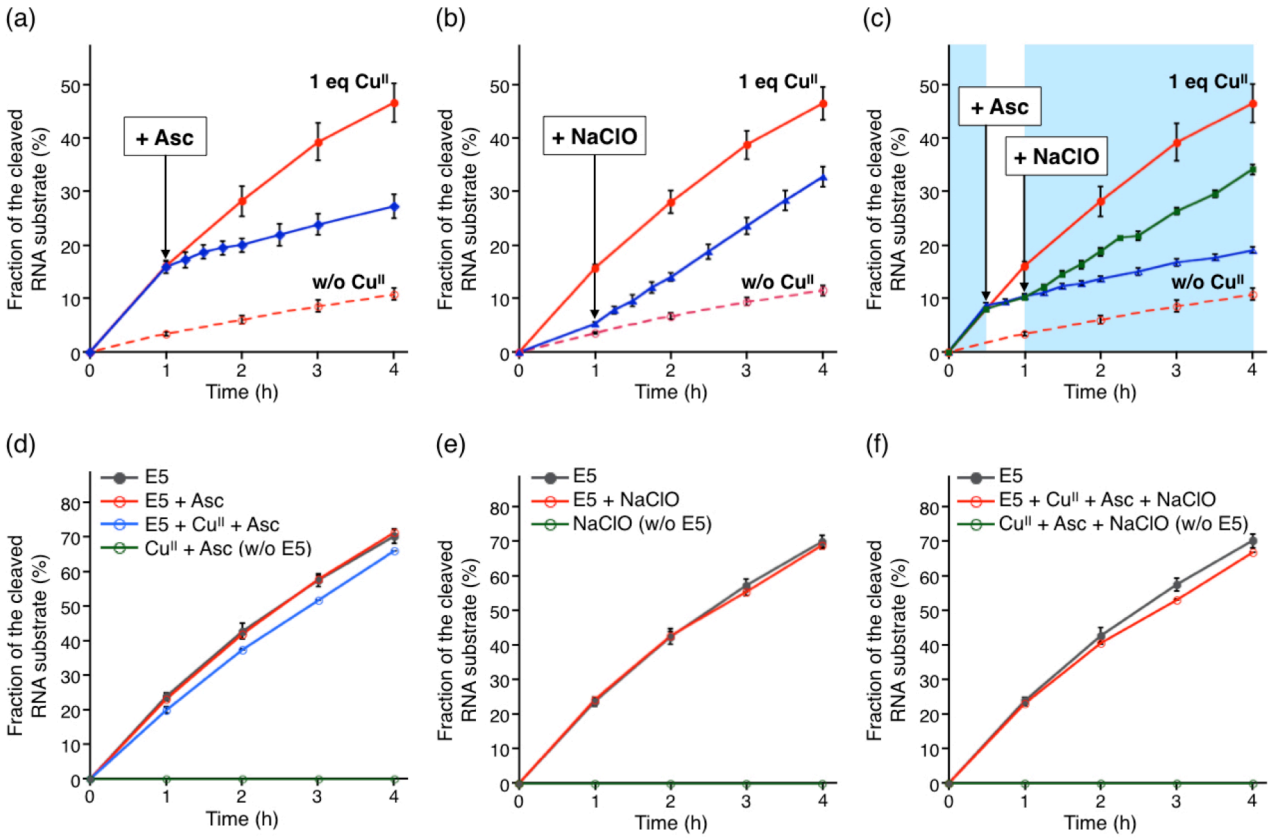

Figure 3-16. Regulation of the RNA-cleaving activity of the split **H**-DNAzyme by the redox reactions of Cu^{II} ions. (a) Deactivation of the **H**-DNAzyme with a reductant. The reaction was initiated in the presence of 1.0 equivalent of Cu^{II} ions. After 1 h, 10 equivalents of sodium ascorbate (Asc) were added. (b) Activation of the **H**-DNAzyme with an oxidant. The reaction was initiated in the presence of 1.0 equivalent of Cu^{II} ions and 10 equivalents of sodium ascorbate. After 1 h, 20 equivalents of an oxidant (NaClO) were added to regenerate Cu^{II} ions. (c) Iterative switching of the activity of the split **H**-DNAzyme. (d,e,f) Control experiments using E5 DNAzyme. [DNAzyme] = 1.0 μM, [substrate] = 10 μM, [$CuSO_4$] = 1.0 μM (1.0 equiv, where applicable), [sodium ascorbate] = 10 μM (10 equiv, where applicable) and [NaClO] = 20 μM (20 equiv, where applicable) in 10 mM HEPES (pH 7.0), 1.0 M NaCl, 10 mM $MgCl_2$. 25 °C. *N* = 3 (a, b, d, e, f), 4 (c). The activities of the **H**-DNAzyme in the presence and in the absence of Cu^{II} ions are also shown in a red solid line and a red dashed line, respectively, in a–c. Error bars indicate standard errors.

3-7. Conclusion

I have developed a Cu^{II}-responsive split DNAzyme, whose activity was modulated through the formation of a **H**–Cu^{II}–**H** base pair. Cu^{II}-responsive split DNAzymes were developed as follows; (i) a reported DNAzyme is separated into two strands, (ii) a pair of **H** nucleotides are incorporated into a stem region of the DNAzyme, and (iii) the position of a **H**–**H** pair and the stem length are adjusted such that the formation of a **H**–Cu^{II}–**H** base pair can associate the two split strands. DNA strands containing a **H** nucleotide were prepared by the polymerase synthesis to optimize the sequence of the DNAzyme. After the sequence screening, a Cu^{II}-responsive DNAzyme (split **H**-DNAzyme), which has a **H**–Cu^{II}–**H** base pair in the third position from the catalytic core, was successfully obtained. The split **H**-DNAzyme was activated by the quantitative formation of a **H**–Cu^{II}–**H** base pair. The DNAzyme exhibited extremely high metal specificity because of the selective formation of a **H**–Cu^{II}–**H** base pair. The reversible regulation of the DNAzyme activity was demonstrated by the alternate addition and removal of Cu^{II} ions. The activity was further regulated by the redox reactions of Cu^{II} ions.

The **H**-DNAzyme developed here is the first example of metal-responsive functional DNAs with the use of a metal-mediated base pair consisting of unnatural nucleotides. The preceding studies exploited only T–Hg^{II}–T and C–Ag^{I}–C base pairs for the regulation of DNAzyme activities.[8,12–14,33] Hg^{II} and Ag^{I} ions can bind to pyrimidine nucleobases in an unspecific manner, which would disrupt a high-order structure of a DNAzyme, often inhibiting its catalytic activity. In contrast, Cu^{II} ions rarely interfere with natural nucleobases, leading to efficient activation of a DNAzyme induced by a single metal-mediated base pair. The incorporation of other unnatural nucleotides would provide DNAzymes that respond to different metal ions. As shown in the section **3-6**, the DNAzyme activities with metallo-base pairs can be regulated by redox reactions of metal ions, including an electrochemical approach.[29,30] Thus, this study would offer a design principle of metal-responsive split DNAzymes with metal-mediated artificial base pairs.

Some reported DNAzymes exhibit their activity by utilizing Cu^{II} ions as a cofactor.[34] On the other hand, the split **H**-DNAzyme was activated through the formation of a **H**–Cu^{II}–**H** base pair

distant from the catalytic site. The whole DNAzyme structure was reconstructed by the formation of only a single **H**–Cu^{II}–**H** pair, resulting in the Cu^{II}-dependent regulation of the catalytic activity. This suggests that various Cu^{II}-responsive DNAzymes can be developed by splitting the DNAzyme strands and incorporating a **H**–Cu^{II}–**H** base pair. Because many kinds of split DNAzymes have been reported so far,[3–15] various Cu^{II}-responsive DNA supramolecules will be developed based on the same strategy.

The split DNAzyme described here regulated its activity by controlling DNA hybridization with the aid of the metal-mediated base pairing. Functional nucleic acids and DNA architectures are often comprised of multiple DNA strands, which undergo self-hybridization to construct an active structure. Accordingly, the design principle would be applicable to metal-dependent regulation of various DNA structures and functions by employing metal-mediated base pairs. I believe that this study would offer a general approach to the development of metal-responsive DNA materials.

3-8. Experimental section

Materials and equipment

All the natural DNA strands, including the primers and the templates, the 6-carboxyfluorescein (FAM)-labeled strands, and the substrate strand containing a riboadenosine (rA) were purchased from Japan Bio Service Co., Ltd. (Saitama, Japan) of HPLC purification grades. Hydroxypyridone nucleoside triphosphate (d**H**TP) was synthesized according to the reported procedures.[35] Natural nucleoside triphosphates (dNTPs) were purchased from Toyobo Co., Ltd. Klenow Fragment (3′→5′ exo–) (KF exo–), Sulfolobus DNA Polymerase IV (Dpo4), and Nt.AlwI were purchased from New England Biolabs, Inc. Metal sources were purchased from FUJIFILM Wako Pure Chemical Industries ($CuSO_4 \cdot 5H_2O$ (99.5% purity), $MnCl_2 \cdot 4H_2O$ (99%), $FeSO_4 \cdot 7H_2O$ (99.0–102.0%), $FeCl_3$ (98%), $CoSO_4 \cdot 7H_2O$ (99.0–102.0%), K_2PtCl_4 (98%), $Hg(ClO_4)_2 \cdot 3H_2O$ (99%), $AgNO_3$ (99.8%)), Soekawa Chemical Co. ($NiSO_4 \cdot 7H_2O$ (99%), $ZnSO_4 \cdot 7H_2O$ (99.9%)), and Tokyo Chemical Industry (Na_2PdCl_4 (98%)) and used without further purification.

Matrix assisted laser desorption ionization time-of-flight (MALDI-TOF) mass spectra were recorded on Bruker ultrafleXtreme and Autoflex III using a mixture of 3-hydroxypicolinic acid (3-HPA) and ammonium citrate as a matrix. Denaturing polyacrylamide gel electrophoresis (PAGE) was carried out with 20% polyacrylamide gel containing 7 M urea. The gels were analyzed using Gel Doc EZ Imager and Image Lab software (Bio-Rad).

Chemical synthesis of DNA strand containing a hydroxypyridone (H) nucleotide

15-mer DNA strands containing a **H** nucleotide (15-bp T_m **1** and **2**; Table 3-4) were synthesized by an NTS M-4-MX DNA/RNA synthesizer (Nihon Techno Service) on a 1-μmol scale in a DMTr-on mode with natural DNA phosphoramidites and standard reagents (Glen Research). A phosphoramidite derivative of **H** nucleoside was synthesized according to the reported procedures.[17] The DNA synthesis was carried out in accordance with the standard procedure except for an extended coupling time (15 min). The products were deprotected using 28% NH_3 aqueous solution at 55 °C for 12 h. The oligonucleotides were firstly purified and detritylated using

a PolyPak II cartridge (Glen Research) and further purified by reverse phase HPLC (Waters XBridge C18 column, 0.1 M TEAA (pH 7.0)/MeCN gradient, 60 °C). The amounts of the oligonucleotides were determined based on the UV absorbance at 260 nm. The molar extinction coefficients of the oligonucleotides were determined by the nearest-neighbor method (Table 3-4, ε_{260} = 5.34 × 10^3 for **H** nucleoside).[17] The products were characterized by MALDI-TOF mass spectrometry (Table 3-4).

Polymerase synthesis of DNAzyme strands containing a H nucleotide

A primer and a template strands (Table 3-2) were mixed in a buffer (10 mM Tris–HCl (pH 7.9), 50 mM NaCl, 10 mM $MgCl_2$, 1 mM dithiothreitol, 6% PEG6000) and annealed prior to the reaction (85 °C → 4 °C, 1.0 °C min^{-1}). After the addition of d**H**TP and KF exo– , the reaction mixture was incubated at 37 °C for 2 h. The concentration of each component was as follows: [primer] = 2.0 μM, [template] = 3.0 μM, [d**H**TP] = 20 μM (10 equiv), and [KF exo–] = 0.08 U μL^{-1}. The reaction mixture was subsequently heated at 85 °C for 10 min to deactivate KF exo– polymerase and annealed again (85 °C → 4 °C, 1.0 °C min^{-1}). After natural nucleoside triphosphates (dNTPs) and Dpo4 polymerase were added, the reaction mixture was incubated at 37 °C for 1 h. The final concentration of each component was as follows: [primer] = 1.0 μM, [template] = 1.5 μM, [d**H**TP] = 10 μM (10 equiv), [dNTPs] = 100 μM (100 equiv), and [Dpo4 polymerase] = 0.02 U μL^{-1}. The reaction progress was monitored by subjecting an aliquot of the reaction mixture to denaturing PAGE analysis. After the reaction was quenched by adding an equal volume of 50 mM EDTA, the reaction mixture was heated at 95 °C for 10 min. The product strand was separated from the template by denaturing PAGE, and the isolated product was further purified by gel filtration (Sephadex G-25 Fine, GE Healthcare) and the subsequent isopropanol precipitation. The amounts of the DNA strands were determined based on the UV absorbance at 260 nm. The molar extinction coefficients (ε_{260}) of the oligonucleotides were determined by the nearest-neighbor method (ε_{260} = 5.34 × 10^3 for **H** nucleoside).

For some of the DNAzyme strands, extra 5′-terminus was removed by a nicking endonuclease,

Nt. AlwI, to prepare the strands with a desired sequence. After the two-step primer extension, the full-length strand was roughly purified with the template strand by isopropanol precipitation. The two DNA strands were annealed (85 °C → 4 °C, 1.0 °C min^{-1}) in a buffer (20 mM Tris–AcOH (pH 7.9), 50 mM AcOK, 10 mM $Mg(AcO)_2$, 0.1 mg mL^{-1} BSA). After adding Nt. AlwI, the reaction mixture was incubated at 37 °C for 20 h. The final concentration of each component was as follows: [primer] = 2.0 μM, [template] = 3.0 μM, and [Nt. AlwI] = 0.2 U μL^{-1}. The product was purified by denaturing PAGE, gel filtration (Sephadex G-25 Fine), and isopropanol precipitation.

MALDI-MS analysis

The enzymatically synthesized DNA strands were desalted by gel filtration (Sephadex G-25 Fine, GE Healthcare) and the subsequent treatment with a cation-exchange resin (Dowex 50W×8, NH_4^+-form). The chemically synthesized DNA strands were directly subjected to MALDI-TOF MS measurement after HPLC purification.

MALDI-TOF MS measurement was conducted using a mixture of 3-hydroxypicolinic acid (3-HPA) and ammonium citrate as a matrix. Oligonucleotide Calibration Standard (Bruker) was used as a calibration standard.

Sequence screening of Cu^{II}-responsive split DNAzymes

Two split DNAzyme strands were mixed in a buffer (10 mM HEPES (pH 7.0), 1 M NaCl, 10 mM $MgCl_2$), and then annealed (85 °C → 25 °C, 1.0 °C min^{-1}) in the presence or in the absence of $CuSO_4$ (1.0 equiv). The RNA-cleaving reaction was initiated by adding a FAM-labeled substrate strand. The final concentration of each component was as follows: [DNAzyme strands] = 1.0 μM each, [substrate strand] = 1.0 μM, [$CuSO_4$] = 0 or 1.0 μM. The reaction mixture was incubated at 25 °C for 3 h. The reaction was quenched by adding a 3:1 mixture of 7 M urea and the loading buffer (30% glycerol, 0.25% bromophenol blue). The cleavage of the RNA substrate was analyzed by denaturing PAGE. The fractions of the cleaved substrate (F) were calculated as follows:

$F\ (\%) = I_c / (I_c + I_u) \times 100$,

where I_c and I_u are the band intensities of the cleaved product and the uncleaved substrate, respectively.

Time-course analysis of the RNA-cleaving reaction by the split H-DNAzyme

The two strands of the split **H**-DNAzyme were annealed (85 °C → 25 °C, 1.0 °C min^{-1}) in a buffer (10 mM HEPES (pH 7.0), 1.0 M NaCl, 10 mM $MgCl_2$) in the presence or in the absence of $CuSO_4$ (1.0 equiv). The RNA-cleaving reaction was initiated by adding 10 equivalents of a FAM-labeled substrate strand, and the reaction mixture was incubated at 25 °C. The final concentration of each component was as follows: [DNAzyme] = 1.0 μM, [substrate] = 10 μM, [$CuSO_4$] = 0 or 1.0 μM. An aliquot of the reaction mixture was taken at the defined time points. After the reaction was quenched by adding a 3:1 mixture of 7 M urea and the loading buffer, the samples were stored at –28 °C until the time course was completed. The reaction progress was analyzed by denaturing PAGE. The apparent first-order rate constants (k_{obs}) were calculated from the initial velocities, which were determined by the reaction progress after 1 h or 3 h.

Assay of the metal specificity of the split H-DNAzyme

The two strands of the split **H**-DNAzyme were annealed (85 °C → 25 °C, 1.0 °C min^{-1}) in a buffer (10 mM HEPES (pH 7.0), 1.0 M NaCl, 10 mM $MgCl_2$) in the presence of one equivalent of metal ions ($MnCl_2$, $FeSO_4$, $FeCl_3$, $CoSO_4$, $NiSO_4$, $CuSO_4$, $ZnSO_4$, Na_2PdCl_4, K_2PtCl_4, $Hg(ClO_4)_2$, and $AgNO_3$). In the experiments with Hg^{II} and Ag^{I} ions, NaCl and $MgCl_2$ in the buffer were replaced by $NaNO_3$ and $Mg(NO_3)_2$, respectively. The RNA-cleaving reaction was initiated by adding one equivalent of the substrate strand. The final concentration of each component was as follows: [DNAzyme] = 1.0 μM, [substrate] = 1.0 μM, [metal ion] = 0 or 1.0 μM. The reaction mixture was incubated at 25 °C for 3 h. The reaction was quenched by adding the loading buffer containing 7 M urea. The cleavage of the RNA substrate was analyzed by denaturing PAGE.

Activation of the split H-DNAzyme with Cu^{II} ions

The two DNAzyme strands (1.0 μM) were mixed in a buffer (10 mM HEPES (pH 7.0), 1.0 M NaCl, 10 mM $MgCl_2$) and then annealed (85 °C → 25 °C, 1.0 °C min^{-1}). The RNA-cleaving reaction was initiated by adding a FAM-labeled substrate (10 equiv), and the reaction mixture was incubated at 25 °C. After 1 h, one equivalent of $CuSO_4$ was added. An aliquot of the reaction mixture was taken at the defined time points. After the reaction was quenched by adding a 3:1 mixture of 7 M urea and the loading buffer, the samples were stored at –28 °C until the time course was completed. The reaction progress was analyzed by denaturing PAGE.

Deactivation of the split H-DNAzyme by the removal of Cu^{II} ions

The two strands of the split **H**-DNAzyme (1.0 μM) and $CuSO_4$ (1.0 equiv) were mixed in a buffer (10 mM HEPES (pH 7.0), 1.0 M NaCl, 10 mM $MgCl_2$) and then annealed (85 °C → 25 °C, 1.0 °C min^{-1}). The reaction was initiated by adding a FAM-labeled substrate (10 equiv), and the reaction mixture was incubated at 25 °C. After 1 h, a Cu^{II}-binding tripeptide (Gly-His-Lys (GHK), 1.0 equiv) was added to remove Cu^{II} ions. An aliquot of the reaction mixture was taken at the defined time points, and the reaction was quenched by adding the loading buffer containing 7 M urea. The reaction progress was analyzed by denaturing PAGE.

Iterative switching of the activity of the split H-DNAzyme

The two DNAzyme strands (1.0 μM) were mixed in a buffer (10 mM HEPES (pH 7.0), 1.0 M NaCl, 10 mM $MgCl_2$) and then annealed (85 °C → 25 °C, 1.0 °C min^{-1}). The RNA-cleaving reaction was initiated by adding 10 equivalents of a two-base shorter substrate strand (5′-CTC TAT rAGG AGC A-3′). The reaction mixture was incubated at 25 °C. $CuSO_4$ (1.0 equiv) and a Cu^{II}-binding peptide (GHK, 1.0 equiv) were alternately added at the defined time points. An aliquot of the reaction mixture was taken at the defined time points, and the reaction was quenched by adding the loading buffer containing 7 M urea. The reaction progress was analyzed by denaturing PAGE.

Deactivation of the split H-DNAzyme by the addition of a reductant

The two strands of the split **H**-DNAzyme (1.0 μM) and $CuSO_4$ (1.0 equiv) were mixed in a buffer (10 mM HEPES (pH 7.0), 1.0 M NaCl, 10 mM $MgCl_2$) and then annealed (85 °C → 25 °C, 1.0 °C min^{-1}). The reaction was initiated by adding a FAM-labeled substrate (10 equiv), and the reaction mixture was incubated at 25 °C. After 1 h, sodium ascorbate (Asc, 10 equiv) was added as a reductant of Cu^{II} ions. An aliquot of the reaction mixture was taken at the defined time points, and the reaction was quenched by adding the loading buffer containing 7 M urea. The reaction progress was analyzed by denaturing PAGE.

Activation of the split H-DNAzyme by the addition of an oxidant

The two strands of the split **H**-DNAzyme (1.0 μM) and $CuSO_4$ (1.0 equiv) were mixed in a buffer (10 mM HEPES (pH 7.0), 1.0 M NaCl, 10 mM $MgCl_2$) and then annealed (85 °C → 25 °C, 1.0 °C min^{-1}). After the addition of sodium ascorbate (Asc, 10 equiv), the reaction was initiated by adding a FAM-labeled RNA substrate (10 equiv). The reaction mixture was left to stand at 25 °C. After 1 h, NaClO (20 equiv) was added as an oxidant. An aliquot of the reaction mixture was taken at the defined time points, and the reaction was quenched by adding the loading buffer containing 7 M urea. The reaction progress was analyzed by denaturing PAGE.

Iterative switching of the activity of the split H-DNAzyme by successive addition of a reductant and an oxidant

The two strands of the split **H**-DNAzyme (1.0 μM) and $CuSO_4$ (1.0 equiv) were mixed in a buffer (10 mM HEPES (pH 7.0), 1.0 M NaCl, 10 mM $MgCl_2$) and then annealed (85 °C → 25 °C, 1.0 °C min^{-1}). The reaction was initiated by adding a FAM-labeled substrate (10 equiv), and the reaction mixture was incubated at 25 °C. After half an hour, sodium ascorbate (Asc, 10 equiv) was added to deactivate the **H**-DNAzyme. After another half hour, NaClO (20 equiv) was added to reactivate the DNAzyme. An aliquot of the reaction mixture was taken at the defined time points,

and the reaction was quenched by adding the loading buffer containing 7 M urea. The reaction progress was analyzed by denaturing PAGE.

Duplex melting analysis

To estimate the melting temperatures (T_m) of the stem duplex of the split **H**-DNAzyme, the DNA strands were annealed (85 °C → 4 °C, 1.0 °C min^{-1}) in the absence and in the presence of $CuSO_4$ (1.0 equiv) in the buffer used for the DNAzyme reaction (10 mM HEPES (pH 7.0), 1.0 M NaCl, 10 mM $MgCl_2$) (Table 3-3).

For the metal-specificity assay, the DNA strands were mixed with metal ions (1.0 equiv) and annealed (85 °C → 4 °C, 1.0 °C min^{-1}) in a buffer (10 mM HEPES (pH 7.0), 100 mM NaCl or 100 mM $NaNO_3$ (for Hg^{II} and Ag^{I})) in the presence of one equivalent of metal ions (Figure 3-14).

Absorbance at 260 nm was recorded on a UV-1700 spectrophotometer (Shimadzu) equipped with a TMSPC-8 temperature controller while the temperature was raised from 5 °C to 85 °C at the rate of 0.2 °C min^{-1}. The normalized absorbance was calculated as follows:

Normalized $A_{260} = \{A_{260}(t\ °C) - A_{260}(4\ °C)\}/\{A_{260}(85\ °C) - A_{260}(4\ °C)\} \times 100$.

The melting temperatures (T_m) were determined as an inflection point of a melting curve using a T_m analysis software LabSolutions (Shimadzu) with a 17-point adaptive smoothing program.

Table 3-4. Sequences of **H**-containing DNA strands prepared by chemical synthesis

Name	Sequence (5′ to 3′)	ε_{260}	$[M–H]^-$	Calcd.[a]	Obs.[b]
15-bp T_m **1**	CAC ATT A**H**T GTT GTA	1.44×10^5	$C_{149}H_{188}N_{49}O_{91}P_{14}$	4555.0	4555.1
15-bp T_m **2**	TAC AAC A**H**T AAT GTG	1.50×10^5	$C_{149}H_{186}N_{55}O_{87}P_{14}$	4573.1	4573.1

a Calculated molecular mass for $[M–H]^-$. *b* Mass observed in MALDI-TOF MS analysis.

3-9. References

[1] (a) S. K. Silverman, *Trends Biochem. Sci.* **2016**, *41*, 595–609. (b) M. Hollenstein, *Molecules* **2015**, *20*, 20777–20804.

[2] (a) I. Willner, B. Shlyahovsky, M. Zayats, B. Willner, *Chem. Soc. Rev.* **2008**, *37*, 1153–1165. (b) L. Gong, Z. Zhao, Y.-F. Lv, S.-Y. Huan, T. Fu, X.-B. Zhang, G.-L. Shen, R.-Q. Yu, *Chem. Commun.* **2015**, *51*, 979–995. (c) R. Orbach, B. Willner, I. Willner, *Chem. Commun.* **2015**, *51*, 4144−4160. (d) Y. Tian, Y. He, Y. Chen, P. Yin, C. Mao, *Angew. Chem. Int. Ed.* **2005**, *44*, 4355–4358. (e) K. Lund, A. J. Manzo, N. Dabby, N. Michelotti, A. Johnson-Buck, S. Taylor, R. Pei, M. N. Stojanovic, N. G. Walter, E. Winfree, H. Yan, J. Nangreave, *Nature* **2010**, *465*, 206–210.

[3] D. M. Kolpashchikov, *ChemBioChem* **2007**, *8*, 2039−2042.

[4] (a) J. Elbaz, O. Lioubashevski, F. Wang, F. Remacle, R. D. Levine, I. Willner, *Nat. Nanotechnol.* **2010**, *5*, 417–422. (b) F. Wang, J. Elbaz, R. Orbach, N. Magen, I. Willner, *J. Am. Chem. Soc.* **2011**, *133*, 17149–17151. (c) J. Elbaz, F. Wang, F. Remacle, I. Willner, *Nano Lett.* **2012**, *12*, 6049−6054. (d) R. Orbach, F. Remacle, R. D. Levine, I. Willner, *Chem. Sci.* **2014**, *5*, 1074–1081.

[5] (a) Y. Xiao, V. Pavlov, R. Gill, T. Bourenko, I. Willner, *ChemBioChem* **2004**, *5*, 374–379. (b) V. Pavlov, Y. Xiao, R. Gill, A. Dishon, M. Kotler, I. Willner, *Anal. Chem.* **2004**, *76*, 2152–2156.

[6] (a) D. M. Kolpashchikov, *J. Am. Chem. Soc.* **2008**, *130*, 2934–2935. (b) M. Deng, D. Zhang, Y. Zhou, X. Zhou, *J. Am. Chem. Soc.* **2008**, *130*, 13095–13102.

[7] J. Elbaz, M. Moshe, B. Shlyahovsky, I. Willner, *Chem. - Eur. J.* **2009**, *15*, 3411−3418.

[8] R. Freeman, X. Liu, I. Willner, *J. Am. Chem. Soc.* **2011**, *133*, 11597–11604.

[9] J. Elbaz, S. Shimron, I. Willner, *Chem. Commun.* **2010**, *46*, 1209–1211.

[10] S. Wang, L. Yue, Z.-Y. Li, J. Zhang, H. Tian, I. Willner, *Angew. Chem. Int. Ed.* **2018**, *57*, 8105–8109.

[11] M. W. Haydell, M. Centola, V. Adam, J. Valero, M. Famulok, *J. Am. Chem. Soc.* **2018**, *140*, 16868−16872.

[12] S. Shimron, J. Elbaz, A. Henning, I. Willner, *Chem. Commun.* **2010**, *46*, 3250−3252.

[13] (a) J. Chen, J. Pan, S. Chen, *Chem. Commun.* **2017**, *53*, 10224–10227. (b) X. Li, J. Xie, B. Jiang, R. Yuan, Y. Xiang, *ACS Appl. Mater. Interfaces* **2017**, *9*, 5733−5738.

[14] D.-M. Kong, N. Wang, X.-X. Guo, H.-X. Shen, *Analyst* **2010**, *135*, 545–549.

[15] (a) J. J. Tabor, M. Levy, A. D. Ellington, *Nucleic Acids Res.* **2006**, *34*, 2167–2172. (b) E.

Mokany, S. M. Bone, P. E. Young, T. B. Doan, A. V. Todd, *J. Am. Chem. Soc.* **2010**, *132*, 1051–1059. (c) J. L. Richards, G. K. Seward, Y.-H. Wang, I. J. Dmochowski, *ChemBioChem* **2010**, *11*, 320–324. (d) B. K. Ruble, J. L. Richards, J. C. Cheung-Lau, I. J. Dmochowski, *Inorg. Chim. Acta* **2012**, *380*, 386–391.

[16] (a) S. Katz, *Biochim. Biophys. Acta* **1963**, *68*, 240–253. (b) Y. Miyake, H. Togashi, M. Tashiro, H. Yamaguchi, S. Oda, M. Kudo, Y. Tanaka, Y. Kondo, R. Sawa, T. Fujimoto, T. Machinami, A. Ono, *J. Am. Chem. Soc.* **2006**, *128*, 2172–2173.

[17] T. Tanaka, A. Tengeiji, T. Kato, N. Toyama, M. Shiro, M. Shionoya, *J. Am. Chem. Soc.* **2002**, *124*, 12494–12498.

[18] R. R. Breaker, G. F. Joyce, *Chem. Biol.* **1995**, *2*, 655–660.

[19] (a) M. K. Schlegel, L.-O. Essen, E. Meggers, *J. Am. Chem. Soc.* **2008**, *130*, 8158−8159. (b) M. K. Schlegel, L. Zhang, N. Pagano, E. Meggers, *Org. Biomol. Chem.* **2009**, *7*, 476−482.

[20] A. Ono, S. Cao, H. Togashi, M. Tashiro, T. Fujimoto, T. Machinami, S. Oda, Y. Miyake, I. Okamoto, Y. Tanaka, *Chem. Commun.* **2008**, *44*, 4825–4827.

[21] Y. Tanaka, J. Kondo, V. Sychrovsky, J. Sebera, T. Dairaku, H. Saneyoshi, H. Urata, H. Torigoe, A. Ono, *Chem. Commun.* **2015**, *51*, 17343–17360.

[22] A. Ono, H. Torigoe, Y. Tanaka, I. Okamoto, *Chem. Soc. Rev.* **2011**, *40*, 5855–5866.

[23] Y. Takezawa, W. Maeda, K. Tanaka, M. Shionoya, *Angew. Chem. Int. Ed.* **2009**, *48*, 1081−1084.

[24] L. Pickart, J. H. Freedman, W. J. Loker, J. Peisach, C. M. Perkins, R. E. Stenkamp, B. Weinstein, *Nature* **1980**, *288*, 715−717.

[25] A. Trapaidze, C. Hureau, W. Bal, M. Winterhalter, P. Faller, *J. Biol. Inorg. Chem.* **2012**, *17*, 37–47.

[26] (a) N. Ma, Y. Li, H. Xu, Z. Wang, X. Zhang, *J. Am. Chem. Soc.* **2010**, *132*, 442–443. (b) M. Nakahata, Y. Takashima, H. Yamaguchi, A. Harada, *Nat. Commun.* **2011**, *2*, 511. (c) M. Huo, J. Yuan, L. Tao, Y. Wei, *Polym. Chem.* **2014**, *5*, 1519–1528

[27] (a) L. Zelikovich, J. Libman, A. Shanzer, *Nature* **1995**, *374*, 790−792. (b) S. Kawano, N. Fujita, S. Shinkai, *J. Am. Chem. Soc.* **2004**, *126*, 8592–8593. (c) A. J. McConnell, C. S. Wood, P. P. Neelakandan, J. R. Nitschke, *Chem. Rev.* **2015**, *115*, 7729−7793.

[28] (a) A. Livoreil, C. O. Dietrich-Buchecker, J.-P. Sauvage, *J. Am. Chem. Soc.* **1994**, *116*, 9399–9400. (b) P. Gavina, J.-P. Sauvage, *Tetrahedron Lett.* **1997**, *38*, 3521–3524. (c) E. R. Kay, D. A. Leigh, F. Zerbetto, *Angew. Chem. Int. Ed.* **2007**, *46*, 72–191.

[29] (a) E. Paleček, *Nature* **1960**, *188*, 656–657. (b) E. M. Boon, D. M. Ceres, T. G. Drummond, M. G. Hill, J. K. Barton, *Nat. Biotechnol.* **2000**, *18*, 1096–1100. (c) T. G. Drummond, M. G.

Hill, J. K. Barton, *Nat. Biotechnol.* **2003**, *21*, 1192–1199. (d) E. Paleček, M. Bartošík, *Chem. Rev.* **2012**, *112*, 3427−3481. (e) W.-W. Zhao, J.-J. Xu, H.-Y. Chen, *Chem. Rev.* **2014**, *114*, 7421−7441.

[30] (a) L. Freage, A. Trifonov, R. Tel-Vered, E. Golub, F. Wang, J. S. McCaskill, I. Willner, *Chem. Sci.* **2015**, *6*, 3544–3549. (b) S. Ranallo, A. Amodio, A. Idili, A. Porchetta, F. Ricci, *Chem. Sci.* **2016**, *7*, 66–71.

[31] (a) P.-J. J. Huang, J. Lin, J. Cao, M. Vazin, J. Liu, *Anal. Chem.* **2014**, *86*, 1816−1821. (b) W. Zhou, M. Vazin, T. Yu, J. Ding, J. Liu, *Chem. - Eur. J.* **2016**, *22*, 9835−9840. (c) J. Liu, Y. Lu, *J. Am. Chem. Soc.* **2007**, *129*, 9838−9839.

[32] B. Jash, J. Müller, *Angew. Chem. Int. Ed.* **2018**, *57*, 9524−9527.

[33] (a) J. Liu, Y. Lu, *Angew. Chem. Int. Ed.* **2007**, *46*, 7587–7590. (b) T. Li, S. Dong, E. Wang, *Anal. Chem.* **2009**, *81*, 2144–2149. (c) T. Li, L. Shi, E. Wang, S. Dong, *Chem. - Eur. J.* **2009**, *15*, 3347–3350. (d) D.-M. Kong, L.-L. Cai, H.-X. Shen, *Analyst*, **2010**, *135*, 1253–1258. (e) X.-H. Zhou, D.-M. Kong, H.-X. Shen, *Anal. Chim. Acta* **2010**, *678*, 124–127. (f) F. Wang, R. Orbach, I. Willner, *Chem. - Eur. J.* **2012**, *18*, 16030–16036. (g) Z. Zhang, D. Balogh, F. Wang, I. Willner, *J. Am. Chem. Soc.* **2013**, *135*, 1934−1940.

[34] (a) C. E. McGhee, R. J. Lake, Y. Lu, In *Artificial Metalloenzymes and Metallo DNAzymes in Catalysis: From Design to Applications*; M. Diéguez, J.-E. Bäckvall, O. Pàmies, Eds.; Wiley-VCH: Weinheim, 2018; pp 41−68. (b) B. Cuenoud, J. W. Szostak, *Nature* **1995**, *375*, 611–614. (c) N. Carmi, L. A. Shultz, R. R. Breaker, *Chem. Biol.* **1996**, *3*, 1039–1046.

[35] T. Kobayashi, Y. Takezawa, A. Sakamoto, M. Shionoya, *Chem. Commun.* **2016**, *52*, 3762–3765.

Chapter 4.

Development of Cu^{II}-responsive Single-stranded DNAzymes

第 4 章

本章については、5 年以内に論文誌で刊行予定のため、非公開。

Chapter 5.

Multimetal-dependent Regulation of DNAzyme Activities

5-1. Introduction

DNA provides a robust platform for the development of sophisticated molecular networks based on sequence-dependent hybridization through Watson–Crick base pairing. Many DNA strands can work together in the same solution by means of a careful sequence design. For the operation of the complicated DNA systems, it is of great importance to endow with responsiveness to multiple external stimuli. In many cases, additional DNA strands, which trigger the strand displacement reactions, have been used as multistimuli.[1] For example, Stojanovic et al. regulated catalytic activities of deoxyribozymes (DNAzymes) to construct a molecular automaton (Figure 5-1a).[2] They operated several DNAzyme-based logic gates in a mixture by adding oligonucleotides as external stimuli. Winfree et al. controlled DNA computing circuits comprising more than 100

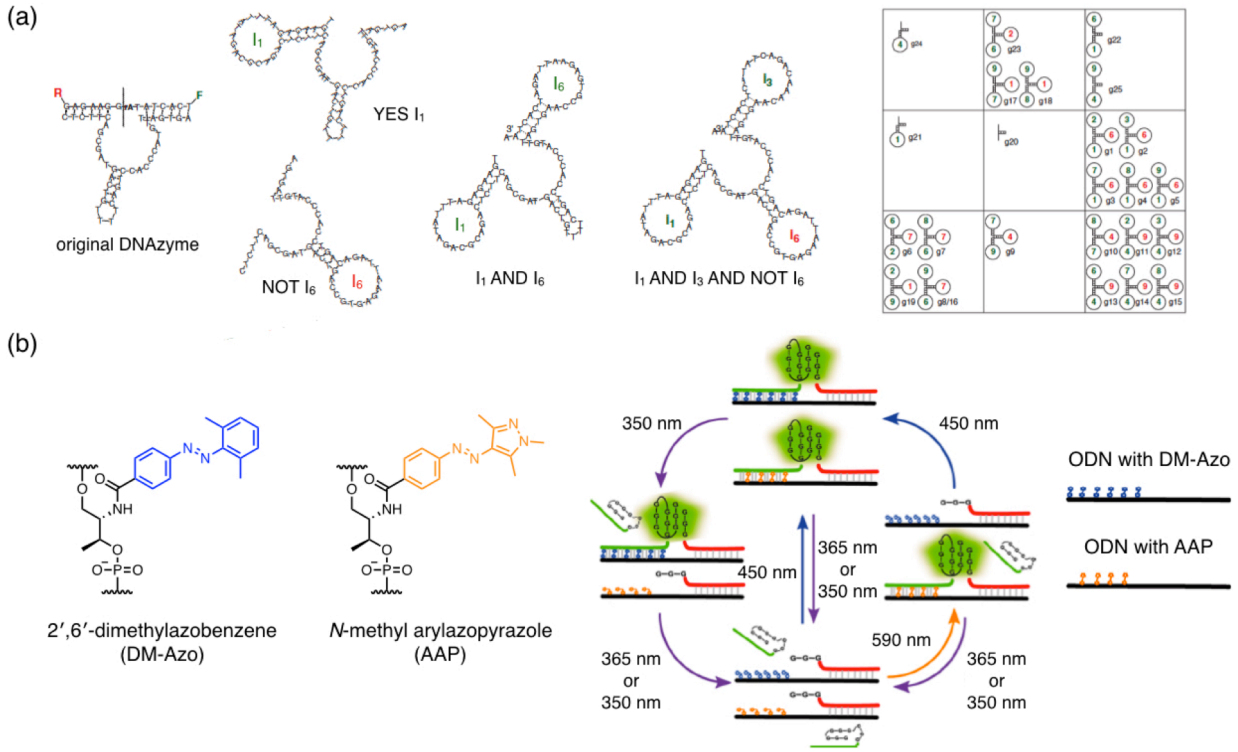

Figure 5-1. Multistimuli-dependent regulation of DNA-based molecular systems. (a) Operation of multiple DNAzymes using DNA strands as external stimuli. The activities of DNAzymes were regulated to construct a molecular automaton. Reproduced from ref. [2]. Copyright 2003 Nature Publishing Group. (b) Orthogonal regulation of DNAzyme activities using light as external stimuli. Two azobenzene derivatives were exploited to respond to light irradiation at different wavelengths. Reproduced from ref. [8]. Copyright 2018 American Chemical Society.

strands with additional multiple DNA stands as inputs.[3] Other external stimuli such as small molecules,[4,5] proteins,[6] pH changes,[7] and light[8,9] have been also exploited for the construction of multistimuli-responsive DNA-based systems. Famulok et al. demonstrated the selective photo-switching of DNAzyme activities by using two azobenzene derivatives (Figure 5-1b).[8] The hybridization of DNA strands was controlled through photoisomerization of the azobenzene derivatives by light irradiation at different wavelengths, resulting in the regulation of the activities of two peroxidase-mimicking DNAzymes in an orthogonal manner.

In contrast to other external stimuli, the use of metal ions as inputs provides mainly three advantages for realizing the multistimuli-dependent regulation. First, various kinds of metal ions can be used with a specific character through the selection of appropriate metal ligands. Second, reversible metal complexation enables the bidirectional regulation of DNA systems. Third, some metal ions can afford responsiveness toward other stimuli such as light and redox agents. The incorporation of metal-mediated base pairs into DNA would be one of the most promising methods to fabricate multimetal-dependent DNA systems. As many types of ligand-type unnatural nucleotides with different metal affinities have been developed so far,[10] metal-mediated base pairing would offer a powerful strategy to impart responsiveness toward diverse metal ions.

In **chapters 3** and **4**, I have developed Cu^{II}-responsive DNAzymes by incorporating hydroxypyridone (**H**) unnatural ligand-type nucleotides into reported DNAzymes. The catalytic activities of the DNAzymes were regulated by Cu^{II}-mediated **H**–Cu^{II}–**H** base pairing. The Cu^{II}-responsive DNAzymes exhibited high metal specificity because of the selective formation of a **H**–Cu^{II}–**H** base pair. I expected that the high metal selectivity can be applied to multimetal-responsive DNA systems, in which Cu^{II} and other metal ions are used as external stimuli.

In this chapter, I describe the multimetal-dependent regulation of DNAzyme activities based on metal-mediated base pairing. In the section **5-2**, the orthogonality of three metal-mediated base pairs, **H**–Cu^{II}–**H**, T–Hg^{II}–T, and C–Ag^{I}–C, was examined. In the section **5-3**, I have demonstrated the metal-dependent orthogonal regulation of DNAzyme activities with the use of two different

metal-mediated base pairs (Figure 5-2a). In addition to **H**–Cu^{II}–**H**, Hg^{II}-mediated thymine base pairing (T–Hg^{II}–T)[11] was exploited for the regulation of DNAzyme activities. A **H**–**H** pair and T–T mismatches were incorporated into two RNA-cleaving DNAzymes to confer responsiveness toward Cu^{II} and Hg^{II} ions, respectively. Owing to the selective formation of **H**–Cu^{II}–**H** and T–Hg^{II}–T base pairs, the catalytic activity of each DNAzyme would be orthogonally regulated in response to Cu^{II} and Hg^{II} ions. In the section **5-4**, I have developed DNAzymes that exhibit an AND logic gate response to two different transition metal ions (Figure 5-2b). I have examined two approaches to the development of AND-gate DNAzymes; (i) a **H**–**H** and T–T pairs were incorporated into a DNAzyme so that the DNAzyme can be activated only when both **H**–Cu^{II}–**H** and T–Hg^{II}–T base pairs are formed, and (ii) a pair of **H** nucleotides were incorporated into a reported Ag^{I}-responsive DNAzyme to endow it with responsiveness to Cu^{II} ions. The **H**-modified DNAzyme would show the catalytic activity only in the presence of both Cu^{II} and Ag^{I} ions. These studies would provide the basis for the construction of multimetal-responsive DNA-based systems by utilizing metal-mediated artificial base pairs.

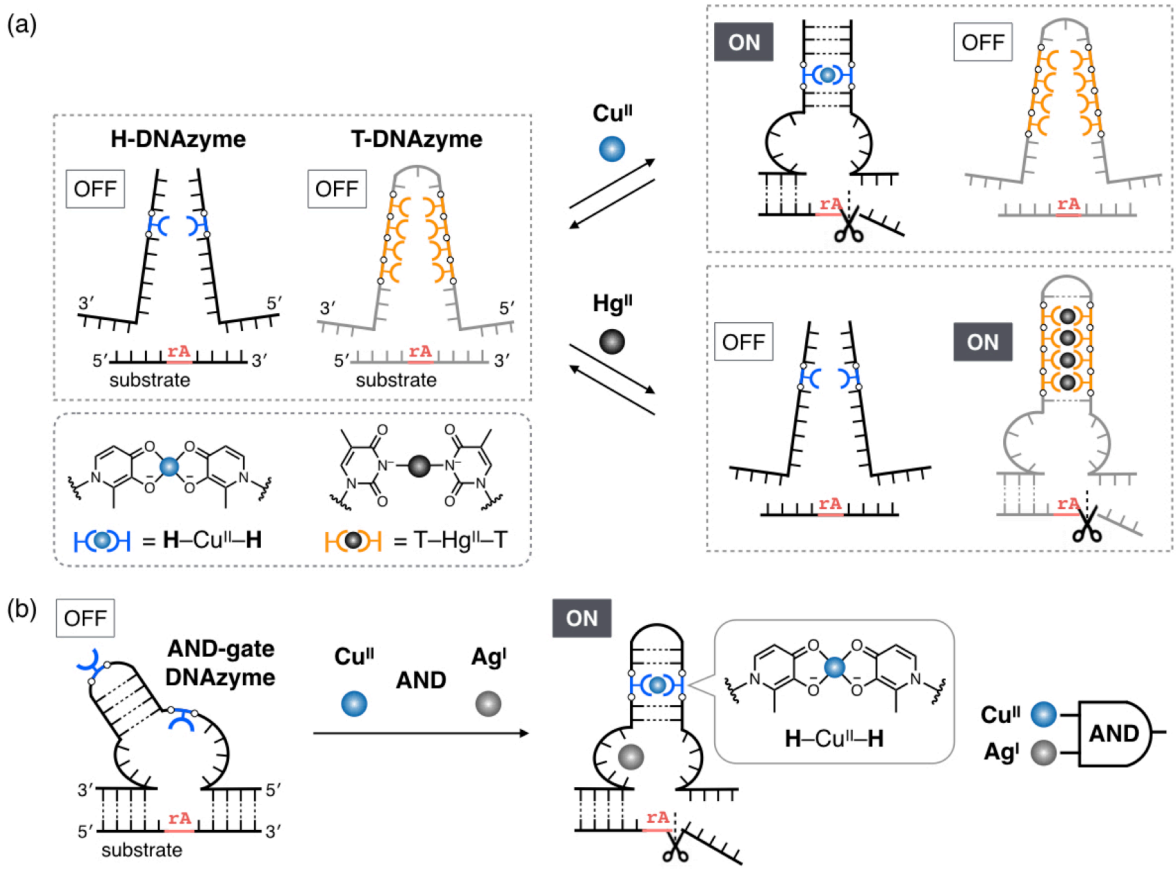

Figure 5-2. Multimetal-dependent regulation of DNAzyme activities based on metal-mediated base pairing. (a) Metal-dependent orthogonal regulation of two different DNAzyme activities by the formation of Cu^{II}- and Hg^{II}-mediated base pairs. (b) Development of AND-gate DNAzymes that respond to two transition metal ions by incorporating hydroxypyridone (**H**) nucleotides.

5-2. Orthogonal formation of metal-mediated base pairs

To demonstrate the multimetal-dependent regulation of DNAzyme activities, I employed Cu^{II}-mediated hydroxypyridone (**H**) base pairing (**H**–Cu^{II}–**H**). In the section **3-5**, it was found that a **H**–Cu^{II}–**H** base pair is selectively formed in the presence of Cu^{II} ions among various transition metal ions. This high metal selectivity enabled the Cu^{II}-specific activation of the split Cu^{II}-responsive DNAzyme containing a **H**–**H** pair (split **H**-DNAzyme). In addition, **H**–Cu^{II}–**H** base pairing was previously applied to construct heterogeneous Cu^{II}/Hg^{II} metal arrays on the basis of orthogonality to Hg^{II}-mediated pyridine base pairing.[12] Thus, **H**–Cu^{II}–**H** base pairing would be suitable for constructing multimetal-responsive DNA systems with Cu^{II} and other metal ions as external multistimuli.

As a **H**–**H** pair binds to neither Hg^{II} nor Ag^{I} ions, I expected that widely utilized Hg^{II}- and Ag^{I}-mediated base pairs consisting of natural pyrimidine bases (i.e. T–Hg^{II}–T[11] and C–Ag^{I}–C,[13] Figure 5-3a)[14] can act as an orthogonal base pair to **H**–Cu^{II}–**H** for the multimetal-dependent regulation. The orthogonality of **H**–Cu^{II}–**H**, T–Hg^{II}–T, and C–Ag^{I}–C base pairs was investigated by melting experiments of DNA duplexes containing a **H**–**H**, a T–T, or a C–C pair (Figure 5-3b).

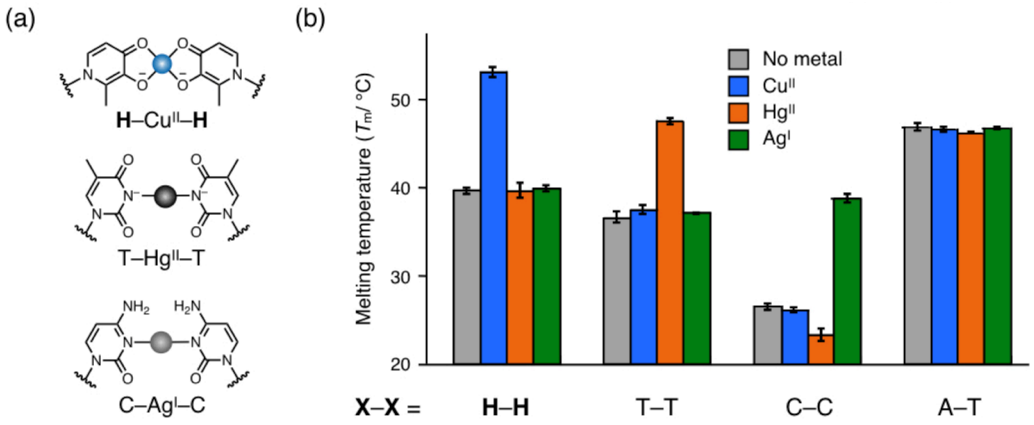

Figure 5-3. Orthogonality of **H**–Cu^{II}–**H**, T–Hg^{II}–T, and C–Ag^{I}–C base pairs. (a) Chemical structures of **H**–Cu^{II}–**H**, T–Hg^{II}–T, and C–Ag^{I}–C. (b) Melting temperatures of DNA duplexes containing a **H**–**H**, a T–T, a C–C, or an A–T pair in the presence of Cu^{II}, Hg^{II}, or Ag^{I} ions. Duplex sequence: (5′-CAC ATT A**X**T GTT GTA-3′)·(3′-GTG TAA T**Y**A CAA CAT-5′) (X–Y = **H**–**H**, T–T, C–C or A–T). [DNA duplex] = 2.0 μM, [metal ions] = 2.0 μM (1.0 equiv) in 10 mM HEPES (pH 7.0), 100 mM $NaNO_3$. 0.2 °C min^{-1}. All the samples were annealed before the measurement. $N \geq 3$. Error bars indicate standard errors.

Melting temperatures (T_m) of the DNA duplexes were measured in the presence of equimolar Cu^{II}, Hg^{II}, or Ag^{I} ions. The T_m value of the DNA duplex possessing a **H**–**H** pair was increased by 13°C in the presence of one equivalent of Cu^{II} ions through the formation of a **H**–Cu^{II}–**H** base pair. In contrast, the addition of Hg^{II} or Ag^{I} ions had no effects on the thermal stability of the **H**-containing duplex, indicating no binding of the metal ions to the **H**–**H** pair. On the other hand, DNA duplexes having a T–T and a C–C pair were specifically stabilized in the presence of equimolar amounts of Hg^{II} and Ag^{I} ions, respectively, indicating the selective formation of T–Hg^{II}–T and C–Ag^{I}–C base pairs. These results clearly verify that the three metal ions, Cu^{II}, Hg^{II}, and Ag^{I}, can be utilized as orthogonal external stimuli for the regulation of DNAzyme activities by exploiting the metal-mediated base pairs. The results also indicate that **H**–Cu^{II}–**H**, T–Hg^{II}–T, and C–Ag^{I}–C base pairs can be selectively formed in the same solution. Thus, the three metal-mediated base pairs can be applied to the multimetal-dependent regulation as the orthogonal base pairs.

5-3. Metal-dependent orthogonal regulation of DNAzyme activities

By exploiting the orthogonal base pairs, **H**–Cu^{II}–**H** and T–Hg^{II}–T, I first examined the metal-dependent orthogonal regulation of catalytic activities of two DNAzymes (Figure 5-2a). A **H**–**H** and T–T pairs were introduced into RNA-cleaving DNAzymes to fabricate a Cu^{II}- and a Hg^{II}-responsive DNAzymes, respectively. The two DNAzymes would be orthogonally regulated in the same solution by the selective formation of a **H**–Cu^{II}–**H** and T–Hg^{II}–T base pairs. As a Cu^{II}-responsive DNAzyme, I used the split **H**-DNAzyme, which was developed in **chapter 3**.

To construct a multimetal-responsive system, I newly developed a Hg^{II}-responsive DNAzyme that worked with the split **H**-DNAzyme. Although Hg^{II}-responsive DNAzymes were previously fabricated using T–Hg^{II}–T base pairs by other groups,[15] a Hg^{II}-responsive DNAzyme was designed so that it shows a comparable activity with that of the split **H**-DNAzyme. T–T mismatches were introduced into the stem region of E5 RNA-cleaving DNAzyme,[16] which had been utilized for the development of Cu^{II}-responsive DNAzymes (**H**-DNAzymes) in **chapters 3** and **4**. Both a split and a single-stranded DNAzymes containing consecutive T–T pairs were examined based on the design strategies presented in **chapters 3** and **4**, respectively. Among them, a single-stranded DNAzyme possessing four T–T mismatches responded to Hg^{II} ions with the largest on–off ratio, which is referred to as T-DNAzyme (Figure 5-4). In a manner similar to the design of the Cu^{II}-responsive single-stranded DNAzymes, the stem-loop sequence was modified to form a catalytically inactive structure in the absence of Hg^{II} ions. In the inactive form, the sequence in the loop region (shown in green) hybridizes to a part of the catalytic domain. In the presence of Hg^{II} ions, the formation of four T–Hg^{II}–T base pairs would induce an intrastrand structure transformation into the active structure, resulting in a Hg^{II}-responsive DNAzyme activation. The sequence of a substrate binding site was altered so that the T-DNAzyme cleaves a substrate different from that of the Cu^{II}-responsive split **H**-DNAzyme.

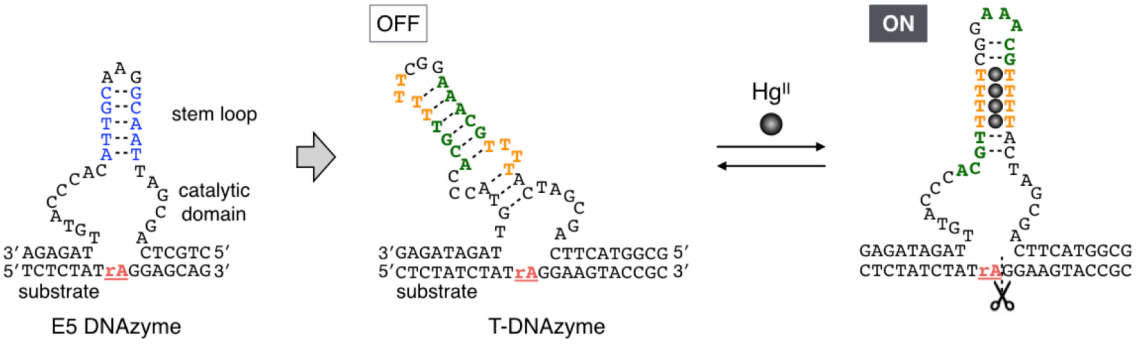

Figure 5-4. Design of a Hg^{II}-responsive DNAzyme (T-DNAzyme) based on E5 RNA-cleaving DNAzyme. "rA" in the substrate strand represents an adenosine ribonucleotide.

The secondary structure and the thermodynamic parameters of T-DNAzyme were estimated by using the mfold program (Figure 5-5).[17] The program suggests that the designed inactive structure (T_m = 57 °C) would be much more thermally stable than the active structure (T_m = 25 °C) in the absence of Hg^{II} ions. For the calculation of the structure in the presence of Hg^{II} ions, the T–Hg^{II}–T base pairs were formally replaced by T–A pairs, considering the comparable thermal stabilities of the two base pairs. The active structure would have higher thermal stability (T_m = 77 °C) than the inactive form (T_m = 57 °C). The secondary-structure prediction supports that T-DNAzyme can fold into the designed inactive and active structures in the absence and in the presence of Hg^{II} ions, respectively.

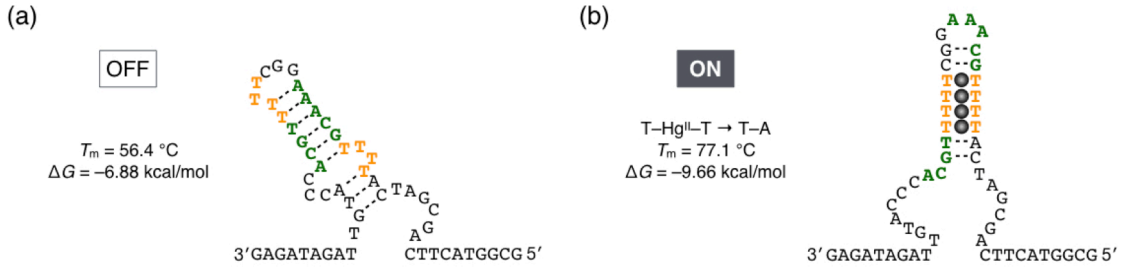

Figure 5-5. Predicted secondary structures and thermodynamic parameters of T-DNAzyme. (a) An inactive structure in the absence of Hg^{II} ions. (b) An active structure in the presence of Hg^{II} ions. The parameters were calculated by the mfold program. The T–Hg^{II}–T pairs were replaced by T–A base pairs. Calculation conditions: [Na^{I}] = 1.0 M, [Mg^{II}] = 10 mM, 25 °C.

Figure 5-6a shows the RNA-cleaving activity of T-DNAzyme in the absence and in the presence of four equivalents of Hg^{II} ions (i.e. 1.0 equiv for a T–T pair). When Hg^{II} ions were added, the DNAzyme activity was enhanced by 11-fold. The result indicates that T-DNAzyme was

activated by the formation of T–Hg^{II}–T base pairs. Moreover, the RNA-cleaving activity was efficiently decreased by the addition of a thymidine oligomer (5′-T_{20}-3′, T20), which served as a scavenger for Hg^{II} ions (Figure 5-6b). Thus, the catalytic activity of T-DNAzyme was reversibly regulated by the addition and removal of Hg^{II} ions.

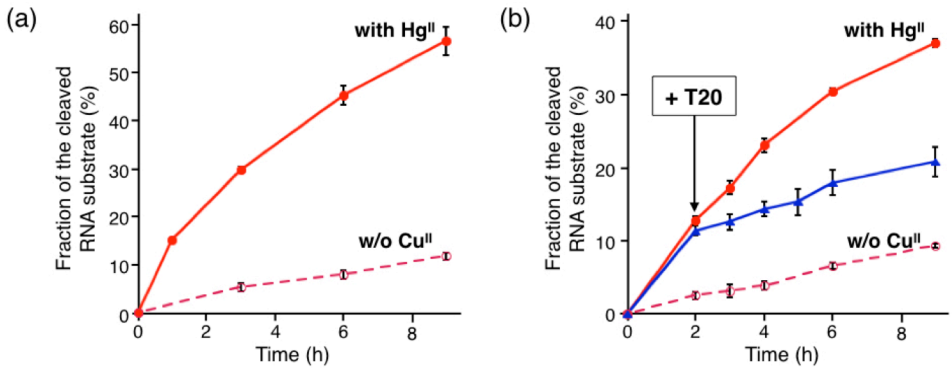

Figure 5-6. (a) RNA-cleaving activity of T-DNAzyme in the absence and in the presence of Hg^{II} ions. [T-DNAzyme] = 1.0 μM, [substrate] = 1.0 μM (1.0 equiv), [$Hg(ClO_4)_2$] = 0 or 4.0 μM (1.0 equiv for a T–T pair) in 10 mM HEPES (pH 7.0), 1.0 M $NaNO_3$, 10 mM $Mg(NO_3)_2$. 25 °C. *N* = 3. (c) Deactivation of T-DNAzyme. A thymidine oligomer (T20, 2.0 equiv) was added as a scavenger. [T-DNAzyme] = 1.0 μM, [substrate] = 2.0 μM (2.0 equiv), [$Hg(ClO_4)_2$] = 4.0 μM (1.0 equiv for a T–T pair), [T20] = 2.0 μM (where applicable), 25 °C. The activity of T-DNAzyme in the absence and in the presence of Hg^{II} ions are also shown in red lines. *N* = 3. Error bars indicate standard errors.

As the Hg^{II}-responsive DNAzyme was successfully obtained, the metal selectivity of the split **H**-DNAzyme and T-DNAzyme was studied. The RNA-cleaving activities of the two DNAzymes were evaluated in the presence of Cu^{II} or Hg^{II} ions under the same buffer condition (Figure 5-7).

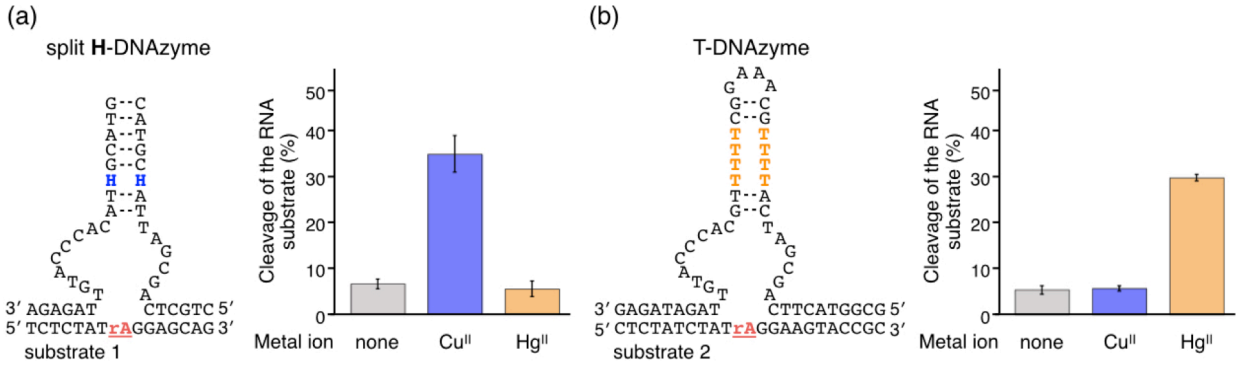

Figure 5-7. Metal selectivity of the split **H**-DNAzyme (a) and T-DNAzyme (b). [DNAzyme] = 1.0 μM, [substrate] = 1.0 μM, [$CuSO_4$] = 0 or 1.0 μM (1.0 equiv for a **H**–**H** pair), [$Hg(ClO_4)_2$] = 0 or 4.0 μM (1.0 equiv for a T–T pair) in 10 mM HEPES (pH 7.0), 1.0 M $NaNO_3$, 10 mM $Mg(NO_3)_2$. 25 °C, 3 h. *N* = 3. Error bars indicate standard errors.

The **H**-DNAzyme was specifically activated with Cu^{II} ions while Hg^{II} ions did not enhance the activity. On the other hand, the activity of T-DNAzyme was increased only when Hg^{II} ions were added. The addition of Cu^{II} ions did not have any effects on the DNAzyme activity. These results validate that the split **H**-DNAzyme and T-DNAzyme can be selectively activated by adding Cu^{II} and Hg^{II} ions, respectively, thus applicable to the orthogonal regulation of DNAzyme activities.

Metal-dependent activation of the two DNAzymes was examined with an equimolar mixture of the split **H**-DNAzyme and T-DNAzyme (Figure 5-8a). The two DNAzymes were operated in the same solution with their substrates in the presence of Cu^{II} and/or Hg^{II} ions. After the DNAzyme strands were annealed, the RNA-cleaving reactions were initiated by adding their substrates and the metal ions. The split **H**-DNAzyme and T-DNAzyme have different substrate-binding arms to cleave distinct substrates. Figure 5-8b represents relative activities, which were normalized by those when each RNA-cleaving reaction was separately conducted under the metal-free condition. When one equivalent of Cu^{II} ions was added, the catalytic activity of the split **H**-DNAzyme was raised eight-fold. In contrast, the activity of T-DNAzyme was the same as that in the absence of the metal ions. The result indicates that **H**–Cu^{II}–**H** base pair was selectively formed in the presence of Cu^{II} ions, thus activating only the split **H**-DNAzyme. In the presence of Hg^{II} ions, only the RNA-cleaving activity of T-DNAzyme was increased by the selective formation of T–Hg^{II}–T base pairs. The activity of the **H**-DNAzyme was slightly decreased presumably because Hg^{II} ions bound not only T–T mismatches of T-DNAzyme but also to other T bases of the **H**-DNAzyme and the substrate. When Cu^{II} and Hg^{II} ions were added, both DNAzyme activities were enhanced two- to three-fold. The nonspecific binding of Hg^{II} ions to natural nucleobases may have also inhibited the active **H**-DNAzyme, resulting in the lower activity than that in the presence of only Cu^{II} ions. As a consequence, the multimetal-dependent orthogonal activation of the DNAzymes was demonstrated using **H**–Cu^{II}–**H** and T–Hg^{II}–T base pairing.

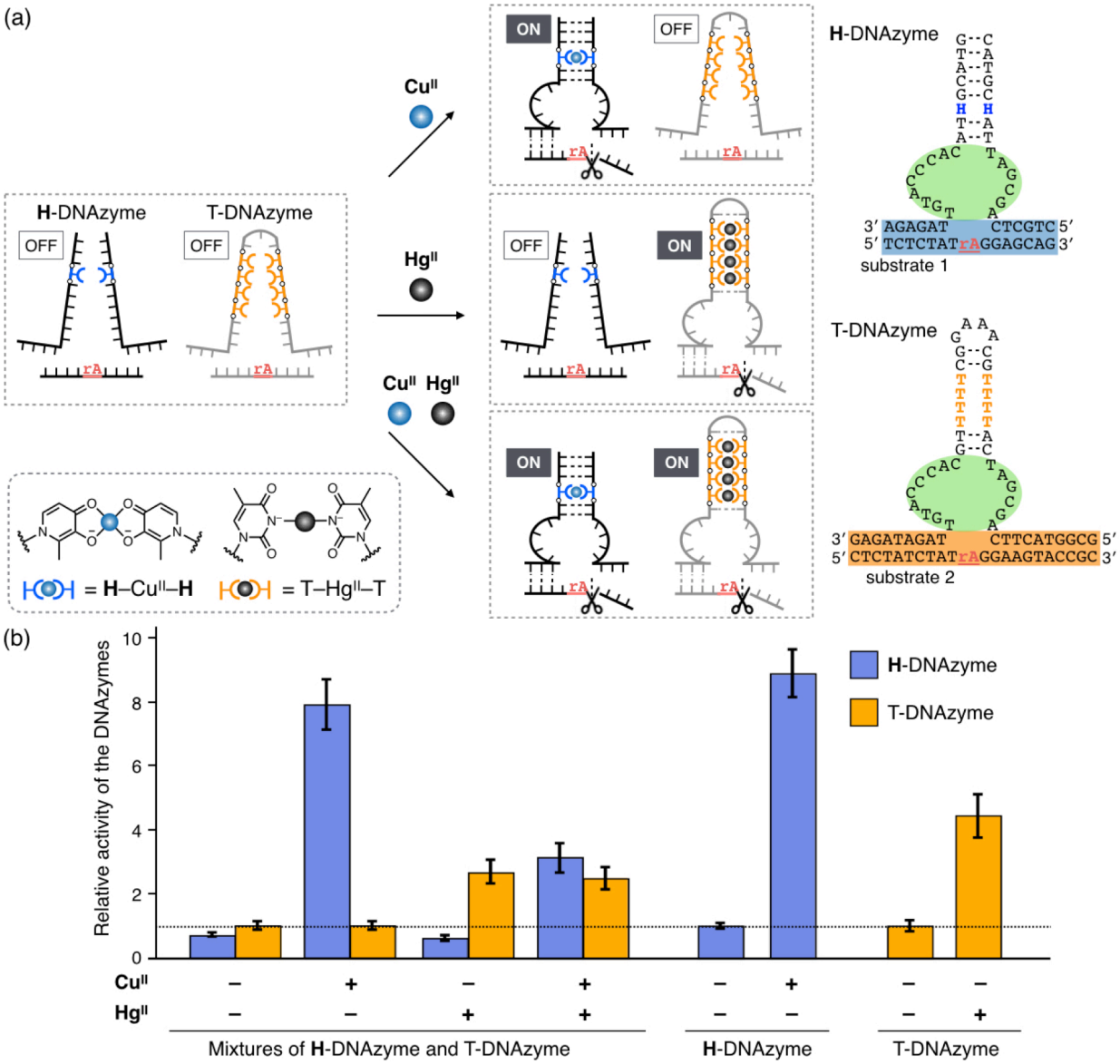

Figure 5-8. Orthogonal activation of a Cu^{II}-responsive DNAzyme and a Hg^{II}-responsive DNAzyme. (a) Design of the orthogonal activation. (b) Metal-dependent activation of the split **H**-DNAzyme and T-DNAzyme. Cu^{II} and/or Hg^{II} ions were added to a mixture of the **H**-DNAzyme and T-DNAzyme. [**H**-DNAzyme] = [T-DNAzyme] = 1.0 μM, [substrate 1] = [substrate 2] = 2.0 μM, [$CuSO_4$] = 0 or 1.0 μM (1.0 equiv for a **H**–**H** pair), [$Hg(ClO_4)_2$] = 0 or 4.0 μM (1.0 equiv for a T–T pair) in 10 mM HEPES (pH 7.0), 1.0 M $NaNO_3$, 10 mM $Mg(NO_3)_2$. 25 °C, 3 h. The activities of the individual DNAzymes under the same condition are also shown. $N \geq 3$. Error bars indicate standard errors.

Even when Cu^{II} and Hg^{II} were added in the course of the reactions, the selective activation was also accomplished (Figure 5-9). The RNA-cleaving reactions were performed in the same mixture of the split **H**-DNAzyme, T-DNAzyme and their substrates as the previous experiment. The

reaction was initiated without the metal ions, and after 2 h, Cu^{II} and/or Hg^{II} ions were added to the reaction mixture. Upon the addition of Cu^{II} ions, the activity of the **H**-DNAzyme was rapidly increased while that of T-DNAzyme was not changed at all (Figure 5-9a). This result shows the selective activation of the **H**-DNAzyme. When Hg^{II} ions were added, only T-DNAzyme was activated through T–Hg^{II}–T base pairing (Figure 5-9b). The addition of Cu^{II} and Hg^{II} ions resulted in the activation of both **H**-DNAzyme and T-DNAzyme (Figure 5-9c). These results corroborate the orthogonal activation of the two DNAzyme activities.

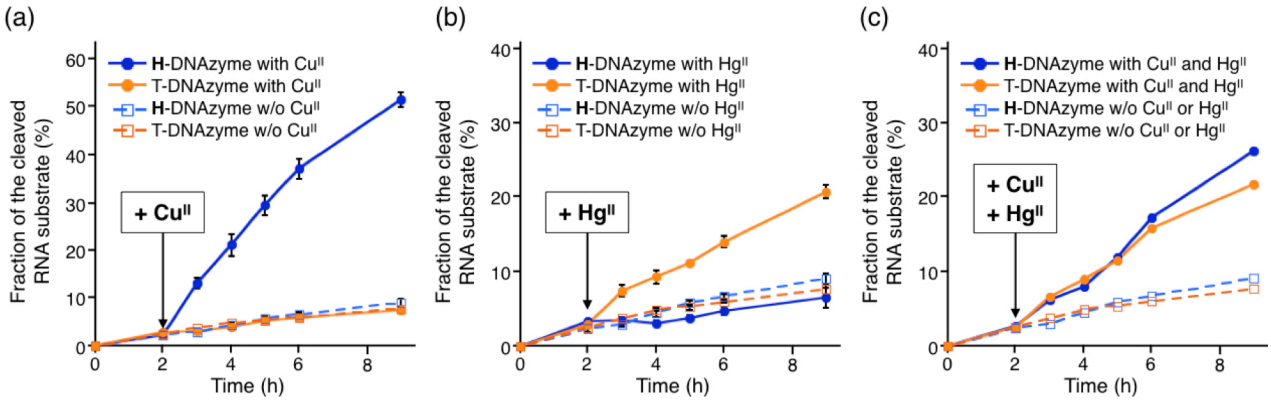

Figure 5-9. Metal-dependent orthogonal activation of the split **H**-DNAzyme and T-DNAzyme. (a) Selective activation of the split **H**-DNAzyme with Cu^{II} ions. (b) Selective activation of T-DNAzyme with Hg^{II} ions. (c) Activation of both **H**- and T-DNAzymes by the simultaneous addition of Cu^{II} and Hg^{II} ions. [**H**-DNAzyme] = [T-DNAzyme] = 1.0 μM, [substrate 1] = [substrate 2] = 2.0 μM (2.0 equiv), [$CuSO_4$] = 0 or 1.0 μM (1.0 equiv for a **H**–**H** pair), [$Hg(ClO_4)_2$] = 0 or 4.0 μM (1.0 equiv for a T–T pair) in 10 mM HEPES (pH 7.0), 1.0 M $NaNO_3$, 10 mM $Mg(NO_3)_2$. 25 °C. Cu^{II} and/or Hg^{II} ions were added after 2 h. *N* = 3. Error bars indicate standard errors.

Furthermore, the selective deactivation of the two DNAzymes was demonstrated by removing Cu^{II} and Hg^{II} ions with the use of corresponding chelating agents (Figure 5-10a). The orthogonal deactivation was studied with an equimolar mixture of the split **H**-DNAzyme and T-DNAzyme. A Cu^{II}-binding peptide (GHK)[18] and a thymidine oligomer (T20) were used to remove Cu^{II} and Hg^{II} ions, respectively. The RNA-cleaving reactions were initiated in the presence of both Cu^{II} and Hg^{II} ions, and one of the chelating agents was added selectively to deactivate the DNAzymes. Figure 5-10b shows the deactivation of the **H**-DNAzyme by the addition of one equivalent of GHK. The addition of one equivalent of GHK immediately decreased the activity of the **H**-DNAzyme while

keeping that of T-DNAzyme. This result shows the selective deactivation of the **H**-DNAzyme by the removal of Cu^{II} ions. On the other hand, when T20 was added, only the activity of T-DNAzyme was diminished (Figure 5-10c). This result demonstrates the selective deactivation of T-DNAzyme by removing Hg^{II} ions. After the removal of Hg^{II} ions, the RNA-cleaving activity of the **H**-DNAzyme was slightly raised. This is presumably due to the fact that the activity of the **H**-DNAzyme was suppressed by the unspecific binding of Hg^{II} ions, which were removed by the addition of T20. All the results demonstrated that the orthogonal deactivation of the DNAzymes was achieved by the selective removal of Cu^{II} and Hg^{II} ions.

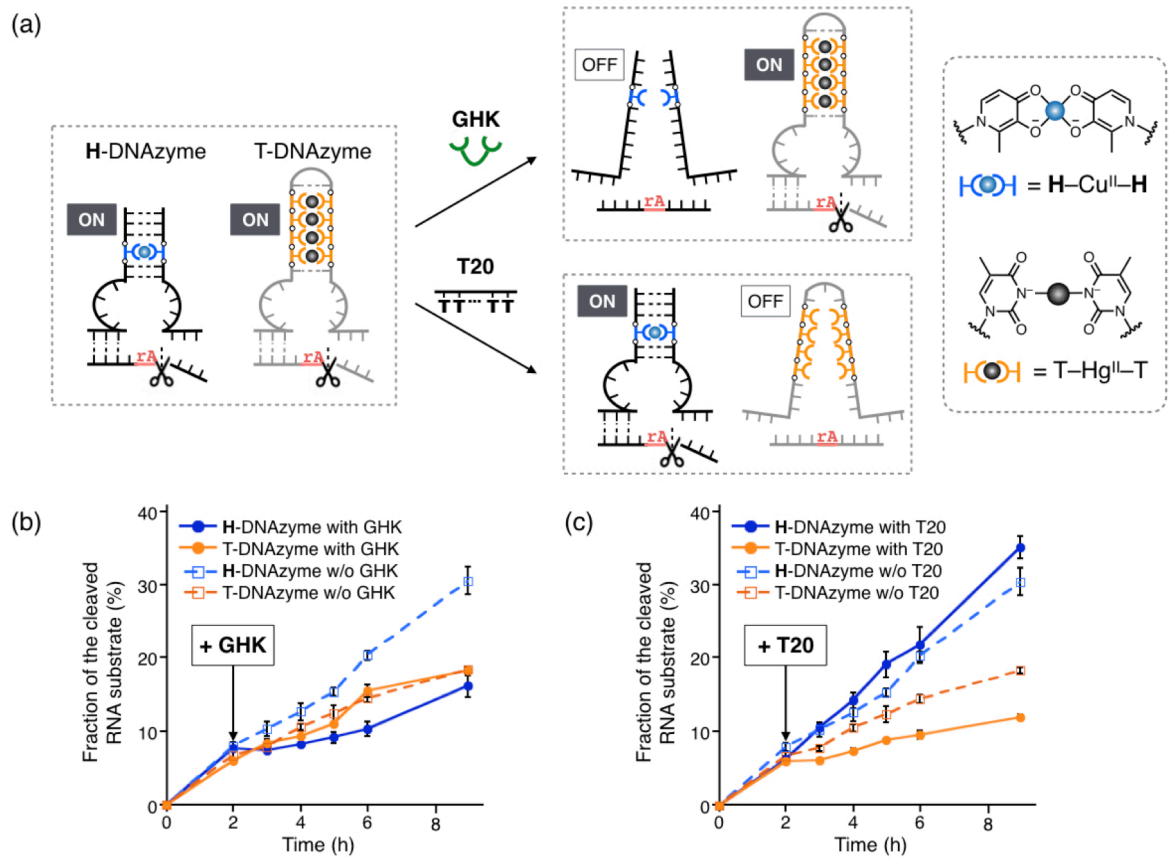

Figure 5-10. Metal-dependent deactivation of **H**-DNAzyme and T-DNAzyme. (a) Selective deactivation of **H**-DNAzyme with a Cu^{II}-binding peptide (GHK) to remove Cu^{II} ions. (b) Selective deactivation of T-DNAzyme with a thymidine oligomer (T20) to remove Hg^{II} ions. [**H**-DNAzyme] = [T-DNAzyme] = 1.0 μM, [substrate 1] = [substrate 2] = 2.0 μM (2.0 equiv), [$CuSO_4$] = 1.0 μM (1.0 equiv for a **H**–**H** pair), [$Hg(ClO_4)_2$] = 4.0 μM (1.0 equiv for a T–T pair), [GHK] = 1.0 μM (where applicable), [T20] = 2.0 μM (where applicable) in 10 mM HEPES (pH 7.0), 1 M $NaNO_3$, 10 mM $Mg(NO_3)_2$. 25 °C. The reactions were initiated in the presence of both Cu^{II} and Hg^{II} ions. After 2 h, GHK or T20 were added. *N* = 3. Error bars indicate standard errors.

Taken all together, the orthogonal regulation of DNAzyme activities was accomplished based on the selective formation of **H**–Cu^{II}–**H** and T–Hg^{II}–T base pairing (Figure 5-11). Each catalytic activity was independently modulated by the addition and removal of Cu^{II} and Hg^{II} ions. The orthogonal metal-dependent regulation will be applied to DNA-based logic gates, multiplexers, and computing circuits.[19] The regulatory system would be also useful for controlling multiple DNA supramolecules.

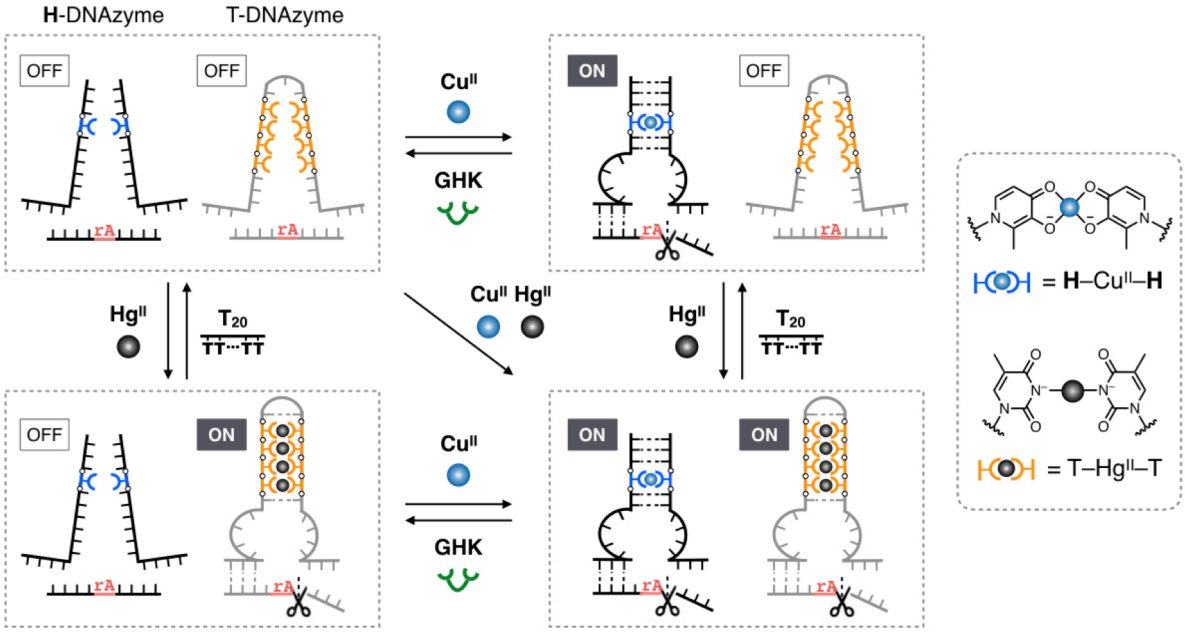

Figure 5-11. Schematic representation of the multimetal-dependent orthogonal regulation of the DNAzyme activities based on **H**–Cu^{II}–**H** and T–Hg^{II}–T base pairing.

Because C–Ag^{I}–C base pairing is orthogonal to **H**–Cu^{II}–**H** and T–Hg^{II}–T (Figure 5-3), the catalytic activities of three DNAzymes would be selectively regulated by exploiting the three metal-mediated base pairs. Other unnatural ligand-type nucleotides can be also applied to the orthogonal regulation. Based on the Hard-Soft Acid-Base (HSAB) theory, artificial nucleotides that bind to soft metal ions such as Pd^{II} and Pt^{II} ions[20] would serve as an orthogonal pair to **H**–Cu^{II}–**H** base pairing.

第 5 章
以降の節(4–6)は 5 年以内に論文誌で刊行予定のため、非公開。

5-7. References

[1] (a) D. Y. Zhang, G. Seelig, *Nat. Chem.* **2011**, *3*, 103–113. (b) F. C. Simmel, B. Yurke, H. R. Singh, *Chem. Rev.* **2019**, *119*, 6326−6369.

[2] M. N. Stojanovic, D. Stefanovic, *Nat. Biotechnol.* **2003**, *21*, 1069–1074.

[3] (a) G. Seelig, D. Soloveichik, D. Y. Zhang, E. Winfree, *Science* **2006**, *314*, 1585–1588. (b) D. Y. Zhang, A. J. Turberfield, B. Yurke, E. Winfree, *Science* **2007**, *318*, 1121–1125. (c) L. Qian, E. Winfree, J. Bruck, *Nature* **2011**, *475*, 368–372. (d) L. Qian, E. Winfree, *Science* **2011**, *332*, 1196–1201. (e) D. Woods, D. Doty, C. Myhrvold, J. Hui, F. Zhou, P. Yin, E. Winfree, *Nature* **2019**, *567*, 366–372.

[4] B. Shlyahovsky, Y. Li, O. Lioubashevski, J. Elbaz, I. Willner, *ACS Nano* **2009**, *3*, 1831–1843.

[5] (a) J. Liu, Y. Lu, *Adv. Mater.* **2006**, *18*, 1667–1671. (b) W. Yoshida, Y. Yokobayashi, *Chem. Commun.* **2007**, 195–197. (c) J. Liu, J. H. Lee, Y. Lu, *Anal. Chem.* **2007**, *79*, 4120–4125. (d) X. Liu, F. Wang, R. Aizen, O. Yehezkeli, I. Willner, *J. Am. Chem. Soc.* **2013**, *135*, 11832–11839.

[6] S. M. Douglas, I. Bachelet, G. M. Church, *Science* **2012**, *335*, 831–834.

[7] J. Elbaz, F. Wang, F. Remacle, I. Willner, *Nano Lett.* **2012**, *12*, 6049−6054.

[8] M. W. Haydell, M. Centola, V. Adam, J. Valero, M. Famulok, *J. Am. Chem. Soc.* **2018**, *140*, 16868−16872.

[9] (a) H. Nishioka, X. Liang, T. Kato, H. Asanuma, *Angew. Chem. Int. Ed.* **2012**, *51*, 1165–1168. (b) M. Škugor, J. Valero, K. Murayama, M. Centola, H. Asanuma, M. Famulok, *Angew. Chem. Int. Ed.* **2019**, *58*, 6948–6951.

[10] (a) Y. Takezawa, J. Müller, M. Shionoya, *Chem. Lett.* **2017**, *46*, 622–633. (b) Y. Takezawa, M. Shionoya, J. Müller, In *Comprehensive Supramolecular Chemistry II*; J. L. Atwood, Eds.; Elsevier Ltd.: Oxford, 2017; Vol. 4, pp 259–293. (c) Y. Takezawa, M. Shionoya, *Acc. Chem. Res.* **2012**, *45*, 2066–2076.

[11] (a) S. Katz, *Biochim. Biophys. Acta* **1963**, *68*, 240–253. (b) Y. Miyake, H. Togashi, M. Tashiro, H. Yamaguchi, S. Oda, M. Kudo, Y. Tanaka, Y. Kondo, R. Sawa, T. Fujimoto, T. Machinami, A. Ono, *J. Am. Chem. Soc.* **2006**, *128*, 2172–2173.

[12] K. Tanaka, G. H. Clever, Y. Takezawa, Y. Yamada, C. Kaul, M. Shionoya, T. Carell, *Nat. Nanotechnol.* **2006**, *1*, 190–194.

[13] A. Ono, S. Cao, H. Togashi, M. Tashiro, T. Fujimoto, T. Machinami, S. Oda, Y. Miyake, I. Okamoto, Y. Tanaka, *Chem. Commun.* **2008**, *44*, 4825–4827.

[14] Y. Tanaka, J. Kondo, V. Sychrovsky, J. Sebera, T. Dairaku, H. Saneyoshi, H. Urata, H. Torigoe, A. Ono, *Chem. Commun.* **2015**, *51*, 17343–17360.

[15] (a) J. Liu, Y. Lu, *Angew. Chem. Int. Ed.* **2007**, *46*, 7587–7590. (b) S. Shimron, J. Elbaz, A. Henning, I. Willner, *Chem. Commun.* **2010**, *46*, 3250−3252. (c) Z. Zhang, D. Balogh, F. Wang, I. Willner, *J. Am. Chem. Soc.* **2013**, *135*, 1934−1940. (d) J. Chen, J. Pan, S. Chen, *Chem. Commun.* **2017**, *53*, 10224–10227. (e) X. Li, J. Xie, B. Jiang, R. Yuan, Y. Xiang, *ACS Appl. Mater. Interfaces* **2017**, *9*, 5733−5738.

[16] R. R. Breaker, G. F. Joyce, *Chem. Biol.* **1995**, *2*, 655–660.

[17] M. Zuker, *Nucleic Acids Res.* **2003**, *31*, 3406−3415.

[18] (a) L. Pickart, J. H. Freedman, W. J. Loker, J. Peisach, C. M. Perkins, R. E. Stenkamp, B. Weinstein, *Nature* **1980**, *288*, 715−717. (b) A. Trapaidze, C. Hureau, W. Bal, M. Winterhalter, P. Faller, *J. Biol. Inorg. Chem.* **2012**, *17*, 37–47.

[19] (a) I. Willner, B. Shlyahovsky, M. Zayats, B. Willner, *Chem. Soc. Rev.* **2008**, *37*, 1153–1165. (b) R. Orbach, B. Willner, I. Willner, *Chem. Commun.* **2015**, *51*, 4144−4160.

[20] (a) K. Tanaka, M. Shionoya, *J. Org. Chem.* **1999**, *64*, 5002–5003. (b) Y. Takezawa, K. Tanaka, M. Yori, S. Tashiro, M. Shiro, M. Shionoya, *J. Org. Chem.* **2008**, *73*, 6092–6098.

[21] R. Saran, J. Liu, *Anal. Chem.* **2016**, *88*, 4014−4020.

[22] R. Saran, K. Kleinke, W. Zhou, T. Yu, J. Liu, *Biochemistry* **2017**, *56*, 1955−1962.

[23] (a) M. N. Stojanovic, T. E. Mitchell, D. Stefanovic, *J. Am. Chem. Soc.* **2002**, *124*, 3555–3561. (b) M. N. Stojanović, D. Stefanović, *J. Am. Chem. Soc.* **2003**, *125*, 6673–6676.

[24] D. M. Kolpashchikov, M. N. Stojanovic, *J. Am. Chem. Soc.* **2005**, *127*, 11348–11351.

[25] (a) H. Lederman, J. Macdonald, D. Stefanovic, M. N. Stojanovic, *Biochemistry* **2006**, *45*, 1194–1199. (b) J. Elbaz, O. Lioubashevski, F. Wang, F. Remacle, R. D. Levine, I. Willner, *Nat. Nanotechnol.* **2010**, *5*, 417–422. (c) R. Pei, E. Matamoros, M. Liu, D. Stefanovic, M. N. Stojanovic, *Nat. Nanotechnol.* **2010**, *5*, 773–777. (d) F. Wang, J. Elbaz, R. Orbach, N. Magen, I. Willner, *J. Am. Chem. Soc.* **2011**, *133*, 17149–17151. (e) R. Orbach, F. Remacle, R. D. Levine, I. Willner, *Chem. Sci.* **2014**, *5*, 1074–1081. (f) R. Orbach, F. Wang, O. Lioubashevski, R. D. Levine, F. Remacle, I. Willner, *Chem. Sci.* **2014**, *5*, 3381–3387. (g) C. W. Brown III, M. R. Lakin, E. K. Horwitz, M. L. Fanning, H. E. West, D. Stefanovic, S. W. Graves, *Angew. Chem. Int. Ed.* **2014**, *53*, 7183–7187.

[26] (a) M. Moshe, J. Elbaz, I. Willner, *Nano Lett.* **2009**, *9*, 1196–1200. (b) S. Bi, Y. Yan, S. Hao, S. Zhang, *Angew. Chem. Int. Ed.* **2010**, *49*, 4438–4442. (c) L. Zhang, Y.-M. Zhang, R.-P. Liang, J.-D. Qiu, *J. Phys. Chem. C* **2013**, *117*, 12352–12357. (d) L. Li, J. Feng, Y. Fan, B. Tang, *Anal. Chem.* **2015**, *87*, 4829−4835. (e) D. Balogh, M. A. A. Garcia, H. B. Albada, I.

Willner, *Angew. Chem. Int. Ed.* **2015**, *54*, 11652–11656.

[27] (a) R. Freeman, T. Finder, I. Willner, *Angew. Chem. Int. Ed.* **2009**, *48*, 7818−7821. (b) K. S. Park, C. Jung, H. G. Park, *Angew. Chem. Int. Ed.* **2010**, *49*, 9757–9760. (c) X. Zhu, H. Xu, X. Gao, X. Li, Q. Liu, Z. Lin, B. Qiu, G. Chen, *Chem. Commun.* **2011**, *47*, 9080–9082. (d) X. Li, L. Sun, T. Ding, *Biosens. Bioelectron.* **2011**, *26*, 3570–3576. (e) F. Wang, R. Orbach, I. Willner, *Chem. - Eur. J.* **2012**, *18*, 16030–16036. (f) H. Pei, L. Liang, G. Yao, J. Li, Q. Huang, C. Fan, *Angew. Chem. Int. Ed.* **2012**, *51*, 9020–9024. (g) G. Zhang, W. Lin, W. Yang, Z. Lin, L. Guo, B. Qiu, G. Chen, *Analyst* **2012**, *137*, 2687–2691.(h) W. Y. Xie, W. T. Huang, N. B. Li, H. Q. Luo, *Chem. Commun.* **2012,** *48*, 82–84. (i) Y.-M. Zhang, L. Zhang, R.-P. Liang, J.-D. Qiu, *Chem. - Eur. J.* **2013**, *19*, 6961–6965. (j) N. Kanayama, T. Takarada, M. Fujita, M. Maeda, *Chem. - Eur. J.* **2013**, *19*, 10794–10798.

[28] T. Kobayashi, Y. Takezawa, A. Sakamoto, M. Shionoya, *Chem. Commun.* **2016**, *52*, 3762–3765.

[29] T. Tanaka, A. Tengeiji, T. Kato, N. Toyama, M. Shiro, M. Shionoya, *J. Am. Chem. Soc.* **2002**, *124*, 12494–12498.

Chapter 6.

Conclusion and Perspectives

第 6 章

本章については、5 年以内に論文誌で刊行予定のため、非公開。

A list of publications

1. “Enzymatic Synthesis of Cu(II)-Responsive Deoxyribozymes through Polymerase Incorporation of Artificial Ligand-Type Nucleotides”

   Yusuke Takezawa, Takahiro Nakama, Mitsuhiko Shionoya, *J. Am. Chem. Soc.* **2019**, *141*, 19342−19350.

Acknowledgement

This research was promoted under supervision of Professor Dr. Mitsuhiko Shionoya (The University of Tokyo). I would like to express my deepest appreciation to him for his generous guidance and thoughtful advice. His passion for science has always encouraged me to tackle difficulties in my research.

I sincerely appreciate Assistant Professor Dr. Yusuke Takezawa (The University of Tokyo) for his daily guidance and aid to my research. His prudent advice and passionate discussion helped me advance my project in the right direction. He kindly taught me all what I need as a scientist.

I would like to acknowledge their warm support and insightful suggestions from Associate Professor Dr. Shohei Tashiro, Assistant Professor Dr. Hitoshi Ube, and Project Assistant Professor Dr. Koichi Nagata (The University of Tokyo).

I am deeply grateful to all the present and former members who shared our life in Shionoya laboratory. Without their support, I could never have gone through my PhD program. I would like to express my thanks especially to Teruki Kobayashi, Daisuke Sasaki, Zhang Wenxuan, Shuntaro Amano, Tong Xing, Lingyun Hu, Keita Mori, Wei-En Huang and Masahiro Wakano, who shared our projects. The discussions with them greatly deepened my understanding of our research.

I appreciate the fruitful discussions with Professor Dr. Takeaki Ozawa (The University of Tokyo), who is my secondary supervisor in the Leading Graduate Course.

I am thankful to Mr. Yoshimitsu Hori (The University of Tokyo), Dr. Shoichi Hosoya (Tokyo Medical and Dental University), and Dr. Natsuhiko Sugimura (Waseda University) for their technical support of MALDI-TOF MS measurement.

For financial support, I thank Advanced Leading Graduate Course for Photon Science (ALPS), which gave me an opportunity to focus on PhD work and to learn science in the different fields.

I am grateful to all my friends, who spent time together, even in difficult days.

Finally, I appreciate my family from the bottom of my heart for their persistent support, encouragement, and love in my life.

Takahiro Nakama